



X-RAY STUDIES OF METHYL 6-AMINO-5-CYANO-2-METHYL-4-(3-NITROPHENYL)-4H-PYRAN-3-CARBOXYLATE

Suresh Sharma^[a], Goutam Brahmachari^[b], Bubun Banerjee^[b], Rajni Kant^[a] and Vivek K. Gupta^{[a]*}

Keywords: crystal structure, direct methods, hydrogen bond.

The title compound, methyl 6-amino-5-cyano-2-methyl-4-(3-nitrophenyl)-4H-pyran-3-carboxylate (C₁₅H₁₃N₃O₅), was synthesized, in 92 % yield, by one-pot multicomponent reaction of 3-nitrobenzaldehyde, malononitrile and methyl acetoacetate using 10 mol% urea as an organo-catalyst at room temperature. It crystallizes in the triclinic space group P -1 with the unit-cell parameters: a= 8.1780(4), b= 8.3787(4), c= 11.8005(6) Å, α = 75.703(4)°, β = 86.017(4)°, γ = 72.983(4)° and Z = 2. The crystal structure was solved by direct methods using single-crystal X-ray diffraction data collected at room temperature and refined by full-matrix least-squares procedures to a final R-value of 0.0538 for 1896 observed reflections. The molecules within the unit cell are stabilized by C-H...O, N-H...O and N-H...N type of hydrogen bonding. In addition π-π interactions are also observed in the crystal structure.

*Corresponding Authors

Tel: +91 9419102467

E-Mail: vivek_gupta2k2@hotmail.com

- [a] X-ray Crystallography Laboratory, Post-Graduate Department of Physics & Electronics, University of Jammu, Jammu Tawi - 180 006, India
 [b] Laboratory of Natural Products & Organic Synthesis, Department of Chemistry, Visva-Bharati (a Central University), Santiniketan – 731235, West Bengal, India.

Introduction

Substituted-pyran scaffolds represent key structural motifs in significant natural bioactive molecules¹⁻⁵ and this has led to the synthesis of a huge number of synthetic analogs of such promising O-heterocycle with a broad range of biological activities including anticancer,⁶⁻⁹ antibacterial and antifungal^{10,11} and anti-rheumatic.¹² In this communication, we wish to report on one-pot facile synthesis of a novel 4H-pyran, namely methyl 6-amino-5-cyano-2-methyl-4-(3-nitrophenyl)-4H-pyran-3-carboxylate *via* multicomponent reaction (MCR) at room temperature using commercially available urea as inexpensive and environmentally benign organocatalyst, and its crystal structure. The structure of the title compound was elucidated by spectral methods and XRD studies.

Experimental

Synthesis

An oven-dried screw cap test tube was charged with a magnetic stir bar, 3-nitrobenzaldehyde (0.151 g, 1 mmol), malononitrile (0.066 g, 1.1 mmol), urea (0.007 g, 10 mol % as organo-catalyst), and EtOH:H₂O (1:1 v/v; 4 mL) in a sequential manner; the reaction mixture was then stirred vigorously at room temperature for about 20 min. After that, methyl acetoacetate (0.116 g, 1 mmol) was added to the stirred reaction mixture, and the stirring was continued for

8h.¹³ The progress of the reaction was monitored by TLC. On completion of the reaction, a solid mass precipitated out that was filtered off followed by washing with aqueous ethanol to obtain crude product. It was purified just by recrystallization from ethanol without carrying out column chromatography. The structure of methyl 6-amino-5-cyano-2-methyl-4-(3-nitrophenyl)-4H-pyran-3-carboxylate was confirmed by analytical as well as spectral studies including FT-IR, ¹H NMR, ¹³C NMR, and TOF-MS. Unit crystal was obtained from DMSO as a solvent. For crystallization 50 mg of compound dissolved in 5 mL DMSO and left for several days at ambient temperature which yielded white block shaped crystals. The chemical structure of title compound is shown in Figure 1.

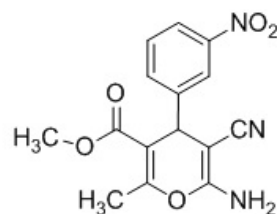


Figure 1. Chemical structure of title compound

White solid. Yield 92%. Mp: 204-206 °C. IR (KBr) ν_{max}cm⁻¹: 3391, 3323, 3207, 3159, 3076, 2945, 2908, 2349, 2183, 1684, 1678, 1601, 1580, 1529, 1423, 1265, 1182, 1067, 906, 835, 787, 729, 683, 623, 523. ¹H NMR (400 MHz, DMSO-*d*₆) δ/ppm: 8.11 (1H, d, J = 7.2 Hz, aromatic H), 7.97 (1H, s, aromatic H), 7.65 (2H, d, J = 7.6 Hz, aromatic H), 7.10, (2H, s, NH₂), 4.52 (1H, s, CH), 3.53 (3H, s, OCH₃), 2.35 (3H, s, CH₃). ¹³C NMR (100 MHz, DMSO-*d*₆) δ/ppm: 166.11, 159.11, 158.41, 148.31, 147.66, 134.43, 130.62, 122.42, 121.90, 119.76, 106.59, 56.79, 52.05, 38.91, 18.83. TOF-MS: 338.0756 [M + Na]⁺. Elemental analysis: Calcd. (%) for C₁₅H₁₃N₃O₅: C, 57.14; H, 4.16; N, 13.33; found: C, 57.16; H, 4.15; N, 13.37.

X-ray structure determination

X-ray intensity data of 8981 reflections (of which 2942 unique) were collected on *X'calibur* CCD area-detector diffractometer equipped with graphite monochromated MoK α radiation ($\lambda = 0.71073$ Å). The crystal used for data collection was of dimensions 0.30 x 0.20 x 0.20 mm. The cell dimensions were determined by least-squares fit of angular settings of 3730 reflections in the θ range 3.49° to 29.14°. The intensities were measured by 'omega scan' mode for θ ranges 3.50° to 26.00°. 1896 reflections were treated as observed ($I > 2\sigma(I)$). Data were corrected for Lorentz, polarization and absorption factors.

The structure was solved by direct methods using SHELXS97.¹⁴ All non-hydrogen atoms of the molecule were located in the best E-map. Full-matrix least-squares refinement was carried out using SHELXL97.¹⁴ The final refinement cycles converged to an $R = 0.0538$ and $wR(F^2) = 0.1255$ for the observed data. Residual electron densities ranged from $-0.205 < \Delta\rho < 0.239$ eÅ⁻³. Atomic scattering factors were taken from International Tables for X-ray Crystallography (1992, Vol. C, Tables 4.2.6.8 and 6.1.1.4). The crystallographic data are summarized in Table 1.

Table 1. Crystal data and other experimental details

CCDC Number	1059815
Crystal description	Block
Crystal size	0.30 x 0.20 x 0.20 mm
Empirical formula	C ₁₅ H ₁₃ N ₃ O ₅
Formula weight	315.28
Radiation, Wavelength	Mo K α , 0.71073 Å
Unit cell dimensions	$a = 8.1780(4)$ Å $b = 8.3787(4)$ Å $c = 11.8005(6)$ Å $\alpha = 75.703(4)^\circ$ $\beta = 86.017(4)^\circ$ $\gamma = 72.983(4)^\circ$
Crystal system, Space group	triclinic, P-1
Unit cell volume	749.23(6) Å ³
No. of molecules per unit cell, Z	2
Absorption coefficient	0.107 mm ⁻¹
F(000)	328
θ range for entire data collection	3.50 < θ < 26.00
Reflections collected / unique	8981 / 2942
Reflections observed $I > 2\sigma(I)$	1896
Range of indices	$h = -9$ to 10 $k = -10$ to 10 $l = -14$ to 14
No. of parameters refined	209
Final R-factor	0.0538
$wR(F^2)$	0.1255
R_{int}	0.0407
R_σ	0.0509
Goodness-of-fit	1.017
Final residual electron density	$-0.205 < \Delta\rho < 0.239$ eÅ ⁻³

Result and discussions

An ORTEP¹⁵ view of the compound with atomic labeling is shown in Figure 2. The geometry of the molecule was calculated using the WinGX,¹⁶ PARST¹⁷ and PLATON¹⁸ software. Packing view of the molecules is shown in Figure 3.

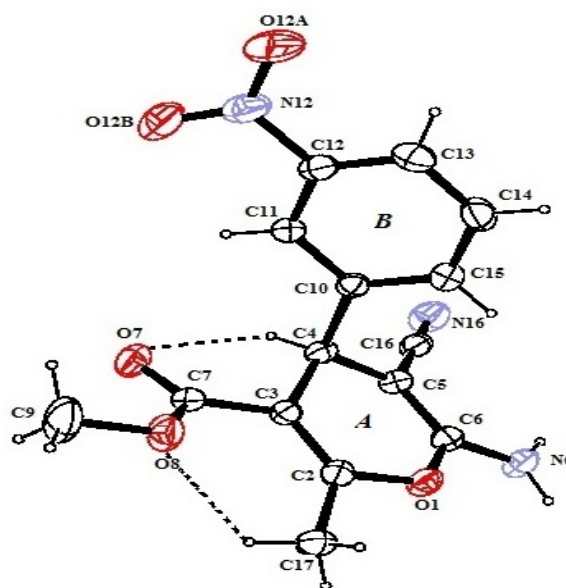


Figure 2. ORTEP view of the molecule with displacement ellipsoids drawn at 40 %

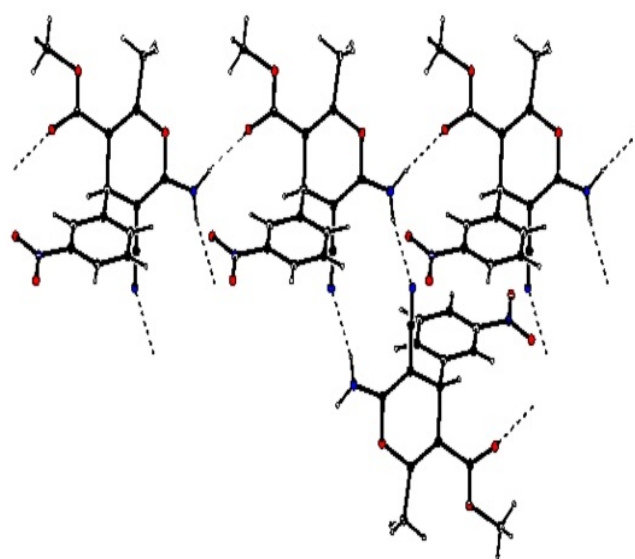


Figure 3. Partial view of hydrogen interactions between the molecules

The title compound comprises of two rings in which phenyl ring (ring-B) is planar and pyran ring (ring-A) deviates significantly from planarity as reflected from the large values of torsion angles in it. It adopts boat conformation with asymmetry parameters $\Delta C_s(O1-C4) = 7.56$ and $\Delta C_2(C2-C3) = 10.17$. The maximum deviation from the mean plane of pyran ring is observed for atom C4 which lies above the mean plane by 0.1648 Å. The bond distances O1-C6 and O1-C2 are 1.368(2) Å and 1.385(2) Å, are close to each other and agree well with the literature values.¹⁹

Table 2. Selected bond lengths (Å) and bond angles (°) for non hydrogen atoms (e.s.d.'s are given in parentheses)

Bond distances(Å)		Bond angles(°)		Torsion angles(°)	
O1-C6	1.368(2)	O12B-N12-O12A	122.8(2)	C16-C5-C6-N6	4.9(4)
O1-C2	1.385(2)	O12B-N12-C12	118.7(2)	C17-C2-C3-C7	-1.0(4)
C7-O7	1.203(2)	O12A-N12-C12	118.5(3)	C2-C3-C7-O7	-153.2(2)
C7-O8	1.326(3)	O8-C7-C3	115.79(18)	C11-C12-N12-O12A	-171.8(3)
O8-C9	1.458(3)	C7-O8-C9	115.66(19)		
N12-O12B	1.207(3)	N16-C16-C5	178.0(2)		
N12-O12A	1.211(3)	C3-C4-C10	110.12(15)		
C4-C10	1.528(3)	C5-C4-C10	113.06(17)		

Table 3. Geometry of intramolecular and intermolecular hydrogen bonds

D-H...A	D-H (Å)	H...A (Å)	D...A (Å)	∠[D-H...A (°)]
C4-H4...O7	0.98	2.457(1)	2.807(2)	100.55(13)
C17-H17C...O8	0.96	2.250(2)	2.898(3)	123.99(16)
N6-H6A...N16 ⁱ	0.86	2.167(2)	3.008(2)	165.65(14)
N6-H6B...O7 ⁱⁱ	0.86	2.023(2)	2.877(3)	171.67(14)
C9-H9C-O12B ⁱⁱⁱ	0.96	2.493(3)	3.405(4)	158.70(20)

Symmetry codes: i. -x+1,-y,-z+2; ii. +x+1,+y,+z; iii. +x,+y+1/2,+z

Table 4. Geometry of π - π hydrogen interactions

CgI-CgJ	CgI-CgJ(Å)	CgI...P(Å)	α (°)	β (°)	Δ (Å)
Cg2-Cg2 ⁱ	3.8139(13)	3.589	0.02	19.80	1.29

Symmetry code: i. -x, 1-y, 1-z; Here Cg₂ represents the centre of gravity of phenyl ring-B.

The bond distance C16-N16 is 1.148(2) Å, verifies its triple bond character. The bond distances N12-O12B and N12-O12A are 1.207(3) Å and 1.211(3) Å, are reasonable. The mean value of endocyclic bond angles in the phenyl ring is close to 120° as expected. The bond angles O12B-N12-O12A, O12B-N12-C12 and O12A-N12-C12 are 122.8(2)°, 118.7(2)° and 118.5(3)° respectively, signifies the planar geometry of nitro group. There is significant deviation of angles C3-C7-O8 and C7-O8-C9 with values 115.79(18)° and 115.66(19)° from the ideal value of 120° and such deviations are also observed in similar structure²⁰. The bond angle N16-C16-C5 with value 178.0(2)° signifies the linear character of carbonitrile group. The dihedral angle C17-C2-C3-C7 has the value -1.0(4)°, reflects that the methyl and carboxylate groups are almost coplanar. The carbonitrile and amino groups are deviated from coplanarity as reflected from the value of torsion angle C16-C5-C6-N6 with value 4.9(4)°. Some important bond lengths, bond angles and torsion angles are listed in Table 2. All other geometrical parameters of the title compound are normal and agree well with the related structure.²⁰

The crystal packing is stabilized by both intra and inter molecular hydrogen interactions. The intramolecular hydrogen interactions lead to formation of two virtual rings [Figure 2]. Both the hydrogen atoms of amino group are involved in intermolecular hydrogen interactions in which N6-H6B...O7 generates a chain like structure and other is responsible for the formation of dimer. The adjacent

chains are linked to each other by N6-H6A...N16 hydrogen interactions [Figure 3]. In addition crystal structure is also stabilized by π - π hydrogen interactions. The geometry of hydrogen interactions is given in Table 3 and Table 4.

Acknowledgments

GB is thankful to the CSIR, New Delhi for financial support [Grant No. 02(0110)/12/EMR-II]. BB is grateful to the UGC, New Delhi for awarding him a Senior Research Fellowship.

References

- Dean, F. M., *Naturally Occurring Oxygen Ring Compounds*; Butterworths: London, **1963**, p. 176.
- Raj, T. Bhatia R. K. Kanur A. Sharma M. Saxena A. K. and Ishar, M. P. S., *Eur. J. Med. Chem.* **2010**, *45*, 790.
- Flavin, M. T., Rizzo, J. D., Khilevich, A., Kucherenko, A., Sheinkina, A. K., Vilavchack, V., Lin, L., Chen, W., Mata, E., Pengsuparp, T., Pezzuto, J. M., Hughes, S. H., Flavin, T. M., Cibulski, M., Boulanger, W. A., Shone, R. L. and Xu, Z.-Q., *J. Med. Chem.* **1996**, *39*, 1303
- Morgan I. R. Jursic B. S. Hooper C. I. Neumann D. M. Thanapalai K. Leblanc, B., *Bioorg. Med. Chem. Lett.*, **2002**, *12*, 3407.

- ⁵Kumar, A., Maurva, R. A., Sharma, S. A., Ahmad, P., Singh, A. B., Bhatia, G. and Srivastava, A. K., *Bioorg Med Chem Lett*, **2009**, *19*, 6447.
- ⁶Skommer, J., Wlodkowic, D., Matto, M., Eray, M. And Pelkonen, J., *Leuk. Res*, **2006**, *30*, 322.
- ⁷Kasibhatla, S., Gourdeau, H., Meerovitch, K., Drewe, J., Reddy, S., Qiu, L., Zhang, H., Bergeron, F., Bouffard, D., Yang, Q., Herich, J., Lamothe, S., Cai, S. X. and Tseng, B., *Mol Cancer Ther*, **2004**, *3*, 1365.
- ⁸Kemnitzner, W., Drewe, J., Jiang, S., Zhang, H., Zhao, J., Grundy, C. C., Xu, L., Lamothe, S., Gourdeau, H., Denis, R., Tseng, B., Kasibhatla, S. and Cai, S. X., *J. Med. Chem.*, **2007**, *50*, 2858.
- ⁹Bhavanarushi, S., Kanakaiah, V., Yakaiah, E., Saddanapu, V., Addlagatta, A. and Rani, V.J., *Med. Chem. Res*, **2013**, *22*, 2446.
- ¹⁰Paliwal, P. K., Jetti, S. R. and Jain, S., *Med. Chem. Res.*, **2013**, *22*, 2984.
- ¹¹Kumar, D., Reddy, V.B., Sharad, S., Dube, U. and Kapur, S., *Eur. J. Med. Chem.*, **2009**, *44*, 3805.
- ¹²Smith, C. W., Bailey, J. M., Billingham, M. E. J., Chandrasekhar, S., Dell, C. P., Harvey, A. K., Hicks, C. A., Kingston, A. F. and Wishart, G. N., *Bioorg. Med. Chem. Lett*, **1995**, *5*, 2783.
- ¹³Brahmachari, G. and Banerjee, B., *ACS Sustainable Chem. Eng.*, **2014**, *2*, 411.
- ¹⁴Sheldrick, G.M., *Acta Cryst.*, **2008**, *A64*, 112.
- ¹⁵Farrugia, L.J. *J Appl Cryst.*, **1997**, *30*, 565.
- ¹⁶Farrugia, L.J., *J Appl Cryst.*, **1999**, *32*, 837.
- ¹⁷Nardelli, M., *J Appl Cryst.*, **1995**, *28*, 659.
- ¹⁸Spek, A.L., *Acta Cryst.*, **2009**, *D65*, 148.
- ¹⁹Allen, F. H., Kennard, O., Watson, D.G., Brammer, L., Orpen, A.G., and Taylor, R., *J. Chem. Soc., Perkin Trans-II.*, **1987**, S1.
- ²⁰Li, Y., Wang, X., Zeng, Z., Shi, D., Wei, X. and Zong, Z., *Acta Cryst. E* **2005**, *E61*, o1115.

Received: 24.04.2015.

Accepted: 04.06.2015.



COLORIMETRIC DETERMINATION OF METOCLOPRAMID HYDROCHLORIDE AND TRANEXAMIC ACID USING 9-CHLOROACRIDINE REAGENT

Theia'a N. Al-Sabha^[a], Maha T. Al-Obaidi^[b] and Thabit S. Al-Ghabsha^[c]

Keywords: metoclopramide hydrochloride, tranexamic acid, 9-chloroacridine, spectrophotometry.

A simple, sensitive and accurate spectrophotometric method is developed for the quantitative determination of metoclopramide hydrochloride and tranexamic acid drugs. The method is based on the interaction between these drugs and 9-chloroacridine reagent. The spectra of the products show maximum absorption at 470 and 479 nm and Beer's law is obeyed in the concentration range of 2-50 and 1-40 $\mu\text{g mL}^{-1}$ with molar absorptivity values 8.50×10^3 and $7074 \times 10^3 \text{ L mol}^{-1} \text{ cm}^{-1}$ for above drugs respectively. The average percent recoveries are 99.90 % and 98.60 % respectively, and relative standard deviation (RSD) is ≤ 0.456 % for both drugs. In addition, the stability constant has been determined and the reaction mechanism is proposed. The method has been applied successfully for the assay of metoclopramide hydrochloride and tranexamic acid in pharmaceutical formulations and compared favourably with the amounts mentioned in formulations.

*Corresponding Authors

E-Mail: dr_theiaa@yahoo.co.uk

[a] Dept. of Chemistry, College of Education, University of Mosul-Iraq

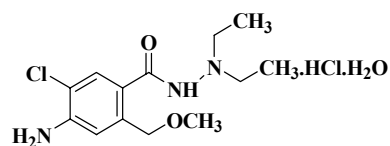
[b] Dept. of Chemistry, College of Science, University of Mosul-Iraq

[c] College of Pharmacy, University of Mosul-Iraq

Introduction

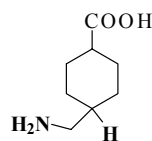
Metoclopramide hydrochloride (MCP.HCl), [4-amino-5-chloro-N-(2-diethylaminoethyl)-2-methoxybenzamide hydro-chloride] [I] is used as an anti-emetic in the treatment of some forms of nausea and vomiting and to increase gastrointestinal motility. It is of little benefit in the prevention or treatment of motion sickness or in the treatment of nausea and vertigo due to Meniere disease or other labyrinth disturbance,¹ also it is used to relieve certain stomach and esophagus problems such as diabetic gastroparesis and gastroesophageal reflux disorder.²

Tranexamic acid (TRA), [Trans 4-(aminomethyl)-cyclohexanecarboxylic acid] [II] is used as antifibrinolytic and haemostatic in the treatment of bleeding associated with excessive fibrinolysis, such as haemorrhage following prostatectomy, tonsillectomy and menorrhagia.³



$\text{C}_{14}\text{H}_{22}\text{ClN}_3\text{O}_2 \cdot \text{HCl} \cdot \text{H}_2\text{O}$
M.wt = 354.3 gm/mol

I



$\text{C}_8\text{H}_{15}\text{NO}_2$
M.wt = 157.2 gm/mol

II

Various analytical techniques have been reported for determination MCP.HCl and TRA in pure or dosage forms. Chromatographic methods,⁴⁻⁸ titrimetry,⁹ voltammetry,¹⁰ atomic absorption,¹¹ flow injection^{12,13} and ion selective electrode¹⁴ are used for determination of MCP.HCl, whereas chromatographic¹⁵⁻¹⁷ and conductometric¹⁸ methods are used for determination of TRA. Of course, the above mentioned techniques are sensitive but expensive. Spectrophotometry is the technique of choice even today due to its inherent simplicity. Many spectrophotometric procedures have been applied for the determination of MCP.HCl and TRA using different reagents such as phenothiazine as coupling reagent and ferric nitrate as oxidizing reagent,¹⁹ o-phenanthroline or bipyridyl in the presence of Fe(III) or Ce(IV) as oxidizing reagents,²⁰ dibenzoyl methane,²¹ aniline as coupling reagent²² and p-dimethylaminocinnamaldehyde²³ in addition to other spectrophotometric methods²⁴⁻²⁸ used for determination of MCP.HCl. Vanilline,²⁹ acetylacetone and formaldehyde,³⁰ 2,6-dichloroquinone-4-chlorimide,³¹ ascorbic acid,³² 1,2-naphthoquinone-4-sodium-sulphonate,³³ DDQ and TCNQ³⁴ p-nitroaniline³⁵ and potassium ferricyanide in the presence of ferric chloride³⁶ reagents are used for determination of TRA. Some of these methods are time-consuming, extraction procedures or heating require strictly controlled reaction conditions. Others are less sensitive. The present work describes a simple and sensitive spectrophotometric method for assay of MCP.HCl and TRA drugs in pure and dosage forms using 9-chloroacridine as chromogenic reagent without any derivatization or catalysis.

Experimental

Apparatus

Shimadzu UV-1650 PC UV-Visible spectrophotometer, equipped with a 1.0-cm path length silica cell, is used for spectral measurements. Philips PW (9421) pH-meter with a

combined glass electrode was used for pH measurements, All calculations in the computing process were done in Microsoft Excel for Windows.

Reagents

All chemicals used are of the highest purity available which are provided by BDH, Fluka and Molekula. 9-Chloroacridine (Eastman chemical Co.) was used as the chromogenic reagent. Absolute ethanol is used. Sodium hydroxide (1×10^{-2} M) and hydrochloric acid (1×10^{-2} M) solution are prepared by appropriate dilution of the concentrated NaOH (1 M) or HCl (1 M) solutions with distilled water. 9-chloroacridine reagent (1×10^{-3} M) (9-CA) solution is prepared by dissolving 0.0053 g of 9-chloroacridine in absolute ethanol and then the volume is completed to 25 ml in a volumetric flask. The solution is freshly prepared and used immediately.

Metoclopramide hydrochloride (MCP.HCl) and tranexamic acid (TRA) ($100 \mu\text{g mL}^{-1}$)

The solutions are prepared by dissolving 0.01g of pure MCP.HCl and TRA (provided from SDI) in distilled water (the solutions were equivalent to $100 \mu\text{g mL}^{-1}$ for each drug).

Recommended procedure

To a series of 5 ml calibrated flasks, increasing volumes of the working MCP.HCl or TRA solutions ($100 \mu\text{g mL}^{-1}$) were transferred to cover the concentration range 2-50 or 1-40 $\mu\text{g mL}^{-1}$ for MCP.HCl or TRA respectively, followed by the addition of 1.5 ml of 1×10^{-3} M 9-CA. The solutions were diluted to the mark with methanol. The solutions were kept in a water bath at room temperature for 5 and 15 min, for MCP.HCl and TRA respectively, and the absorbance was measured at 470 and 479 nm respectively against the respective blank reagent.

Procedure for MCP.HCl and TRA assay in dosage forms

Tablet

Weighed and finely powdered 10 tablets (each containing 10 mg MCP.HCl and 500 mg TRA), an accurately weighed amount of powder, equivalent to one tablet, was dissolved in 10 ml ethanol, shaken to increase the solubility and filtered into 100 ml calibrated flask, then the solution was made to the volume with the distilled water (the solution was equivalent to $100 \mu\text{g mL}^{-1}$ for MCP.HCl and $5000 \mu\text{g mL}^{-1}$ for TRA). A suitable volume was diluted with distilled water and followed the recommended procedure.

Syrup

The content of MCP.HCl syrup (5 mg/5 mL) was homogenized well and 10 ml of syrup was quantitatively transferred into 100 ml volumetric flask and completed to the mark with distilled water. An aliquot of diluted drug was taken and treated as mentioned in the recommended procedure.

Injection

For the analysis of injection, 2ml vial containing 10 mg/2 ml of MCP.HCl and 1ml containing 250 mg/5 mL TRA were transferred into 100 ml volumetric flask separately, and diluted up to the mark with distilled water. Working standard was prepared by suitable dilution and the recommended procedure was followed.

Results and discussion

In the preliminary investigation work, it was found that 9-CA reagent reacted selectively with MCP.HCl and TRA in alcoholic medium of ethanol and produced an orange colored solutions immediately with maximum absorption at 470 and 479 nm for above drugs respectively. Whereas the reagent blank which shows low absorbance at these wavelengths but have a maximum absorption at 386 nm (Fig. 1). However, the wavelength of maximum absorption 470 and 479 nm for MCP.HCl and TRA respectively were used in all subsequent experiments.

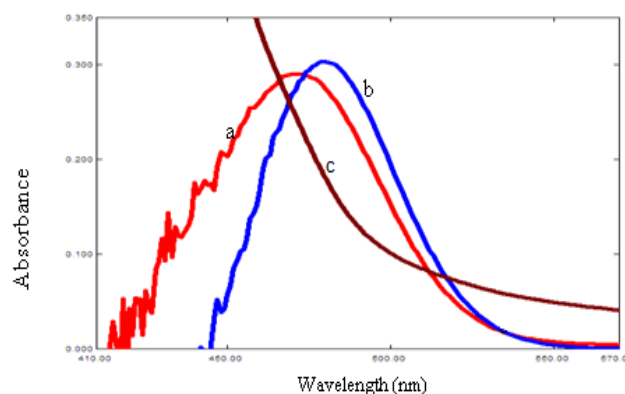


Figure 1. Absorption spectra of a) MCP.HCl ($6.0 \mu\text{g mL}^{-1}$), b) TRA ($6.0 \mu\text{g mL}^{-1}$) products with 9-CA (1×10^{-3} M) against reagent blank and c) Reagent blank against ethanol.

Selecting optimum reaction conditions

The effect of various parameters on the absorption intensity of the colored products were investigated and the reaction conditions were optimized.

Effect of solvent

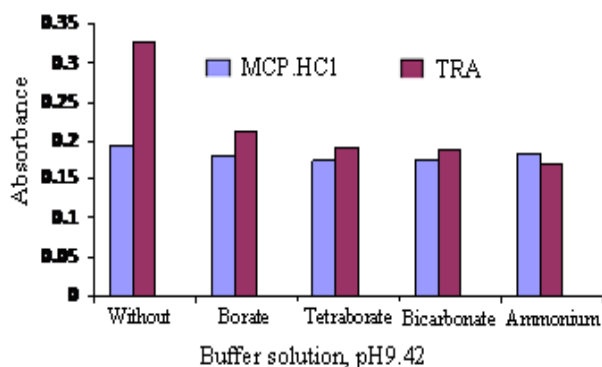
A number of mixtures were prepared by mixing 0.3 and 0.5 ml of MCP.HCl and TRA solutions, containing $100 \mu\text{g}$ of the drug mL^{-1} , with 1 ml of 1×10^{-3} M 9-CA and the volume was made to 5 ml with solvents such as water, methanol, ethanol, acetone, acetonitrile and tetrahydrofuran in calibrated flasks as given in Table 1. It was observed that the mixtures prepared from the solution of 9-CA in methanol and drug solutions in water made to 5 ml with the methanol gave maximum absorbance for MCP.HCl and TRA at 470 and 479 nm respectively, Therefore, this combination of solvents and wavelengths was chosen in the subsequent experiments.

Table 1. Effect of solvent on color intensity of drug-9-CA products.

Drug dissolved in	9-CA solvent	Dilution by	MCP.HCl		TRA	
			λ_{\max} (nm)	Abs.	λ_{\max} (nm)	Abs.
water	methanol	water	309	0.051	473	0.151
water	methanol	methanol	479	0.191	470	0.327
methanol	methanol	methanol	548	0.001	471	0.045
water	ethanol	water	458	0.035	473	0.112
water	ethanol	ethanol	439	0.112	472	0.268
ethanol	ethanol	ethanol	454	0.009	470	0.031
water	acetone	water	464	0.031	463	0.067
water	acetone	acetone	435	0.092	428	0.170
acetone	acetone	acetone	416	0.012	421	0.021
water	acetonitrile	water	472	0.025	472	0.092
water	acetonitrile	acetonitrile	435	0.145	475	0.181
acetonitrile	acetonitrile	acetonitrile	417	0.030	473	0.033
water	THF	water	499	0.02	473	0.023
water	THF	THF	419	0.103	476	0.133
THF	THF	THF	307	0.093	473	0.015

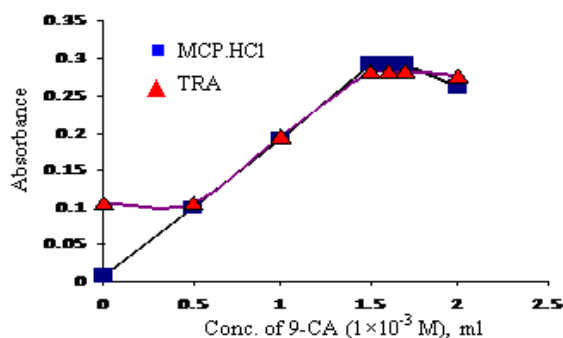
Effect of pH

The effect of pH on the colour intensity in the pH range between 1.32 and 12.0, obtained by suitable addition of 0.01 M of HCl and NaOH, was examined. It was found that the sensitivity of products decreased on addition of HCl or NaOH. However; the pH of the final dilution, measured in the absence of HCl and NaOH, was found 9.42. Different buffer solutions (bicarbonate, borate, tetraborate and ammonium of pH 9.5) were also examined. These showed a negative effect on the absorbance of the products (Fig. 2).

**Figure 2.** Effect of buffer solutions on the absorbance of $6 \mu\text{g mL}^{-1}$ MCP.HCl and $10 \mu\text{g mL}^{-1}$ TRA products with 9-CA reagent

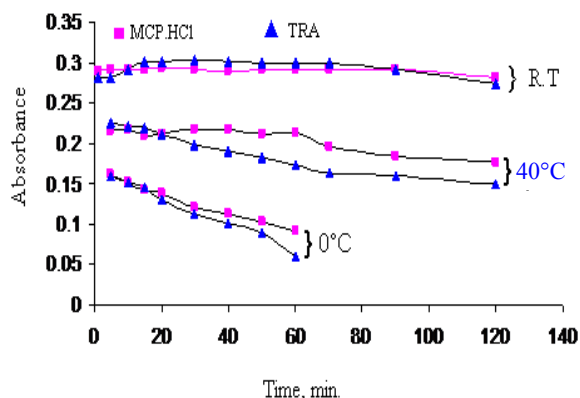
Effect of reagent concentration

Different volumes of 9-CA (1×10^{-3} M), in the range 0-2.0 ml, were added to solutions containing same amounts of MCP.HCl and TRA ($6 \mu\text{g mL}^{-1}$) separately, and making the final volume to 5 ml. The absorbance was measured at 470 and 479 nm at room temperature against their respective reagent blank, respectively. It was evident that the absorbance increases with increasing 9-CA concentration and reached maximum value when 1.5-1.7 ml of 9-CA was used for both drugs (Fig.3). Finally, 1.5 ml of 9-CA was used in subsequent experiments.

**Figure 3.** Effect of 9-CA reagent concentration

Effect of temperature and development time

The effect of temperature on the rate of reaction for drug-9-CA products was studied at room temperature (25°C), 40°C and 0°C at the previous optimum reaction conditions. The results indicated that the products were formed after the addition of reagent immediately and reached its maximum absorbance at room temperature after 5 and 15 min and remained constant for 85 and 55 min for MCP.HCl and TRA after which the absorbance decreased indicating dissociation (Fig. 5).

**Figure 5.** Effect of temperature and developing time for the absorption of $6 \mu\text{g mL}^{-1}$ MCP.HCl and $6 \mu\text{g mL}^{-1}$ TRA.

Effect of surfactants

Effect of various surfactants, SDS, CTAB, Tween-80 and Triton X-100, of 0.2 % concentration was examined on the absorption intensity of the drug – 9-CA products. It was found that the chosen surfactants had a negative effect on the absorbance of the products.

Quantitation

The results for the determination of MCP.HCl and TRA by 9-CA reagent are summarized in Table 2. The Beer's law limits and molar absorptivity values were evaluated and the results indicated that the method is sensitive. The linearity was represented by the regression equation and the corresponding correlation coefficient for drugs determined by the proposed method represents excellent linearity. The relative standard deviation (RSD) and accuracy (average recovery %) for the analysis of four replicates of each three different concentrations for paracetamol indicated that the method is precise and accurate. Limit of detection (LOD) and limit of quantitation (LOQ) were calculated according to the following equations:

$$LOD = \frac{3.3\sigma}{b} \quad \text{and} \quad LOQ = \frac{10\sigma}{b}$$

where σ is the standard deviation of five reagent blank determinations and b is the slope of the calibration curve. The results obtained are in the accepted range below the lower limit of Beer's law range.

Study of interferences

The extent of interference by some excipients which often accompany pharmaceutical preparations were studied by measuring the absorbance of solutions containing fixed amount of drug ($10 \mu\text{g mL}^{-1}$) and various amounts of diverse species in a final volume of 5 ml. It was found that the studied excipients did not interfere seriously even in the presence of 30 fold excess (Table 3). However; an error of 5.0 % in the absorbance readings was considered tolerable. This indicated that the method was free from interferences.

Table 2. Summary of optical characteristics and statistical data for the proposed method

Parameter	MCP.HCl	TRA
λ_{max} (nm)	470	479
Linear range ($\mu\text{g mL}^{-1}$)	2-50	1-40
Molar absorptivity ($\text{L mol}^{-1} \text{cm}^{-1}$)	8.503×10^3	7.074×10^3
LOD ($\mu\text{g mL}^{-1}$)	0.110	0.055
LOQ ($\mu\text{g mL}^{-1}$)	0.368	0.182
Sandell sensitivity ($\mu\text{g cm}^{-2}$)	0.0417	0.0222
Average recovery (%) [*]	99.90	98.60
Correlation coefficient	0.996	0.998
Regression equation (Y) ^{**}		
Slope, a	0.024	0.045
Intercept, b	0.105	0.007
RSD [*]	≤ 0.456	≤ 0.279

^{*} Average of five determinations, ^{**} $Y = aX + b$, where X is the concentration of MCP.HCl and TRA in $\mu\text{g mL}^{-1}$.

Analytical applications

The proposed method was successfully applied to determine MCP.HCl and TRA in pharmaceutical tablet, syrup and injection preparations using three concentrations for each drug. The average recovery % was in the range 99.48 - 102.5 % for MCP.HCl and 96.67 - 101.29 % for TRA indicating that the method is accurate (Table 4). The obtained results were compared statistically by a Student's t -test for accuracy and a variance ratio F -test for precision with the official method procedures^{37,38} at the 95 % confidence level with four degrees of freedom, As cited in Table 5, the results showed that the experimental t -test and F -test were less than the theoretical value ($t = 3.182$, $F = 9.12$), indicating that there was no significant difference between the proposed method and official method.

Stoichiometry and stability constant

The molar ratio of the products formed between each of MCP.HCl and TRA with 9-CA reagent were investigated by applying the continuous variation (Job's) and mole ratio methods.³⁹ The results indicated that products were formed in the ratio of 1:1 (Figure 6). This finding supports that these products are formed through amino group present in MCP.HCl and TRA. The stability constant (K_{st}) of the products were determined according to the previous ratio and found 2.962×10^4 and $8.026 \times 10^4 \text{ L mol}^{-1}$ respectively, indicating good stability.

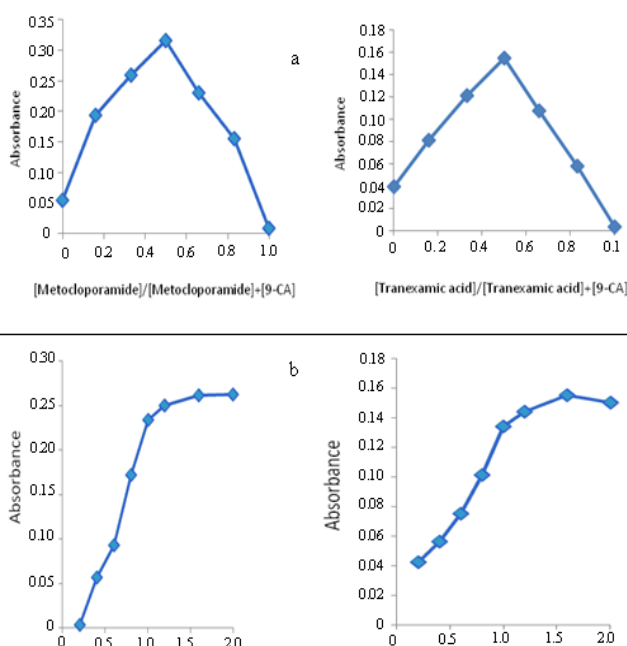


Figure 6. Continuous variation (a) and mole ratio (b) plots for drug- 9-CA products

Reaction mechanism

The colour produced from the interaction of MCP.HCl and TRA with 9-CA suggested that a free amino function in the molecule is necessary for the reaction. This finding is in agreement with the interaction of primary aromatic amines with the acridine^{40,41} to form highly coloured solutions. The reaction mechanism has been postulated in Scheme 1.

Table 3. Effect of excipients on the determination of MCP.HCl and TRA

Excipient	Recovery % of 10 µg mL ⁻¹ of target compounds in the presence of excipient in µg mL ⁻¹							
	MCP.HCl				TRA			
	50	100	200	300	50	100	200	300
Glucose	99.86	98.29	100.85	102.27	99.60	98.19	101.41	100.81
Lactose	100.28	101.70	102.27	101.98	98.99	99.60	97.38	100.40
Arabic gum	99.86	98.29	100.85	102.27	100.40	100.81	102.62	103.02
Sodium chloride	99.15	99.43	97.73	103.13	98.99	100.81	101.01	101.41
Sucrose	99.72	98.30	97.73	98.01	98.58	100.40	99.66	100.81
Starch	98.58	96.31	98.01	97.73	101.01	103.02	98.99	97.38

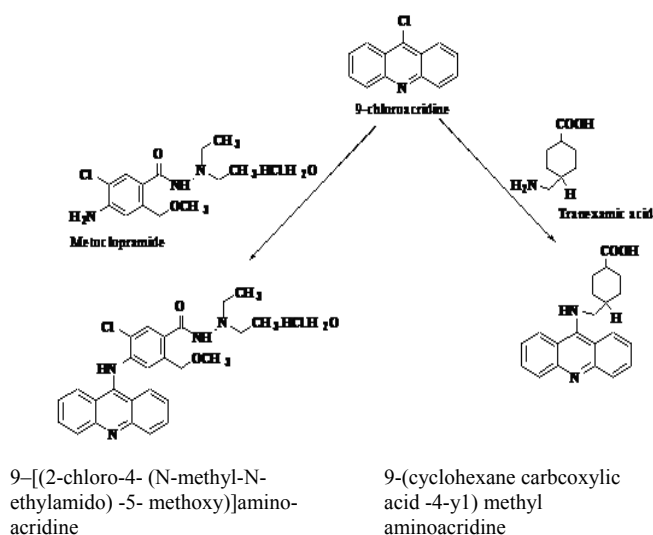
Table 4. Results of Assay of MCP.HCl and TRA in pharmaceutical preparations using the proposed method

Average recovery (mg)	Drug content Found * (mg)	Recovery* (%)	Amount present (µg.mL ⁻¹)	Certified value	Pharmaceutical preparation
10.2	10.25	102.5	10	10mg	Meclodin tablet ^a
	10.15	101.5	14		
	10.2	102.0	18		
5.03	5.09	101.7	10	5 mg/5 ml	Clopram syrup ^b
	4.97	99.48	14		
	5.02	100.46	18		
10.09	10.13	101.30	10	10 mg/2 ml	Metoclopramide.HCl injection ^c
	10.03	100.30	14		
	10.12	101.16	18		
505.64	508.0	101.16	10	500 mg	Transamine tablet ^d
	506.43	101.29	14		
	502.5	100.5	18		
245.86	249.50	99.8	10	250 mg/5 ml	Transamine injection ^d
	246.42	98.57	14		
	241.67	96.67	18		

*Average of four determinations, ^aSamarra drug industries, Iraq (S.D.I-Iraq), ^bThe Arab pharmaceutical manufacturing Co. Ltd., Sult-Jordan, ^cNanjinghuaxinbiopharm. CO. Ltd, manufactured in china, ^dActavis, Istanbul, Turkey.

Table 5. Comparison of the proposed method with official method

F_{test}	t_{exp}	Recovery (%)		Pharmaceutical preparation	Drug
		Standard method ^{36,37}	Present method		
4.5	1.36	101.29	102.5	Meclodin tablet	MCP.HCl
5.9	2.1	101.29	99.48	Clopram syrup	
4.9	0.15	101.29	101.16	Metoclopramid. HCl injection	
5.1	0.23	100.40	100.46	Transamine tablet	TRA
1.53	1.57	100.42	99.83	Transamine injection	



Scheme 1. Proposed reaction mechanism of 9-CA with MCP.HCl and TRA

Conclusion

A simple, selective and sensitive spectrophotometric method has been developed for the determination of microgram amounts of MCP.HCl and TRA based on their reaction with 9-CA reagent to form colored product having maximum absorption at 470 and 479 nm in methanolic medium respectively. The proposed method was applied successfully for the assay of the pharmaceutical formulations as tablet, syrup and injection.

References

- Martindal "The Extra Pharmacopoeia", 46th ed., The Pharmaceutical Press, London, **2000**, 1200.
- Ponte, C. D. and Nappi, J. M., *Am. J. Hosp. Pharm.*, **1981**, 38, 829.
- Bennet, P. N. and Brown, M. J., *Clin. Pharm.*, **2008**, 522.
- Fatmi, A. A., Williams, G. V. *Drug. Dev. Ind. Pharm.*, **1989**, 15, 1365.
- Ross, L. M., Eadie, M. J., Bochner, F., Hooper, W. D. and Tyrer, J. H., *J. Chromatogr. Biomed. Appl.*, **1980**, 9, 175.
- Riggs, K. W., Szetz, A., Runak, D. W., Mull, A. E., Abbote, B. F. S and Axeison, J. E., *J. Chromatogr. B. Biomed. Appl.*, **1994**, 660, 315.
- Bryson, S. M. and Gibert, L. M., *J. Clin. Pharm. Therap.*, **2008**, 9, 263.
- Vejendla, R., Kudidhi, V., Sravanthi, S., Taruni, G., Musthafa, M. D., *Int. J. Pharm. Phytopharmacol. Res.*, **2013**, 3, 83.
- Jawan, B. and Owas, L. *Int. J. Pharm.*, **1986**, 28, 44.
- Wang, Z. H., Zhary, H. Z., Zhou, S. P. and Dong, J., *Talanta*, **2001**, 53, 1133.
- Park, M. K., Lim, B. R., Yu, K. S. and Yong, K. H., *Yakhar Hoe Chi*, **1978**, 22, 27.
- Buna, M., Haron, J., Prognen, P. and Mah, F., *Analyst*, **1996**, 121, 1551.
- Al-Arfa, N. A., *Talanta*, **2004**, 62, 255.
- Al-Haideri, A. A., Abdulla, N. I. and Malih, I. J. K., *Iraqi J. Pharm Sci.*, **2012**, 21, 70.
- Patil, K. R., Rane, V. P., Sangshetti, J. N. and Shinde, D. B., *Eurasian J. Anal. Chem.*, **2010**, 5, 204.
- Khuhawar, M. Y. and Rind, F. M. A., *Chromatographia*, **2001**, 53, 709.
- Tampubolon, H. B. and Sumarlik, E., *J. Liq. Chromatogr. Related. Techn.*, **2005**, 28, 3243.
- Elazazy, M. S., El-Mammli, M. Y., Shalaby, A. and Ayad M. M., *Chem. Anal. (Warsaw)*, **2008**, 53, 725.
- Al-Abachi, M. Q. and Al-Ward, H. S., *Natl. J. Chem.*, **2002**, 7, 363.
- Amin, A. S. and Ragab, G. H., *Anal. Sci.*, **2003**, 19, 747.
- Revanasiddappa, H. D. and Manju, B., *J. Pharm. Biomed. Anal.*, **2001**, 25, 631.
- Shah J., Rasul J. M., Azam K., M. and Amin S., *J. Anal. Chem.*, **2005**, 60, 633.
- Moussa, B. A., *J. Pharm. Biomed. Anal.*, **2000**, 23, 1045.
- El-Gendy, A. E., *Spectroscopy Lett.*, **1992**, 25, 1297.
- Fan, J., Wang, A. J., Feng, S. L. and Wang, J. J., *Talanta*, **2005**, 66, 236.
- Abdel-Gawad, F. M., El-Guindi, N. M., *Anal. Lett.*, **1995**, 28, 1437.
- Herrero, M. R., Romero, A. M. and Calatayud, J. M., *Talanta*, **1998**, 47, 223.
- Ramappa, P. G. and Revanasiddappa, H. D., *Indian Drugs*, **1999**, 36, 381.
- Rind, E. M., Laghari, M. G., Memon, A. H., Mughal, U. R., Almai, F., Memon, N., Khuhawar, M. Y. and Maneshwari, M. L., *Yaoxue XueBao*, **2009**, 44, 125.
- Abulghasem, El A. K. and Mohamed, A. A., *Chem. Pharm. Bull.*, **2007**, 55, 364.
- Kariem, El R. A., Jabbir, M. A. A., *World App. Sci. J.*, **2012**, 19, 1263.
- Mohamed, M. A., Kariem, E. A. and Jabbir, M. A. A., *J. Anal. Techn.*, **2012**, 1, 2.
- Agarwa, S. L. and Murthy, R., *Int. J. Res. Pharm. Biomed. Sci.*, **2012**, 3, 2.
- Raza A., *Anal. Lett.*, **2006**, 39, 2217.
- Dhamra, M. Y., *J. Educ. Sci.*, **2011**, 24, 21.
- Mohite, P. B., Pandhare, R. B., Khanage, S. G., and Bhaskar, V. H., *Asian J. Res. Chem.*, **2009**, 2, 273.
- British Pharmacopoeia*, CD-Rom. The Stationery Office, London, **2010**.
- British Pharmacopoeia* on CD-Rom, 3rd Edn., System Simulation Ltd. The Stationery Office, London, **2000**.
- Hargis, L.G., "Analytical Chemistry, Principles and Techniques", Prentice-Hall Inc., New Jersey. **1988**, 424-427.
- Stewart J. T., Ray, A. B. and Fackler, W. B., *J. Pharm. Sci.*, **1969**, 58, 1261.
- Gammans, R. E., Stewart, J. T. and Sternson, L. A., *Anal. Chem.*, **1974**, 46, 62.

Received: 13.04.2015.

Accepted: 05.06.2015.



SYNTHESIS OF SOME NEW HETEROCYCLIC COMPOUNDS CONTAINING COUMARIN RING AND EVALUATION OF THEIRS PHARMACOLOGICAL EFFECT

Reda M. Fikry^{[a]*}, Nabila A. Ismail^[a], Mohammed El-Garby^[a], Enaiat M. Kamel^[a] and Ahmed D. H. Deeb^[a,b]

Keywords: 3-Acetyl coumarin, Nicotino-nitrile, Pyridopyrimidine, Naphthyridine, Antitumor.

2-Amino-6-(2-oxo-2H-chromen-3-yl)-4-phenylnicotino-nitrile was reacted with cyclohexanone, formic acid, acetic anhydride, acetophenone, triethylorthoformate and hydrazine hydrate to give the corresponding pyridopyrimidine and pyridopyridine derivatives. On the other hand, 2-amino-4-(3-chloro-phenyl)-6-(2-oxo-2H-chromen-3-yl)nicotinonitrile was cyclized by reacting it with urea, thiourea, formamide, triethylorthoformate, hydrazine hydrate and cyclohexanone to give the corresponding cyclic pyridopyridine, pyridopyrimidine and pyridotriazine derivatives. The potential cytotoxicity activity of compounds 7, 8, 16 and 17 was tested against breast carcinoma cell line by SRB (Sulphorhodamine-B) assay.

* Corresponding Authors

E-Mail: redmof56@yahoo.com

[a] Department of Chemistry, Faculty of Science, Zagazig University, Zagazig, Egypt

[b] Department of Chemistry, Faculty of Science, Jazan University, Jizan, 2097, Saudi Arabia

Introduction

Coumarin and coumarin-related compounds have been proved for many years to have significant therapeutic potential. Coumarins could be synthesized by various methods, such as Pechmann,¹ Perkin,² Knoevenagel,³ Reformatsky,⁴ Witting,⁵ Claisen⁶ and flash vacuum pyrolysis reaction.⁷ It has shown numerous biological activities, such as antitumor,⁸ anti-HIV (NNRTI),⁹ antioxidation,¹⁰ antimicrobial activity¹¹ and anticancer activity.¹²

Material and methods

All melting points are uncorrected and were determined on Gallenkamp electric melting point apparatus. IR spectra (KBr discs, cm⁻¹) were recorded on a FT/IR-400 spectrophotometer (Perkin Elmer). ¹HNMR spectra were recorded on a Varian-300 (CDCl₃, DMSO-d₆) solution. Chemical shifts are reported as δ (ppm) values relative to tetramethylsilane (TMS) as internal reference. The elemental analyses were carried out at Micro analytical center, Cairo University.

3-Acetyl-2H-chromen-2-one (3)

3-Acetylcoumarin was prepared according to the procedure reported.¹³ A mixture of salicylaldehyde (50 mmol) and ethyl acetoacetate (50 mmol) was stirred with cooling. To this mixture, 1 g of piperidine was added with shaking. The mixture was maintained at freezing

temperature for 2-3 h, resulting in a yellow colored solid mass, which was separated out. It was recrystallized from ethanol to get the target compound **3**.

2-Amino-6-(2-oxo-2H-chromen-3-yl)-4-phenylnicotinonitrile (4a)

A mixture of 3-acetylcoumarin (10 mmol), benzaldehyde (10 mmol), malononitrile (10 mmol) and ammonium acetate (20 mmol) in acetic acid 30 ml was refluxed for 3 hrs, cooled and filtered off to get the solid mass, dried and recrystallized from acetic acid. Yield 61 %, m.p. 262 °C. Anal. Calcd. For C₂₁H₁₃N₃O₂ (339.35): C, 74.33; H, 3.86; N, 12.38; O, 9.43. Found: C, 74.31; H, 3.81; N, 12.35; O, 9.41. IR (KBr): 3492, 3360, 2214 and 1726 cm⁻¹ attributed to (NH₂), (CN) and (C=O), respectively.

2-Amino-4-(3-chlorophenyl)-6-(2-oxo-2H-chromen-3-yl)nicotinonitrile (4b)

A mixture of 3-acetyl coumarin (10 mmol), 3-chlorobenzaldehyde (10 mmol), malononitrile (10 mmol) and ammonium acetate (20 mmol) in acetic acid 30 ml was refluxed for 3 h, cooled and filtered off to get the solid mass, dried and recrystallized from acetic acid. Yield 58 %, m.p. 258-260°C. Anal. Calcd. For C₂₁H₁₂ClN₃O₂ (373.79): C, 67.48; H, 3.24; N, 11.24; O, 8.56. Found: C, 67.44; H, 3.21; N, 11.21; O, 8.51. IR (KBr): 3313, 3193, 2202 and 1732 cm⁻¹ attributed to (NH₂), (CN) and (C=O), respectively, ¹H NMR of compound **4b** revealed signals at δ 7.1 (s, 2H, NH₂) and δ 7.4 - 8.4 (m, 10H, ArH's).

3-(5-Amino-4-phenyl-6,7,8,9-tetrahydrobenzo[b][1,8]naphthyridin-2-yl)-2H-chromen-2-one (5)

To a solution of **4a** (10 mmol) in cyclohexanone (15 ml), anhydrous ZnCl₂ (10 mmol) was added and the reaction mixture was refluxed for 30 minutes. The complex with zinc

chloride was separated from the solution, the mixture dissolved in 40 % sodium hydroxide (20 ml), and extracted with benzene. The benzene layer was dried (Na_2SO_4) and evaporated to give **5**, which recrystallized from acetic acid. Yield 48 %, m.p. 312 °C. Anal. Calcd. For $\text{C}_{27}\text{H}_{21}\text{N}_3\text{O}_2$ (419.47): C, 77.31; H, 5.05; N, 10.02; O, 7.63. Found: C, 77.27; H, 5.01; N, 10.05; O, 7.59. IR (KBr): 3384, 3210 and 1726 cm^{-1} attributed to (NH_2) and ($\text{C}=\text{O}$), respectively.

7-(2-Oxo-2H-chromen-3-yl)-5-phenylpyrido[2,3-d]pyrimidin-4(3H)-one (6)

A solution of **4a** (5 mmol) in formic acid (20 ml) was heated under reflux for 24 h then cooled, poured into crushed-ice, filtered off, dried and recrystallized from methanol to give **6**. Yield 52 %, m.p. 210-212 °C. Anal. Calcd. For $\text{C}_{22}\text{H}_{13}\text{N}_3\text{O}_3$ (367.36): C, 71.93; H, 3.57; N, 11.44; O, 13.07. Found: C, 71.90; H, 3.52; N, 11.41; O, 13.02. IR (KBr): 3243, 1680 and 1738 cm^{-1} attributed to (NH), ($\text{C}=\text{O}$) and ($\text{C}=\text{O}$), respectively; ^1H NMR of compound **6** revealed signals at δ 6.6 – 8.2 (m, 12H, ArH s) and δ 12.00 (s, 1H, NH).

4-Amino-7-(2-oxo-2H-chromen-3-yl)-5-phenyl-1,8-naphthyridin-2(1H)-one (7)

A mixture of compound **4a** (5 mmol), acetic anhydride (8 ml) and phosphoric acid (8 ml) was heated under reflux for 10 h, cooled, poured into ice-water then neutralized with solid sodium carbonate to $\text{pH} = 7$, filtered off, dried and recrystallized from acetic acid. Yield 67 %, m.p. 300 °C. Anal. Calcd. For $\text{C}_{23}\text{H}_{15}\text{N}_3\text{O}_3$ (381.38): C, 72.43; H, 3.96; N, 11.02; O, 12.59. Found: C, 72.45; H, 3.91; N, 11.00; O, 12.55. IR (KBr): 3434, 3313, 3193 and 1725 cm^{-1} attributed to (NH), (NH_2) and ($\text{C}=\text{O}$), respectively; ^1H NMR of compound **7** revealed signals at δ 2.88 (s, 2H, NH_2) and δ 7.36 - 8.66 (m, 12H, ArH s) and δ 11.8 (s, 1H, NH).

3-(5-Amino-4,7-diphenyl-1,8-naphthyridin-2-yl)-2H-chromen-2-one (8)

A mixture of **4a** (5 mmol), acetophenone (5 mmol) and few drops of TEA in 1,4-dioxan (30 ml) was heated under reflux for 5 h then cooled and poured into ice-water to precipitate, filtered off, dried and recrystallized from 1,4-dioxan. Yield 63 %, m.p. 310-312 °C. Anal. Calcd. For $\text{C}_{23}\text{H}_{19}\text{N}_3\text{O}_2$ (441.48): C, 78.90; H, 4.34; N, 9.52; O, 7.25. Found: C, 78.82; H, 4.31; N, 9.48; O, 7.21. IR (KBr): 3390, 3220 and 1726 cm^{-1} attributed to (NH_2) and ($\text{C}=\text{O}$), respectively; ^1H NMR of compound **8** revealed signals at δ 4.99 (s, 2H, NH_2) and δ 7.36 - 8.92 (m, 17H, ArH s).

Ethyl-N-(3-cyano-6-(2-oxo-2H-chromen-3-yl)-4-phenylpyridin-2-yl)formimidate (9)

Compound **4a** (5 mmol) was refluxed in triethylorthoformate (30 ml) for 8 h, cooled, poured into petroleum ether, filtered off, dried and recrystallized from benzene to give **9**. Yield 65 %, m.p. 222-224 °C. Anal. Calcd. For $\text{C}_{24}\text{H}_{17}\text{N}_3\text{O}_3$ (395.41): C, 72.90; H, 4.33; N,

10.63; O, 12.14. Found: C, 72.84; H, 4.35; N, 10.60; O, 12.12. IR (KBr): 2979, 2225, 1738 and 1640 cm^{-1} attributed to ($\text{CH}_{\text{aliphatic}}$), (CN), ($\text{C}=\text{O}$) and ($\text{C}=\text{N}$), respectively.

3-(4-Hydrazinyl-5-phenylpyrido[2,3-d]pyrimidin-7-yl)-2H-chromen-2-one (10)

A mixture of compound **9** (25 mmol), hydrazine hydrate (1.5 ml, 98 %) in dry benzene (20 ml) was stirred for 4 h. at room temperature, filtered off, dried and recrystallized from methanol to give compound **10**. Yield 42 %, m.p. 274-276 °C. Anal. Calcd. For $\text{C}_{24}\text{H}_{21}\text{N}_5\text{O}_3$ (427.46): C, 67.44; H, 4.95; N, 16.38; O, 11.23. Found: C, 67.41; H, 4.91; N, 16.32; O, 11.23. IR (KBr): 3390, 3315, 3174 and 1723 cm^{-1} attributed to (NH_2), (NH) and ($\text{C}=\text{O}$), respectively; ^1H NMR of compound **10** revealed signals at δ 2.4 (s, 2H, NH_2) and δ 4.2 (s, 1H, NH) and δ 7.3-8.9 (m, 12H, ArH s).

2-(6-Amino-5-cyano-4-phenylpyridin-2-yl)-3-(2-hydroxyphenyl)acrylohydrazide (11)

A mixture of compound **4a** (25 mmol) and equivalent amount of hydrazine hydrate in ethanol (25 ml) was heated under reflux for 4 h, cooled, filtered off, dried and recrystallized from methanol to give **11**. Yield 57 %, m.p. 304-306 °C. Anal. Calcd. For $\text{C}_{21}\text{H}_{17}\text{N}_5\text{O}_2$ (371.39): C, 67.91; H, 4.61; N, 18.86; O, 8.62. Found: C, 67.85; H, 4.58; N, 18.82; O, 8.61. IR (KBr): 3470, 3344, 3212, 2215 and 1691 cm^{-1} attributed to (NH , NH_2), (OH), (CN) and ($\text{C}=\text{O}$)_{hydrazide}, respectively; ^1H NMR of compound **11** revealed signals at δ 2.00 (s, 2H, NH_2 of NHNH_2) and δ 5.53 (s, 1H, OH) and δ 6.7 – 7.6 (m, 10H, ArH s and Pyridine proton) and δ 7.8 (s, 2H, NH_2) and δ 8.00 (s, 1H, NH) and δ 8.6 (s, 1H, cinnamoyl proton).

4-Amino-5-(3-chlorophenyl)-7-(2-oxo-2H-chromen-3-yl)pyrido[2,3-d]pyrimidin-2(1H)-one (12a)

A mixture of compound **4b** (25 mmol) and urea (30 mmol) was heated to be fused for 2 h, then dissolved in a solution of sodium hydroxide (10 %) with stirring for 2 h, then neutralized by HCl to obtain solid product, filtered off, washed with water, dried and recrystallized from acetic acid to give **12a**. Yield 45 %, m.p. 285 °C. Anal. Calcd. For $\text{C}_{22}\text{H}_{13}\text{ClN}_4\text{O}_3$ (416.82): C, 63.39; H, 3.14; N, 13.44; O, 11.52. Found: C, 63.35; H, 3.11; N, 13.40; O, 11.53. IR (KBr): 3475, 3410, 1728 and 1724 cm^{-1} attributed to (NH_2), ($\text{C}=\text{O}$) and ($\text{C}=\text{O}$), respectively; ^1H NMR of compound **12a** revealed signals at δ 2.8 (s, 2H, NH_2) and δ 7.36 - 8.9 (m, 10H, ArH s) and δ 9.2 (s, 1H, NH).

3-(4-Amino-5-(3-chlorophenyl)-2-thioxo-1,2-dihydropyrido[2,3-d]pyrimidin-7-yl)-2H-chromen-2-one (12b)

A mixture of compound **4b** (25 mmol) and thiourea (30 mmol) was heated to be fused for 2 h, then dissolved in a solution of sodium hydroxide (10 %) with stirring for 2 h, then neutralized by HCl to obtain solid product, filtered off, washed with water, dried and recrystallized from acetic acid to give **12b**. Yield 47 %, m.p. 235 °C. Anal. Calcd. For $\text{C}_{22}\text{H}_{13}\text{ClN}_4\text{O}_2\text{S}$ (432.88): C, 61.04; H, 3.03; N, 12.94; O, 7.39. Found: C, 61.01; H, 3.05; N, 12.91; O, 7.36. IR (KBr):

3463, 3400, 1724 and 1270 cm^{-1} attributed to (NH_2), ($\text{C}=\text{O}$) and ($\text{C}=\text{S}$), respectively.

3-(4-Amino-5-(3-chlorophenyl)pyrido[2,3-d]pyrimidin-7-yl)-2H-chromen-2-one (13)

A mixture of compound **4b** (5 mmol) and formamide (15 ml) was refluxed for 90 minutes then cooled, poured into crushed-ice to obtain the solid product, filtered off, washed, dried and recrystallized from acetic acid to give **13**. Yield 53 %, m.p. 286-288 °C. Anal. Calcd. For $\text{C}_{22}\text{H}_{13}\text{ClN}_4\text{O}_2$ (400.82): C, 65.92; H, 3.27; N, 13.98; O, 7.98. Found: C, 65.87; H, 3.22; N, 13.91; O, 7.95. IR (KBr): 3432, 3390, 1725 and 1604 cm^{-1} attributed to (NH_2), ($\text{C}=\text{O}$) and ($\text{C}=\text{N}$), respectively.

Ethyl-N-(4-(3-chlorophenyl)-3-cyano-6-(2-oxo-2H-chromen-3-yl)pyridin-2-yl)formimide (14)

Compound **4b** (5 mmol) was heated under reflux in triethylorthoformate (30 ml) for 8 h, cooled, poured into petroleum ether to completely precipitation, filtered off, dried and recrystallized from benzene. Yield 50 %, m.p. 210 °C. Anal. Calcd. For $\text{C}_{24}\text{H}_{16}\text{ClN}_3\text{O}_3$ (429.86): C, 67.06; H, 3.75; N, 9.78; O, 11.17. Found: C, 67.09; H, 3.71; N, 9.72; O, 11.18. IR (KBr): 3061, 2993, 2220, 1733 and 1651 cm^{-1} attributed to ($\text{CH}_{\text{aromatic}}$), ($\text{CH}_{\text{aliphatic}}$), (CN), ($\text{C}=\text{O}$) and ($\text{C}=\text{N}$), respectively.

3-(5-(3-Chlorophenyl)-4-hydrazinylpyrido[2,3-d]pyrimidin-7-yl)-2H-chromen-2-one (15)

A mixture of compound **15** (25 mmol) and hydrazine hydrate (1.5 ml) in dry benzene (25 ml) was stirred at room temperature for 4 hrs, filtered off, dried and recrystallized from benzene to give **15**. Yield 42 %, m.p. 298 °C. Anal. Calcd. For $\text{C}_{22}\text{H}_{13}\text{ClN}_4\text{O}_2$ (415.83): C, 63.54; H, 3.39; N, 16.84; O, 7.70. Found: C, 63.55; H, 3.36; N, 16.80; O, 7.67. IR (KBr): 3390, 3340, 1725 and 1604 cm^{-1} attributed to (NH , NH_2), ($\text{C}=\text{O}$) and ($\text{C}=\text{N}$), respectively; ^1H NMR of compound **15** revealed signals at δ 2.5 (s, 2H, NH_2) and δ 3.1 (s, 1H, NH) and δ 7.4 - 9.08 (m, 11H, ArH's).

3-(5-(3-Chlorophenyl)-4-hydroxypyrido[2,3-d][1,2,3]triazin-7-yl)-2H-chromen-2-one (16)

A solution of sodium nitrite (10 mmol) in 10 ml of water was added to a cold solution of **4b** (5 mmol) in acetic acid (30 ml) and concentrated HCl (15 ml), after completion of addition, the ice bath was removed and stirring continued at room temperature for additional 2 h. The crude product obtained was recrystallized from acetic acid. Yield 61 %, m.p. 292-294 °C. Anal. Calcd. For $\text{C}_{21}\text{H}_{11}\text{ClN}_4\text{O}_3$ (402.79): C, 62.62; H, 2.75; N, 13.91; O, 11.92. Found: C, 62.58; H, 2.80; N, 13.92; O, 11.88. IR (KBr): 3432, 1726 and 1607 cm^{-1} attributed to (OH), ($\text{C}=\text{O}$) and ($\text{C}=\text{N}$), respectively; ^1H NMR of compound **16** revealed signals at δ 7.4 - 9.00 (m, 10H, ArH's) and δ 9.06 (s, 1H, OH).

3-(5-(3-Chlorophenyl)-4-hydroxypyrido[2,3-d]pyrimidin-7-yl)-2H-chromen-2-one (17)

A mixture of compound **4b** (5 mmol) and triethylorthoformate (10 ml) in dimethylformamide (20 ml) was heated under reflux for 45 minutes, cooled, filtered off, dried and recrystallized from acetic acid to give yellow crystals of **17**. Yield 70 %, m.p. 296-298 °C. Anal. Calcd. For $\text{C}_{22}\text{H}_{12}\text{ClN}_3\text{O}_3$ (401.80): C, 65.76; H, 3.01; N, 10.46; O, 11.95. Found: C, 65.71; H, 3.04; N, 10.41; O, 11.91. IR (KBr): 3405, 1724 and 1607 cm^{-1} attributed to (OH), ($\text{C}=\text{O}$) and ($\text{C}=\text{N}$), respectively; ^1H NMR of compound **17** revealed signals at δ 7.3 - 8.1 (m, 11H, ArH's) and δ 8.8 (s, 1H, OH).

2-(6-Amino-4-(3-chlorophenyl)-5-cyanopyridin-2-yl)-3-(2-hydroxyphenyl)acrylo-hydrazide (18)

A mixture of compound **4b** (25 mmol) and equivalent amount of hydrazine hydrate in ethanol (25 ml) was heated under reflux for 4 h, cooled, filtered off, dried and recrystallized from methanol to give **18**. Yield 69 %, m.p. 200 °C. Anal. Calcd. For $\text{C}_{21}\text{H}_{16}\text{ClN}_5\text{O}_2$ (405.84): C, 62.15; H, 3.97; N, 17.26; O, 7.88. Found: C, 62.11; H, 3.92; N, 17.22; O, 7.86. IR (KBr): 3510, 3420, 3304, 3163, 2212 and 1652 cm^{-1} attributed to (OH), (NH), (NH, NH_2), (CN) and ($\text{C}=\text{O}$), respectively; ^1H NMR of compound **18** revealed signals at δ 2.00 (s, 2H, NH_2 of NHNH_2) and δ 5.53 (s, 1H, OH) and δ 6.7 - 7.6 (m, 9H, ArH's and Pyridine proton) and δ 7.8 (s, 2H, NH_2) and δ 8.00 (s, 1H, NH) and δ 8.6 (s, 1H, cinnamoyl proton).

3-(5-Amino-4-(3-chlorophenyl)-6,7,8,9-tetrahydrobenzo[b]-[1,8]naphthyridin-2-yl)-2H-chromen-2-one (19)

To a solution of **4b** (5 mmol) in cyclohexanone (8 ml) anhydrous ZnCl_2 (5 mmol) was added and the reaction mixture was refluxed for 50 minutes. The complex with zinc chloride was separated from the solution. Thereafter, the mixture was dissolved in 40 % sodium hydroxide (20 ml) and extracted with benzene and then benzene was evaporated to give **19** which was recrystallized from ethanol. Yield 56 %, m.p. >300°C. Anal. Calcd. For $\text{C}_{27}\text{H}_{20}\text{ClN}_3\text{O}_2$ (453.92): C, 71.44; H, 4.44; N, 9.26; O, 7.05. Found: C, 71.38; H, 4.41; N, 9.21; O, 7.09. IR (KBr): 3480, 3395, 2932 and 1698 cm^{-1} attributed to (NH_2), ($\text{CH}_{\text{aliphatic}}$) and ($\text{C}=\text{O}$), respectively.

Antitumor assay

Reagents: Fetal bovine serum (FBS) and L-glutamine, were from GibcoIvitrogen Co. (Scotland, UK). RPMI-1640 medium was from cambrex (New Jersey, USA). Dimethylsulfoxide (DMSO), doxorubicin, penicillin, streptomycin and sulforhodamine B (SRB) were from Sigma Chemical Co. (Saint Louis, USA).

Cell cultures: Three human tumor cell lines, MCF-7 breast adenocarcinoma was obtained from the European Collection of cell cultures (ECACC, Salisbury, UK).

They grew as monolayer and routinely maintained in RPMI-1640 medium supplemented with 5 % heat inactivated FBS, 2 mM glutamine and antibiotics (penicillin 100 U mL⁻¹, streptomycin 100 µg mL⁻¹), at 37 °C in a humidified atmosphere containing 5 % CO₂.

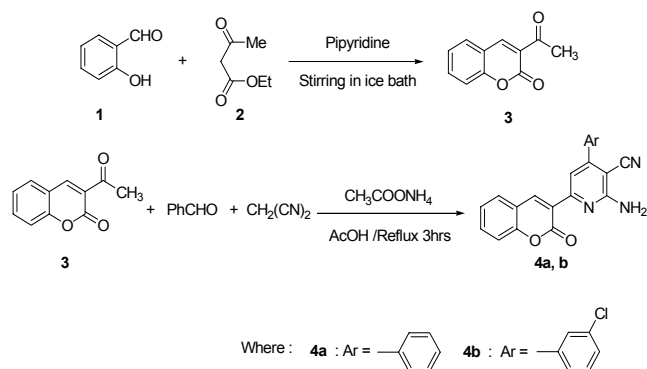
Exponentially growing cells were obtained by plating 1.5 x 10⁵ cells mL⁻¹ for MCF-7 followed by 24 h of incubation. The effect of the vehicle solvent (DMSO) on the growth of these cell lines was evaluated in all the experiments by exposing untreated control cells to the maximum concentration (0.5 %) of DMSO used in each assay.

Tumour cell growth assay

The effects of compounds of **7**, **8**, **16** and **17** on the in vitro growth of human tumor cell lines were evaluated according to the procedure¹⁴⁻¹⁷ adopted by the National Cancer Institute (NCI, USA) in the "In vitro Anticancer Drug Discovery Screen" that uses the protein-binding dye Sulforhodamine B to assess cell growth. Briefly, exponentially, cells growing in 96-well plates were then exposed for 48 h to five serial concentrations of each compound, starting from a maximum concentration of 150 µM. Following this exposure period adherent cells were fixed, washed and stained. The bound stain was solubilized and the absorbance was measured at 492 nm in a plate reader (Bio-Tek Instruments Inc., Power wave XS, Wincoski, USA). For each test compound and cell line, a dose-response curve was obtained and the growth inhibition of 50 % (GI₅₀), corresponding to the concentration of the compounds that inhibited 50% of the net cell growth was calculated as described elsewhere. Doxorubicin was used as a positive control and tested in the same manner.

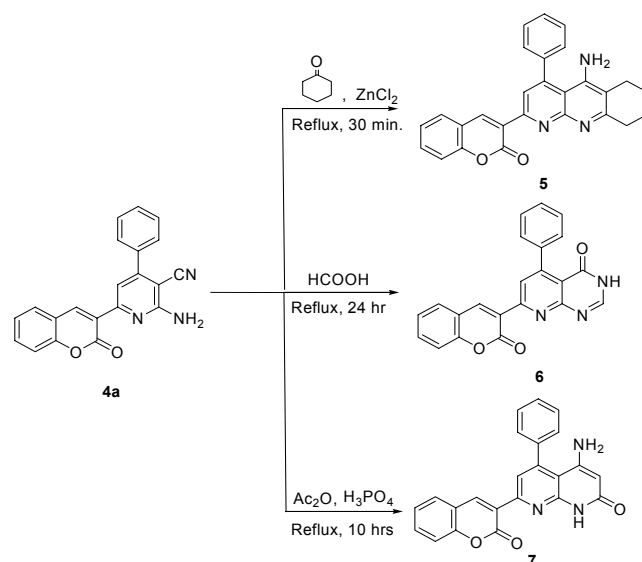
Results and discussion

3-Acetylcoumarin-2-one **3** was prepared and was allowed to react with malononitrile, benzaldehyde and/or 3-chlorobenzaldehyde in the presence of ammonium acetate and acetic acid under reflux to give the corresponding 2-amino-6-(2-oxo-2H-chromen-3-yl)-4-phenylnicotino-nitrile **4a**¹⁸ or 2-amino-4-(3-chloro-phenyl)-6-(2-oxo-2H-chromen-3-yl)nicotinonitrile **4b** (Scheme 1).

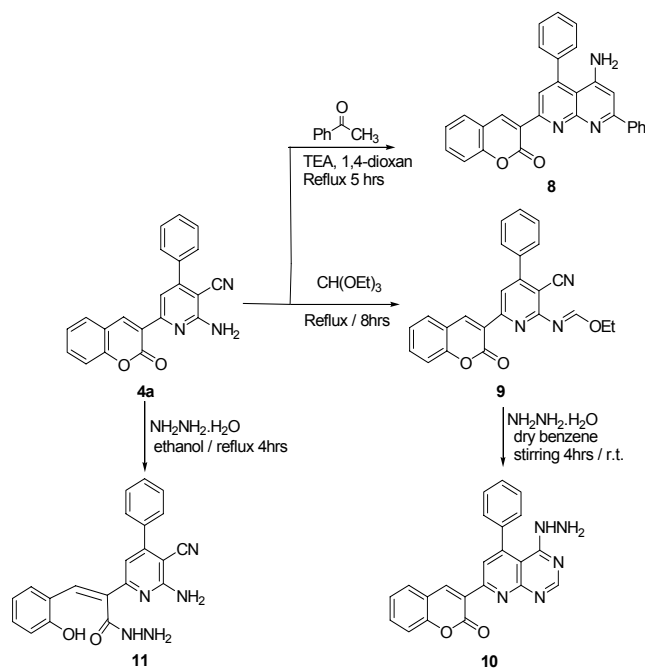


Scheme 1

Continually, compound **4a** was condensed with cyclohexanone in the presence of anhydrous zinc chloride to give the corresponding 3-(5-amino-4-phenyl-6,7,8,9-tetrahydrobenzo[*b*][1,8]naphthyridin-2-yl)-2H-chromen-2-one **5**. The synthesis of 7-(2-oxo-2H-chromen-3-yl)-5-phenylpyrido[2,3-*d*]pyrimidin-4(3*H*)-one **6** was achieved by the reaction of compound **4a** with formic acid. Treatment of compound **4a** with acetic anhydride in the presence of phosphoric acid underwent cyclization affording 4-amino-7-(2-oxo-2H-chromen-3-yl)-5-phenyl-1,8-naphthyridin-2(1*H*)-one **7** (Scheme 2).



Scheme 2



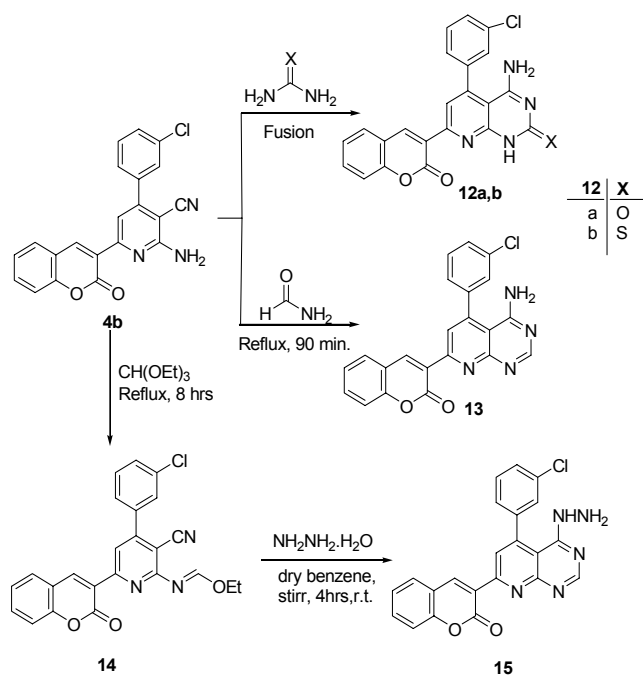
Scheme 3.

Table 1. The antitumor activity of compounds **7**, **8**, **16** and **17** against breast carcinoma cell line (MCF-7)

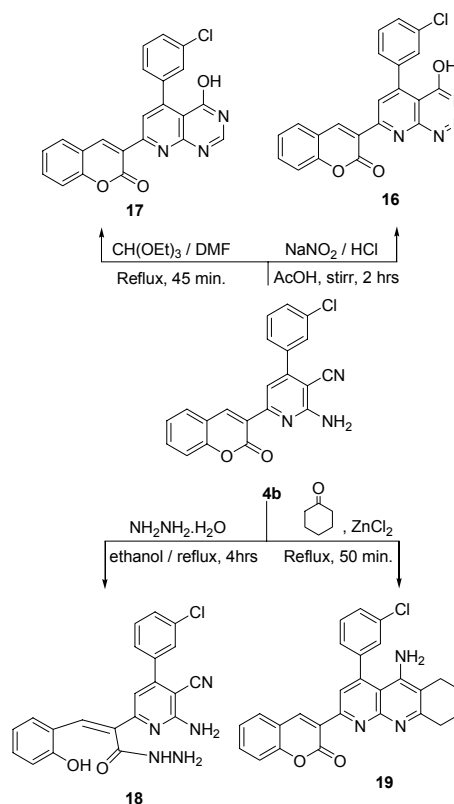
Compound	Viability rate (%)			IC ₅₀ (mg mL ⁻¹)
	0.1 µg mL ⁻¹	1 µg mL ⁻¹	10 µg mL ⁻¹	
7	54.22 ± 6.42	50.06 ± 4.87	46.49 ± 4.20	56.34 ± 4.82
8	77.58 ± 4.36	72.43 ± 4.36	68.30 ± 8.63	14.32 ± 2.58
16	80.27 ± 10.63	83.46 ± 8.69	70.19 ± 6.48	28.50 ± 2.46
17	62.34 ± 4.38	58.28 ± 7.56	52.39 ± 8.69	2.32 ± 3.87

Also cyclization of compound **4a** with acetophenone in the presence of triethylamine yielded 3-(5-amino-4,7-diphenyl-1,8-naphthyridin-2-yl)-2*H*-chromen-2-one **8**. The condensation of compound **4a** with triethylorthoformate gave ethyl-N-3-cyano-6-(2-oxo-2*H*-chromen-3-yl)-4-phenylpyridine-2-yl formimidate **9** which reacted with hydrazine hydrate under reflux giving compound **10**. On the other hand, when compound **4a** reacted with hydrazine hydrate, the coumarin ring opened to obtain the corresponding compound 2-(6-amino-5-cyano-4-phenylpyridin-2-yl)-3-(2-hydroxyphenyl)acryloylhydrazide **11** (Scheme 3).

While compound **4b** underwent cyclization upon treatment with urea and/or thiourea giving 4-amino-5-(3-chlorophenyl)-7-(2-oxo-2*H*-chromen-3-yl)pyrido-[2,3-*d*]pyrimidin-2(1*H*)-one **12a** and 3-(4-amino-5-(3-chlorophenyl)-2-thioxo-1,2-dihydropyrido[2,3-*d*]pyrimidin-7-yl)-2*H*-chromen-2-one **12b**. Cyclization of compound **4b** also can be achieved by allowing to react with formamide to afford 3-(4-amino-5-(3-chlorophenyl)pyrido[2,3-*d*]pyrimidin-7-yl)-2*H*-chromen-2-one **13**. By the same way, compound **4b** reacted with triethylorthoformate to yield compound **14** which underwent further cyclization upon treatment with hydrazine hydrate at room temperature affording 3-(5-(3-chlorophenyl)-4-hydrazinylpyrido-[2,3-*d*]pyrimidin-7-yl)-2*H*-chromen-2-one **15** (Scheme 4).

**Scheme 4**

Diazotization of compound **4b** with sodium nitrite and conc. Hydrochloric acid in the presence of acetic acid led to formation of 3-(5-(3-chlorophenyl)-4-hydroxypyrido[2,3-*d*][1,2,3]triazin-7-yl)-2*H*-chromen-2-one **16**. The reaction of compound **4b** with triethylorthoformate in the presence of dimethylformamide underwent cyclization yielding compound **17** and the structure was established by infrared spectrum revealed no absorption in the CN region, furthermore, it displayed absorption bands at (3448-3400cm⁻¹) as a broad band (NH₂, OH). By the same way compound **4b** reacted with hydrazine hydrate and cyclohexanone to give compounds **18**, **19**, respectively (Scheme 5).

**Scheme 5**

Antitumor activity

The potential cytotoxicity activity of compounds **7**, **8**, **16** and **17** was tested against breast carcinoma cell line (MCF-7) by SRB (Sulphorhodamine-B) assay. Results are given in concentrations that were able to cause 50% of cell growth inhibition (GI₅₀) after a continuous exposure of 48 h and show means ± SEM of three-independent experiments performed in duplicate.

References

- ¹Pechmann, V. H., Duisberg, C., *Chem. Ber.*, **1884**, 17, 929.
- ²Johnson, J. R., *Org. React.*, **1942**, 1, 210.
- ³Brufola, G., Fringuelli, F., Piermatti, O., Pizzo, F., *Heterocycles*, **1996**, 43, 1257.
- ⁴Shirner, R. L., *Org. React.*, **1942**, 1, 1.
- ⁵Yavari, I., Hekmat, S. R., Zonouzi, A., *Tetrahedron Lett.*, **1998**, 39, 2391.
- ⁶Cairns, N., Harwood, L. M., Astles, D. P., *J. Chem. Soc., Perkin Trans.*, **1994**, 1, 3101. Cartwright, G. A., McNab, W., *J. Chem. Res.*, **1997**, S, 296.
- ⁷Weber, U. S., Steffen, B., Siegers, C. P., *Res. Commun. Mol. Pathol. Pharmacol.*, **1998**, 99, 193.
- ⁸Patil, A. D., Freyer, A. J., Drake, S. E., Haltiwanger, R. C., Bean, M. F., Taylor, P. B., Caranfa, M. J., Breen, A. L., Bartus, H. R., Johnson, R. K., Hertzberg, R. P., Westley, J. W., *J. Med. Chem.*, **1993**, 36, 4131.
- ⁹Yun, B. S., Lee, I. K., Ryoo, I. J., Yoo, I. D., *J. Nat. Prod.*, **2001**, 64, 1238.
- ¹⁰Zaha, A. A., Hazem, A., *Microbiologica.*, **2002**, 25, 213.
- ¹¹Maly, D. J., Leonetti, F., Backes, B. J., Dauber, D. S., Harris, J. L., Craik, C. S., Ellman, J. A., *J. Org. Chem.*, **2002**, 67, 910.
- ¹³Heravi, M. M., Sadjadi, S., Oskooie, H. A., Shoar, R. H., Bamoharram, F. F., *Catal. Commun.*, **2008**, 9, 470–474.
- ¹⁴Campaigne, E., *Compr. Heterocycl. Chem.*, **1984**, 4, 863.
- ¹⁵Skehan, P., Storeng, R., Scudiero, D., Monks, A., McMahon, J., Vistica, D., Warren, J. T., Bokesch, H., Kenny, S., Boyd, M. R., *J. Natl. Cancer Inst.*, **1990**, 82, 1107.
- ¹⁶Monks, A., Scudiero, D., Skehan, P., Shoemaker, R., Paul, K., Vistica, D., Hose, C., Langley, J., Cronise, P., Vaigro-Wolff, A., Gray-Goodrich, M., Campbell, H., Mayo, J., Boyd, M., *J. Natl. Cancer Inst.*, **1991**, 83, 757-776.
- ¹⁷Campbell, M., Mayo, H., Boyd, J., *J. Natl. Cancer Inst.*, **1991**, 83, 757.
- ¹⁸Zhou, J. F., Gong G. X., Zhu, F. X., Zhi, S. J., *Chin. Chem. Lett.*, **2009**, 20, 37-39.

Received: 20.04.2015.

Accepted: 14.06.2015.



CRYSTAL STRUCTURE OF BIS(O-AMYLDITHIOCARBONATO)BIS(3-BROMOPYRIDINE)NICKEL(II)

Gurvinder Kour^[a], Neerupama^[b], Renu Sachar^[b] and Rajni Kant^{[a]*}

Keywords: xanthates, crystal structure, direct methods, interactions, octahedral.

The complex crystallizes in orthorhombic crystal system with space group *Pbca*. The unit cell parameters are: $a=12.346(15)$ Å, $b=9.0931(9)$ Å, $c=25.136(5)$ Å, $Z=4$. The asymmetric unit comprises of half molecule with nickel(II) cation lies on an inversion centre. The Ni(II) atom is coordinated in a distorted octahedral arrangement. The variation in C–S bond lengths involving the xanthate ligands indicates the presence of double bond character due to delocalization over the two C–S bonds. The crystal structure was refined to a final reliability index (R-value) of 0.0594 for 1714 observed reflections. The amyl chain attached to the dithiocarbonato group contains disorder over two sets of sites with occupancy ratios of 0.683: 0.317. The crystal structure is stabilized by weak C–H... π interactions.

* Corresponding Authors

Fax: +91 191 243 2051

E-Mail: rkant.ju@gmail.com

- [a] X-ray Crystallography Laboratory, Post-Graduate Department of Physics & Electronics, University of Jammu, Jammu Tawi - 180 006, India.
[b] Department of Chemistry, University of Jammu, Jammu Tawi - 180 006, India.

3-bromopyridine (0.82 g, 0.0052 mol) was added. The mixture was stirred for two to three hours and kept undisturbed for one to two days when dark green colored micro-crystals of the adduct were obtained. The product so obtained was filtered and dried in vacuum desiccator over anhydrous calcium chloride. Chemical structure of the complex is shown in Figure 1.

Introduction

Dithiocarbonates are sulfur and oxygen containing ligands which can form complexes with various transition metals through the mechanism of coordinated complex formation. Transition metal dithiolate complexes exhibited versatile and interesting chemistry that have been studied extensively during the last decades.¹ Xanthates can form bidentate, monodentate, or network solids, showing a wide range of coordination behaviour.²⁻⁵ Metal xanthates are extensively used as corrosion inhibitors⁶ and agricultural reagents.^{7,8} Dithiocarbonates have also found important use in medicine as antitumor agents^{9,10} and for treating Alzheimer's disease.¹¹ Nickel thiolate complexes have received special attention in recent years because sulfur-ligated nickel complexes mimic the [Fe–Ni] hydrogenase active site and dimeric metal complexes based on nickel thiolate hydrides have been shown to be catalytically active for proton reduction.¹²

Experimental

Synthesis

Bis(O-amyldithiocarbonato)nickel(II) required for preparation of the adduct was obtained by mixing aqueous solutions of potassium salt of O-amyldithiocarbonate (4.04 g, 0.02 mol) and $\text{NiCl}_2 \cdot 6\text{H}_2\text{O}$ (2.37 g, 0.01 mol). The precipitates of bis(O-amyldithiocarbonato)nickel(II) were formed which were filtered immediately and dried in vacuum desiccators. Bis(O-amyldithiocarbonato)nickel(II) (1 g, 0.0026 mol) was then dissolved in acetone (60 ml) and stirred for about 10-20 minutes. To the resulting solution,

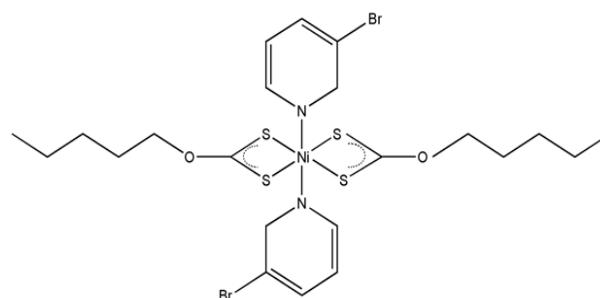


Figure 1. Chemical structure of bis(O-amyldithiocarbonato)bis(3-bromopyridine)nickel(II)

Crystal structure determination and refinement

A green block shaped single crystal having good morphology (0.3 x 0.2 x 0.1 mm) was chosen for three-dimensional X-ray intensity data collection using X'calibur CCD area-detector diffractometer equipped with graphite monochromated Mo K_α radiation ($\lambda = 0.71073$ Å). The crystal selection was made by Leica polarizing microscope. The diffractometer provides reflections of a large number of individual planes and their corresponding intensities were recorded electronically with the help of a CCD camera. The unit cell dimensions were determined by least squares fit of angular settings of 1597 reflections in the θ range 3.99 to 27.85°. A total of 7072 reflections were recorded for θ ranging from 3.64 to 25.98° and out of these reflections, 2754 were found unique. 1714 reflections were treated as observed ($-15 \leq h \leq 14$, $-11 \leq k \leq 10$, $-15 \leq l \leq 31$) using ($I > 2\sigma(I)$) as criterion. Data were corrected for Lorentz-polarization, extinction and multi-scan absorption corrections.

The structure was solved by direct methods using SHELXS97.¹³ All non-hydrogen atoms of the molecule were located from the E-map. Full-matrix least-squares refinement was carried out by using SHELXL97 software.¹³ The geometry of the molecule is determined by PLATON.¹⁴ All H atoms were positioned geometrically and were treated as riding on their parent C atoms, with C-H distances of 0.93–0.97 Å; with $U_{\text{iso}}(\text{H}) = 1.2U_{\text{eq}}(\text{C})$, except for the methyl group where $U_{\text{iso}}(\text{H}) = 1.5U_{\text{eq}}(\text{C})$. The final refinement cycles yielded an *R*-factor of 0.0594 ($wR(F^2) = 0.1195$) for the observed data. The residual electron density ranges from -0.62 to 0.59 eÅ⁻³.

Atomic scattering factors were taken from International Tables for X-ray Crystallography (1992, Vol. C, Tables 4.2.6.8 and 6.1.1.4). The crystallographic data are summarized in Table 1. CCDC – 1061096 contains the supplementary crystallographic data for this paper.

Table 1: Crystal data and other experimental details

CCDC Number	1061096
Crystal description	Block
Crystal size	0.30 x 0.20 x 0.10 mm
Empirical formula	C ₂₂ H ₃₀ Br ₂ N ₂ NiO ₂ S ₄
Formula weight	701.25
Radiation, Wavelength	Mo K α , 0.71073 Å
Unit cell dimensions	$a = 12.346(15)$ Å, $b = 9.0931(9)$ Å, $c = 25.136(5)$ Å, $\alpha = \beta = \gamma = 90^\circ$
Crystal system, Space group	Orthorhombic, <i>Pbca</i>
Unit cell volume	2821.9(7) Å ³
No. of molecules per unit cell, <i>Z</i>	4
Absorption coefficient	3.838 mm ⁻¹
<i>F</i> (000)	1416
θ range for entire data collection	$3.99 < \theta < 27.85^\circ$
Reflections collected / unique	7072 / 2754
Reflections observed $I > 2\sigma(I)$	1714
Range of indices	$h = -15$ to 14, $k = -11$ to 10, $l = -15$ to 31
No. of parameters refined	158
Final <i>R</i> -factor	0.0594
$wR(F^2)$	0.1195
<i>R</i> _{int}	0.0496
<i>R</i> _{sigma}	0.0753
Goodness-of-fit	1.096
(Δ/σ) _{max}	0.001
Final residual electron density	-0.62 < $\Delta\rho$ < 0.59 e Å ⁻³

Results and discussion

The X-ray crystal structure analysis reveals that the Ni atom lies on a crystallographic center of symmetry and has octahedral coordination geometry. An ORTEP¹⁵ view of the molecule with atomic labeling is shown in Figure 2. Its geometry was calculated using the PLATON¹⁴ and PARST¹⁶ software. The Ni atom is six-coordinated by the tertiary N donor atom of two bromopyridine molecules (situated axially intranspositions, N–Ni–N=180°) and four S atoms of two coordinated dithiocarbonato ligands which are situated

in the equatorial plane. The Ni atom is located on a centre of inversion. The Ni–S bond lengths involving the xanthates ligands are 2.4484(16) Å for Ni–S1 and 2.4418(18) Å for Ni–S2 and these values of bond distances are in good agreement with those reported for other analogous Ni-dithiocarbonato complexes.^{17–19} Selected bond lengths and bond angles are given in Table 2.

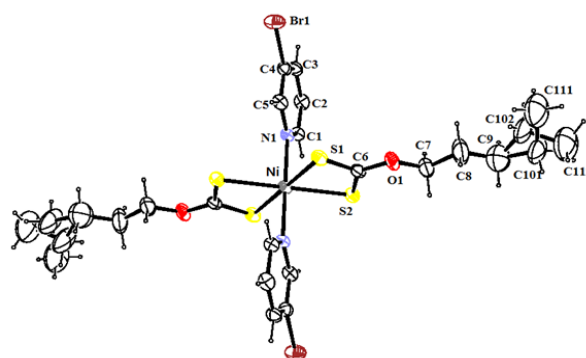


Figure 2. ORTEP plot of the molecule with 40% probability thermal ellipsoids

The dihedral angle between the pyridine ring and the four planar atoms Ni/S1/C6/S2 is 84.57(14)°. The mean value of C_{ar}=N (pyridine) distance is 1.356(7) Å. The sum of the bond angles [C5–N1–Ni, C1–N1–Ni, C5–N1–C1] around N1 is 360.00(13)° indicating sp² hybridization. The C–S bond lengths involving the xanthate ligands are: C6–S1 = 1.681(7) Å and C6–S2 = 1.684(7) Å. These values are approximately same and shows a double bond character due to delocalization over the two C–S bonds.²⁰ As a consequence of the hybridization of the carbon atom, the O1–C6 bond has a distance [1.317(7) Å] shorter than that of O1–C7 [1.438(9) Å].

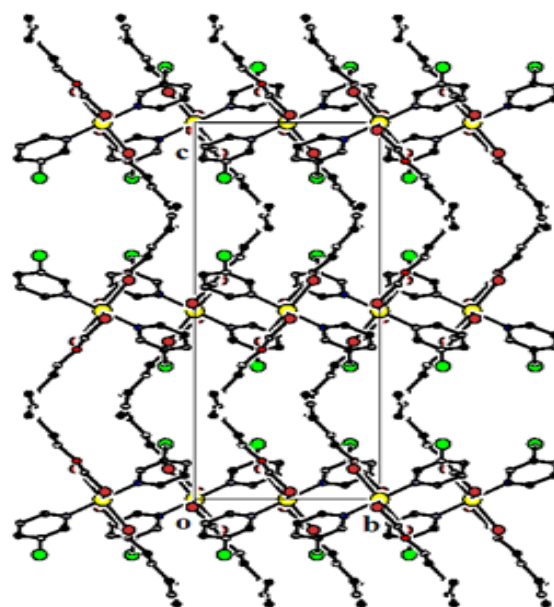


Figure 3. The crystal packing of the complex viewed down a-axis

Table 2. Selected bond lengths (Å) and bond angles (°) for non hydrogen atoms (e.s.d.'s are given in parentheses)

Bond lengths, Å		Bond angles, °	
Ni-N1	2.117(5)	N1-Ni-N1 ⁱ	180.0(1)
Ni-S1	2.448(2)	N1-Ni-S2	88.5(1)
Ni-S2	2.442(2)	N1-Ni-S1	89.9(1)
C6-O1	1.317(7)	N1 ⁱ -Ni-S2	91.5 (1)
O1-C7	1.438(9)	N1-Ni-S2 ⁱ	91.5 (1)
S1-C6	1.681(7)	N1 ⁱ -Ni-S2 ⁱ	88.5(1)
S2-C6	1.684(7)	C5-N1-Ni	120.6 (4)
Br1-C4	1.887(6)	C1-N1-C5	118.0(5)
		C1-N1-Ni	121.4(4)

The short value of bond distance for O1–C6 is consistent with a significant contribution of the resonance form of the xanthate anion that features a formal C=O and a negative charge on each of S atom.²¹ The Br–C4 bond length of 1.887(6) Å is comparable with those reported for related structures.^{22,23} The amyl chain attached to the dithiocarbonato group contains disorder over two sets of sites with occupancy ratios of 0.683: 0.317.

The crystal structure is stabilized by weak C-H... π interactions. Details of the geometry of C-H... π interactions are given in Table 3. Crystal packing viewed down the a-axis (Figure 3) shows that the molecules are stacked in parallel layers forming a zig-zag pattern along bc-plane.

Table 3. Geometry of intra and inter molecular hydrogen bonds

D-H...A	D-H, Å	H...A, Å	D...A, Å	θ [D-H...A], °
C8-H8B...Cg1 ⁱ	0.97	3.031	3.764	133

Symmetry codes: (i) $\frac{1}{2}+x, \frac{1}{2}-y, -z$; Cg1 represents center of gravity of pyridine ring (N1/C1/C2/C3/C5/C5)

Acknowledgements

One of the authors (Rajni Kant) acknowledges the Indian Council of Medical Research, New Delhi for research funding under research project no. BIC/12(14)/2012. And also the Department of Science & Technology for single crystal X-ray diffractometer as a National Facility under Project No. SR/S2/CMP-47/2003.

References

- Gorgulu, A. O., Celikkan, H., and Arslan, M., *Acta Chim. Slov.*, **2009**, 56(2), 334.
- Winter, G., *Rev. Inorg. Chem.*, **1980**, 2, 253.
- Tiekink, E. R. T. and Winter, G., *Rev. Inorg. Chem.*, **1992**, 12, 183.
- Hoskins, B. F. and Pannan, C. D., *J. Chem. Soc., Chem. Comm.*, **1975**, 11, 408.
- Dakternieks, D., Di Giacomo, R., Gable, R.W. and Hoskins, B.F., *J. Amer. Chem. Soc.*, **1988**, 110(20), 6762.
- Scendo, M., *Corr. Sci.*, **2005**, 47(7), 1738.
- Doane, W. M., Shasha, B. S. and Russel, C. R., *Controlled Releases. Pestic.*, **1977**, 53, 74.
- Orts, W. J., Sojka, R. E. and Glenn, G. M., *Agro Food Ind. Hi-Tech*, **2002**, 13(4), 37.
- Larsson, A.-C. and Oberg, S., *J. Phys. Chem., A*, **2011**, 115(8), 1396.
- Adibhatla, R. M., Hatcher, J. F. and Gusain, A., *Neurochem. Res.*, **2012**, 37, 671.
- Perluigi, M., Joshi, G., Sultana, R., et al., *Neuroscience*, **2006**, 138(4), 1161.
- Han, Z., McNamara, W. R., Eum, M., Holland, P. L. and Eisenberg, R., *Angew. Chem. Int. Ed.*, **2012**, 51, 1667.
- Sheldrick, G. M., *Acta Cryst.*, **2008**, A64, 112.
- Spek, A. L., *Acta Cryst.*, **2009**, D65, 148.
- Farrugia, L. J., *J. Appl. Cryst.*, **2012**, 45, 849.
- Nardelli, M., *J. Appl. Cryst.*, **1995**, 28, 659.
- Kant, R., Kour, G., Anthal, S., Neerupama & Sachar, R., *Acta Cryst.*, **2015**, E71, m12.
- Kapoor, S., Sachar, R., Singh, K., Gupta, V. K., and Rajnikant, J., *Chem. Cryst.*, **2012**, 42, 222.
- Kaur, I., Singh, K., Kaur, G., Sachar, R., Gupta, V K & Kant, R., *J. Crystallogr.*, **2014**, 1.
- Jiang, X. H., Zhang, W. G., Zhong, Y., and Wang, S.L., *Molecules*, **2002**, 7, 549.
- Alam, N., Ehsan, M.A., Zeller, M., Mazhar, M., and Arifin, Z., *Acta Cryst.* **2011**, E67, m1064.
- Hemamalini, M. and Fun, H. K., *Acta Cryst.*, **2010**, E66, o663.
- Lu, Y. B. and Jian, F. M., *Acta Cryst.*, **2012**, E68, m101.

Received: 19.05.2015.

Accepted: 16.06.2015.



PATHWAYS FOR THE SYNTHESIS OF PYRIMIDINE AND PYRAN BASED HETEROCYCLIC DERIVATIVES: A CONCISE REVIEW

Ayaz Mahmood Dar^{[a]*} and Shamsuzzaman^[a]

Keywords: heterocycles, pyrimidines, pyrans, diethyl malonate, malononitrile.

Pyrimidines and pyrans are the special class of heterocyclic compounds with a broad spectrum of biological activities such as anticancer, antiviral, antibacterial, antioxidant, antiallergic and antidepressant. The use of pyran derivatives is not only limited in cosmetics, pigments and biodegradable agrochemicals but also constitute a structural unit of many natural products. Therefore researchers have synthesized these condensed heterocycles through different complex pathways as target structures for biological studies. This review focuses on the various strategies followed for the convenient synthesis of pyrimidine and pyran based heterocyclic compounds. The steps included condensation followed by cyclization or MCR, either in a step-wise manner or in one pot has been achieved successfully to obtain these two classes of heterocycles under different conditions. Diethyl oxalate, diethyl malonate, malononitrile and ethyl cyanoacetate are the most common reagents used for the synthesis of pyrimidines and pyrans appended on different heterocyclic skeletons.

* Corresponding Authors

E-Mail: ayazchem09@gmail.com

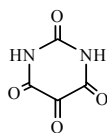
[a] Department of chemistry, Aligarh Muslim University, Aligarh 202002 India

Introduction

Polyfunctionalized heterocyclic compounds play important roles in the drug discovery process and analysis of drugs in late development or in the market shows that 68 % of them are heterocycles.^{1,2} hence it is not surprising that research on the synthesis of polyfunctionalized heterocyclic compounds has received significant attention in the recent years. Pyrimidine or 1,3-diazine (1) is a 6-membered aromatic heterocycle with two nitrogen atoms in the ring at 1,3-positions.³ It may be regarded as being derived from benzene by the replacement of two *meta* "CH" groups by "N". The pyrimidine ring system has wide occurrence in nature as substituted and fused ring derivatives, like the nucleotides, thiamine and alloxan (2).⁴ It is also found in many synthetic compounds such as barbiturates and the HIV drug, Zidovudine.



(1)



(2)

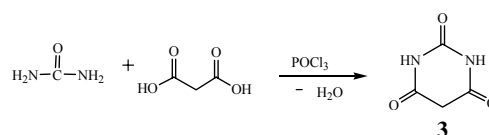
Its derivatives have been known to display a wide range of pharmacological activities as regards the tyrosine kinase domain of epidermal growth factor receptor,⁵ 5-phosphoribosyl-1-pyrophosphate synthetase⁶ and dihydrofolate reductase⁷ have been fully demonstrated. Numerous reports delineate the antitumour, antiviral, antioxidant and hepatoprotective activity of these compounds.⁸⁻¹¹ Similarly, in recent years, considerable attention has been focused on the development of new methodologies to synthesize many kinds of pyrazole based

pyrimidine ring system.¹² Indeed, these compounds are, by now widely recognized as important organic materials showing interesting biological activities.¹³ In addition, these fused heterocyclic systems like pyrazolopyridopyrimidines, pyrazoloquinolines and pyrazolopyridines present the interesting biological properties such as virucidal, anticancer, fungicidal, bactericidal and vasodilatory activities.¹⁴

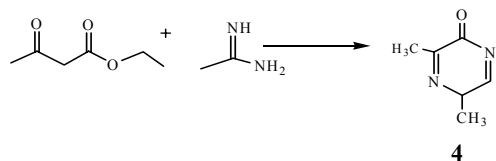
The pyrimidine heterocyclic core is an important subunit because of its widespread abundance in the basic structure of numerous natural products.¹⁵ A number of synthetic pharmacophores based upon the pyrimidyl structure exhibit antibacterial, anticancer, anti-HIV-1 and antirubella virus activities.¹⁶⁻¹⁸ The fused pyrimidine ring systems containing substituted six-membered ring have been proved to have cytotoxic nature^{19,20} and the reason for the bio-toxicity of the pyrimidine heterocycles may be attributed to the presence of a subunit such as >N-CS-N<.²¹ As such the development of clinically useful anticancer drug (5-fluorouracil)²² and antiviral drugs (AZT, DDI, BVDU)²³⁻²⁵ has renewed the interest in the synthetic manipulation of pyrimidine derivatives.²⁶ Here in we report the different strategies including cyclization, multi component reaction, reduction and oxidation approaches for the synthesis of pyrimidine and pyran based heterocycles.

Synthesis of pyrimidine derivatives

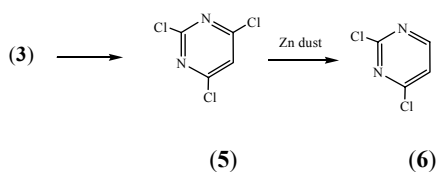
Although pyrimidine derivatives such as uric acid and alloxan were known in the early 19th century, a laboratory synthesis of a pyrimidine was not carried out until 1879,⁴ when Grimaux²⁷ reported the preparation of barbituric acid (3) from urea and malonic acid in the presence of phosphorus oxychloride.



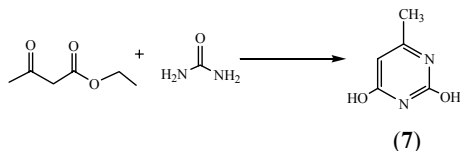
The systematic study of pyrimidines began in 1884 with Pinner²⁸ who synthesized 3,5-dimethyl-5H-pyrazin-2-one (**4**) by condensing ethyl acetoacetate with acetamidine. Pinner²⁹ first proposed the name “pyrimidin” in 1885 which later got modified as “pyrimidine”.



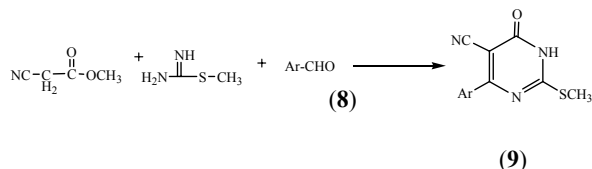
Gabriel and Colman³⁰ in 1900 reported the conversion of barbituric acid (**3**) into trichloropyrimidine (**5**) by POCl₃. The compound (**5**) upon selective reduction yielded dichloropyrimidine (**6**).



Benhard³¹ reported the reaction of ethyl acetoacetate with urea that yielded a pyrimidine derivative (4-methyluracil) (**7**) in better amounts.

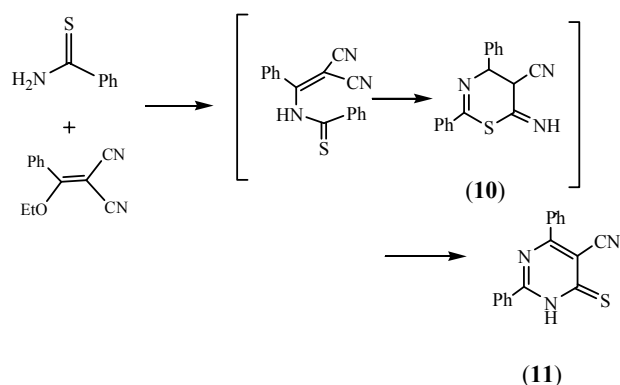


Hussain and co-workers³² reported that heating the mixture of methyl cyanoacetate, S-methyl isothiurea and aldehydes (**8a-d**) yielded corresponding 4-aryl-5-cyano-2-methylthio-6-oxypyrimidine derivatives (**9a-d**).

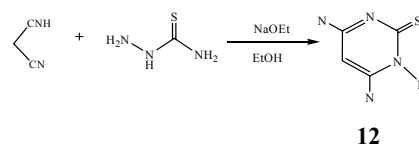


Ar: (a) C₆H₅, (b) *p*-NO₂-C₆H₄, (c) *o*-CH₃O-C₆H₄, (d) *o*-NO₂-C₆H₄

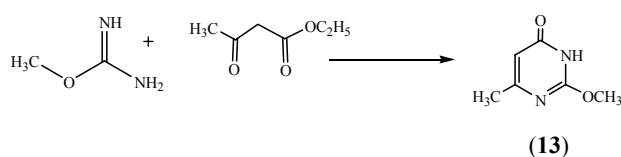
Soto and co-workers³³ reported the reaction of thiobenzamide with 3-ethoxy-3-phenyl-2-cyanoacrylonitrile (**10**) in presence of sodium isopropoxide in 2-propanol to afford 5-cyano-2,6-diphenyl-4-thioxo-3,4-dihydro-pyrimidine (**11**) through formation of the 3-phenyl-2-cyano-3-thiobenzamide acrylonitrile as an intermediate.



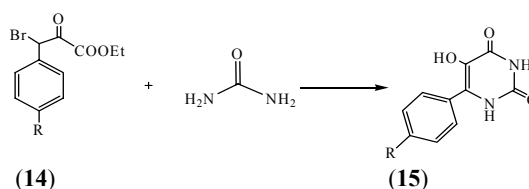
Taylor and Morrison³⁴ reported the synthesis of 1,4,6-triamino-2(2H)-pyrimidine-2-thione (**12**) by reacting malononitrile with thiosemicarbazide in presence of sodium ethoxide in ethanol.



Botta and co-workers³⁵ reported the synthesis of 2-methoxy-6-methyl-3(2H)-pyrimidin-4-one (**13**) after reacting ethyl acetoacetate and O-methylisourea in an aqueous medium.

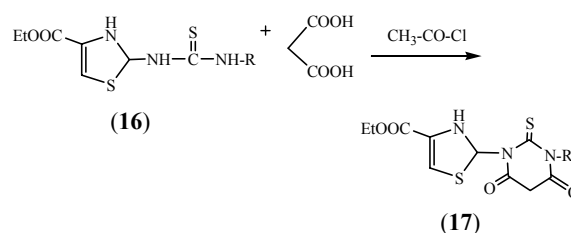


Andereichikov and co-workers³⁶ reported the synthesis of uracil derivatives (**15a-d**) by the reaction of aryl substituted bromopyruvate esters (**14a-d**) with urea.



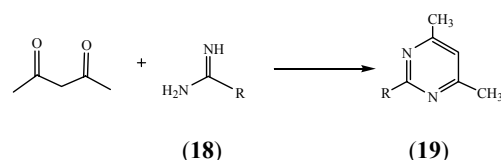
R: (a) OCH₃, (b) OH, (c) Cl, (d) H

El-Subbagh³⁷ reported the synthesis of pyrimidine derivative (**17a,b**) by reacting thiazolyl thiourea derivatives (**16a,b**) with malonic acid in the presence of acetyl chloride.



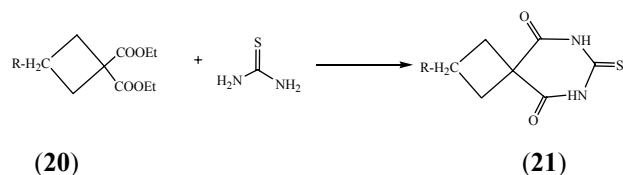
R: (a) CH₃, (b) C₂H₅

Bowman and co-workers³⁸ reported that acetyl acetone condensed with acetamidine derivatives (**18a-e**) and gave corresponding pyrimidine derivatives (**19a-e**) in good yields.



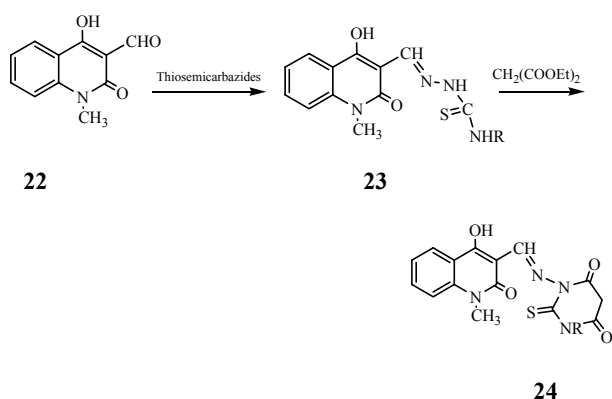
R: (a) NH-C₆H₅, (b) SH, (c) NH-C₆H₄CH₃, (d) NHHN.NO₂, (e) C₂H₅

Yossef and co-workers³⁹ reported the reaction of 1,1-cycloalkane dicarboxylic acid diethyl esters (**20a-c**) with thiourea which gave *spiro*-barbituric acid derivatives (**21a-c**).

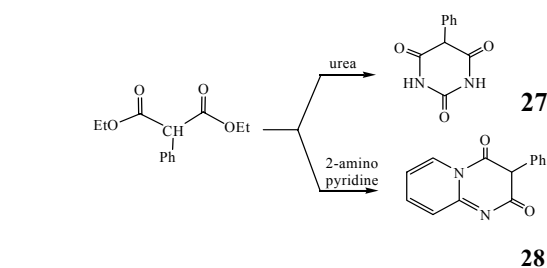


R: (a) CH_3 , (b) C_2H_5 , (c) isopropyl

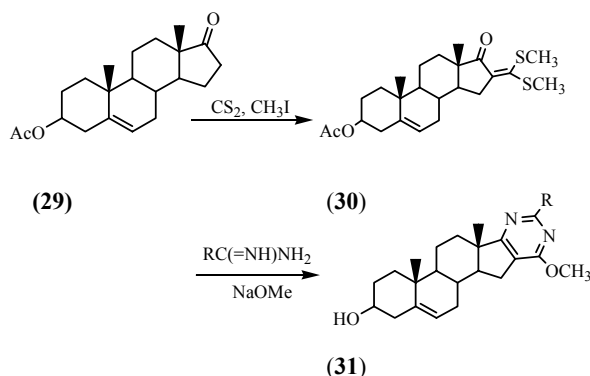
Mohamed⁴⁰ reported the reaction of 1,2-dihydro-4-hydroxy-1-methyl-2-oxoquinoline-3-carbaldehyde (22) with thiosemicarbazides to yield desired thiosemicarbazones (23a-d). These thiosemicarbazones then reacted with diethyl malonate which resulted into corresponding pyrimidine derivatives (24a-d) in good yields.



R: (a) H, (b) C_6H_5 , (c) $p\text{-CH}_3\text{OC}_6\text{H}_4$, (d) $\text{H}_2\text{C}=\text{CH}-\text{CH}_2$

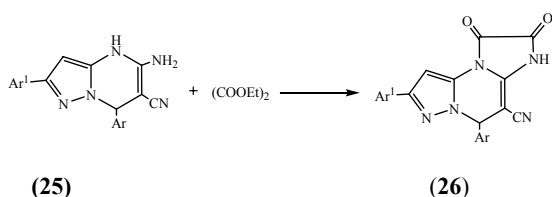


Peseke and co-workers⁴³ reported the reaction of androst-5-en-17-one (29) with CS_2 and CH_3I that yielded 3 β -acetoxy-16-[[bis(methylthio)methylene]androst-5-en-17-one (30) which later reacted with different amidines in presence of sodium methoxide to provide corresponding steroidal pyrimidine derivatives (31a-e).



R: (a) H, (b) C_2H_5 , (c) C_6H_5 , (d) NH_2 , (e) OCH_3

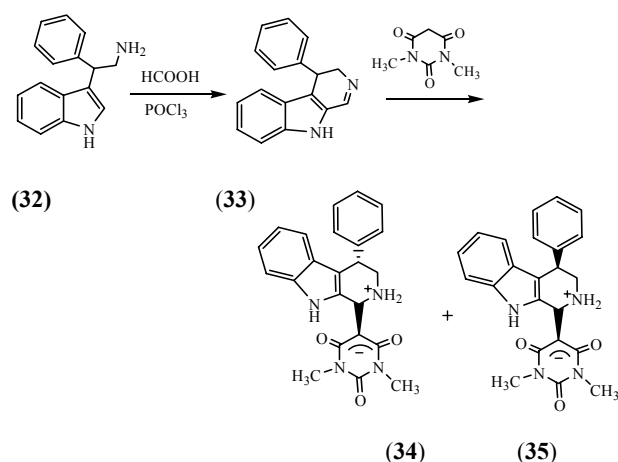
Eldin and Attaby⁴¹ reported the reaction of pyrazole[3,2-b]pyrimidine derivatives (25a-p) with diethyl oxalate which yielded imidazo[1,2:3',4']pyrazole[3,2-b]pyrimidine derivatives (26a-p) in good yields.



Ar, Ar¹: (a) C_6H_5 , C_6H_5 , (b) $p\text{-Cl-C}_6\text{H}_4$, C_6H_5 (c) $p\text{-CH}_3\text{OC}_6\text{H}_4$, C_6H_5 , (d) $p\text{-O}_2\text{NC}_6\text{H}_4$, C_6H_5 , (e) $\text{C}_4\text{H}_3\text{O-}\alpha$, C_6H_5 , (f) $\text{C}_4\text{H}_3\text{S-}\alpha$, C_6H_5 , (g) C_6H_5 , $p\text{-CH}_3\text{C}_6\text{H}_4$, (h) $p\text{-ClC}_6\text{H}_4$, $p\text{-CH}_3\text{C}_6\text{H}_4$, (i) $p\text{-CH}_3\text{OC}_6\text{H}_4$, $p\text{-CH}_3\text{C}_6\text{H}_4$, (j) $p\text{-NO}_2\text{C}_6\text{H}_4$, $p\text{-CH}_3\text{C}_6\text{H}_4$, (k) $\text{C}_4\text{H}_3\text{O-}\alpha$, $p\text{-CH}_3\text{C}_6\text{H}_4$, (l) $\text{C}_4\text{H}_3\text{S-}\alpha$, $p\text{-CH}_3\text{C}_6\text{H}_4$, (m) C_6H_5 , $p\text{-BrC}_6\text{H}_4$, (n) $p\text{-ClC}_6\text{H}_4$, $p\text{-BrC}_6\text{H}_4$, (o) $p\text{-CH}_3\text{OC}_6\text{H}_4$, $p\text{-BrC}_6\text{H}_4$, (p) $\text{C}_4\text{H}_3\text{O-}\alpha$, $p\text{-BrC}_6\text{H}_4$.

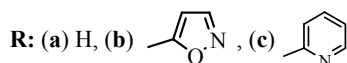
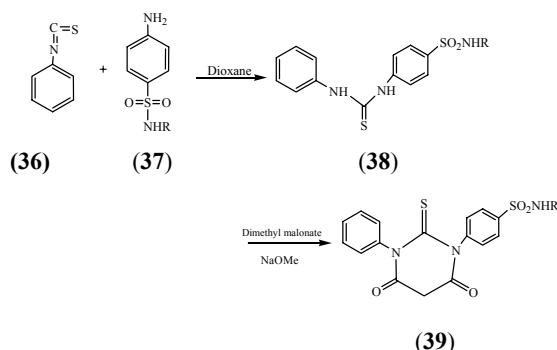
Stadlbauer and co-workers⁴² reported the reaction of diethyl malonate with urea and 2-aminopyridine which gave barbituric acid derivative (27) and pyrido[1,2-a]pyrimidine-2,4-dione derivative (28), respectively in better yields.

Semenov *et al.*⁴⁴ reported the reaction of β -phenyl-tryptamine (32) with formic acid under Bischler-Napieralski conditions that yielded 4-phenyl-3,4-dihydro- β -carboline (33) which upon reaction with 1,3-dimethylbarbituric acid provided two diastereomers of substituted pyrimidinones [34 (RR), 35 (RS)].

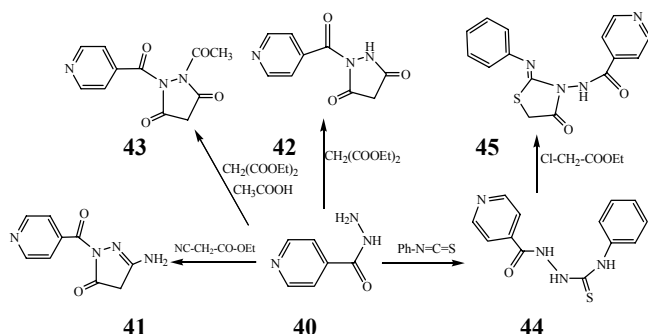


Bawazir and co-workers⁴⁵ reported the reaction of phenylisothiocyanate (36) with sulfa drugs (37a-c) in 1,4-dioxane that yielded N,N'-disubstituted thiourea derivatives

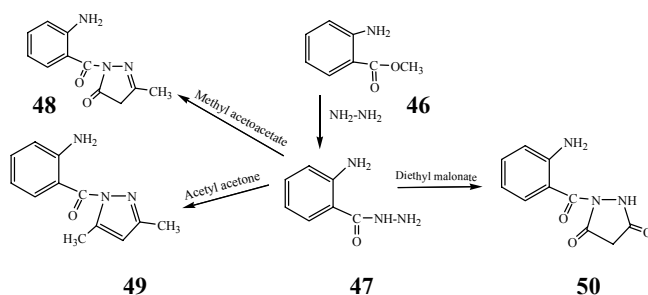
(38a-c) which later on reaction with dimethyl malonate in presence of sodium methoxide provided corresponding 1,3-disubstituted thiobarbituric acid derivatives (39a-c).



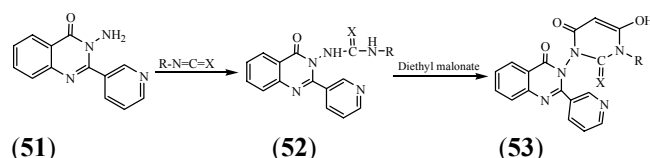
Parashar and co-workers⁴⁶ reported the reaction of isonicotinohydrazide (40) with ethyl cyanoacetate, diethyl malonate, diethyl malonate with acetic acid and phenylisothiocyanate, which gave 3-amino-1-isonicotinoyl-1H-pyrazol-5(4H)-one (41), 1-isonicotinoyl-pyrazolidine-3,5-dione (42), 1-acetyl-2-isonicotinoyl-pyrazolidine-3,5-dione (43), 1-isonicotinoyl-4-phenylthiosemicarbazide (44), respectively. The compound (44) on further reaction with ethyl chloroacetate gave N-(4-oxo-2-(phenylimino)thiazolidin-3-yl) isonicotinamide (45).



Hassan⁴⁷ reported the reaction of methyl anthranilate (46) with hydrazine hydrate that gave 2-aminobenzhydrazide (47) which in turn on reaction with methyl acetoacetate, acetyl acetone and diethyl malonate, yielded (2-aminobenzoyl)-3-methyl-1H-pyrazole-5-(4H)-one (48), (2-aminobenzoyl)(3,5-dimethyl-1H-pyrazole-1-yl)methanone (49) and (2-aminobenzoyl)pyrazolidine-3,5-dione (50), respectively in good amounts.

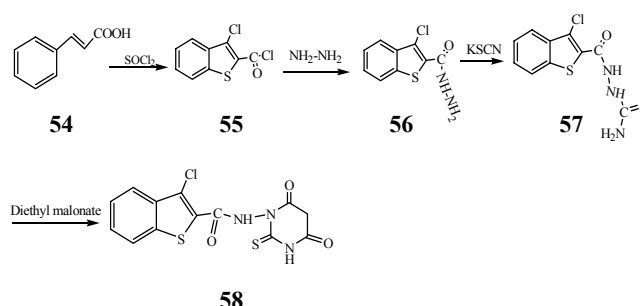


Abbas and co-workers⁴⁸ reported the reaction of 3-amino-2-(pyridin-3-yl)-4-quinazolinone (51) with *p*-hydroxyphenyl isocyanate and phenyl isothiocyanate provided 1-(4-oxo-2-(pyridin-3-yl)quinazolin-3(4H)-yl)-3-phenylurea (52a) and 1-(4-oxo-2-(pyridin-3-yl)quinazolin-3(4H)-yl)-3-phenylthiourea (52b). The compounds (52a and 52b) upon reaction with diethyl malonate and after keto-enol tautomerism, yielded 6-hydroxy-3-(4-oxo-2-(pyridin-3-yl)quinazolin-3-(4H)-yl)-1-phenylpyrimidine-2,4-(1H,3H)-dione (53a) and 3-(4-hydroxy-6-oxo-3-phenyl-2-thioxo-2,3-dihydropyrimidin-1(6H)-yl)-2-(pyridin-3-yl)quinazolin-4-(3H)-one (53b).



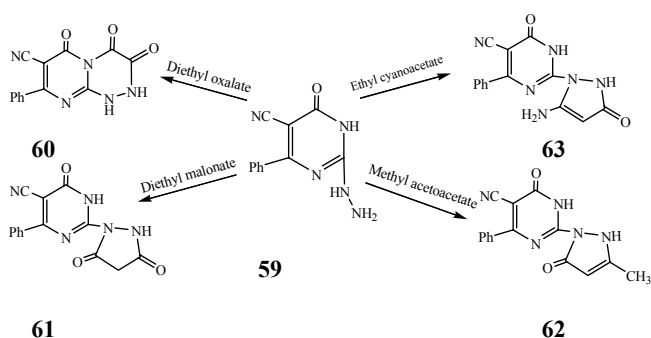
X: R: (a) O, C₆H₅, (b) S, C₆H₄OH-p

Naganagowda and co-workers⁴⁹ reported the synthesis of 3-chloro-1-benzothiophene-2-carbonylchloride (55) from cinnamic acid (54). The compound (55) reacted with hydrazine and gave 3-chloro-1-benzof[b]thiophene-2-carboxylic acid hydrazide (56) which on reaction with potassium thiocyanate provided 2-[(3-chloro-1-benzof[b]thiophen-2-yl)carbonyl]hydrazine carbothioamide (57) which on reaction with diethyl malonate yielded 3-chloro-N(4,6-dioxo-2-thioxotetrahydropyrimidin-1(2H)-yl)-1-benzothiophene-2-carboxamide (58).

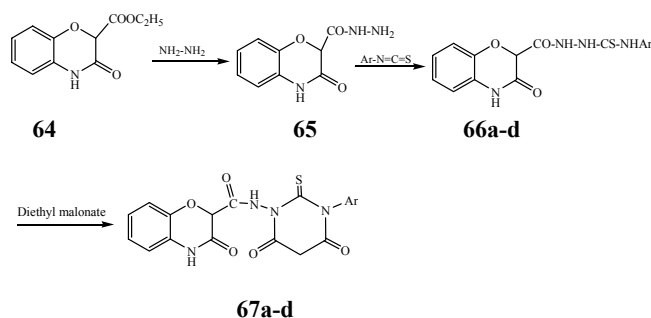


El-zahar and co-workers⁵⁰ reported the reaction of 2-hydrazino-6-oxo-4-phenyl-1,6-dihydropyrimidine-5-carbonitrile (59) with diethyl oxalate, diethyl malonate, methyl acetoacetate and ethyl cyanoacetate that provided corresponding 3,4,6-trioxo-8-phenyl-tetrahydro-2H-pyrimido[2,1-c][1,2,4]triazine-7-carbonitrile (60), 2-(3,5-dioxo-pyrazolidin-1-yl)-6-oxo-4-phenyl-1,6-dihydropyrimidine-5-carbonitrile (61), 2-(3-methyl-5-oxo-2,5-dihydro-pyrazol-1-yl)-6-oxo-4-phenyl-1,6-dihydropyrimidinecarbonitrile (62) and 2-(5-amino-3-oxo-2,3-dihydro-pyrazol-1-yl)-6-oxo-4-phenyl-1,6-dihydropyrimidine-5-carbonitrile (63), respectively, in good yields.

Dabholkar and Gavande⁵¹ reported the reaction of 2H, 4H-2-ethoxycarbonyl-3, 4-dihydro-3-oxo-1,4-benzoxazine (64) with hydrazine and provided 2H, 4H-2-hydrazino carbonyl-3,4-dihydro-3-oxo-1,4-benzoxazine (65) which upon reaction with arylisothiocyanate derivatives yielded 2H,4H-2-[(4'-substituted)arylthiosemicarbazino]carbonyl-3,4-dihydro-3-oxo-1,4-benzoxazine derivatives (66a-d).

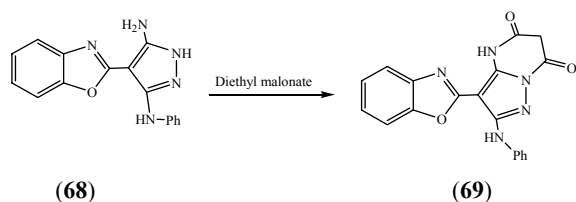


The compounds (**66a-d**) later on reaction with diethyl malonate and gave 2H,4H-2-[5'-H-5'-dihydro-2'-thioxo-3'-aryl-4',6'-dioxo-1,3-diazine]aminocarbonyl-3,4-di-hydro-3-oxo-1,4-benzoxazines (**67a-d**).

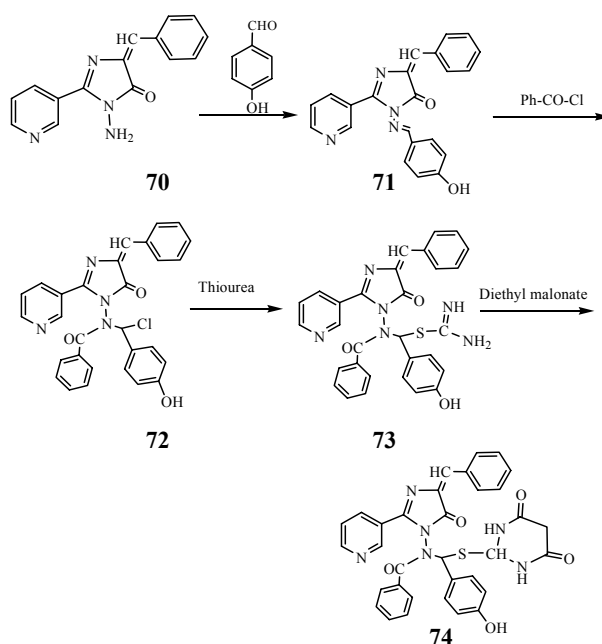


Ar: (a) Ph, (b) C₆H₄CH₃, (c) C₆H₄NO₂, (d) C₆H₃(NO₂)₂

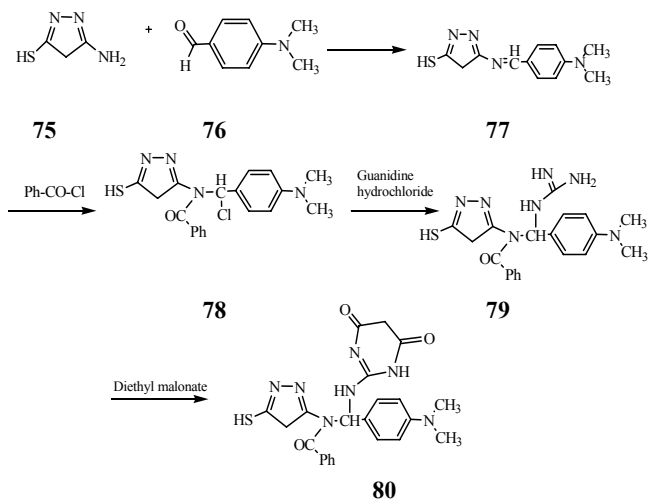
Wahab and Mohamed⁵² reported the reaction of N-[3-amino-4-(benzoxazol-2-yl)pyrazol-5-yl]phenylamine (**68**) with diethyl malonate which provided 3-benzoxazol-2-yl-2-phenylamino-4H-pyrazolo[1,5-a]pyrimidine-5,7-dione (**69**) in 80 % yield.



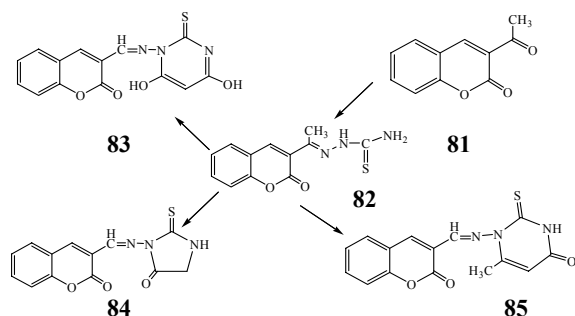
Abodi and co-workers⁵³ reported the reaction of 3-amino-5-(benzylidene)-2-(pyridin-3-yl)-3,5-dihydro-4H-imidazol-4-one (**70**) with *p*-hydroxybenzaldehyde which gave 5-(benzylidene)-3-[(*p*-hydroxybenzylidene)amino]-2-(pyridin-3-yl)dihydro-4H-imidazol-4-one (**71**). The compound (**71**) reacted with benzoyl chloride and provided N-[chloro(4'-phenyl)methyl]-N-[4'-*p*-hydroxybenzylidene-5'-oxo-2-(pyridin-3-yl)-4,5-dihydro-1H-imidazol-1-yl]benzamide (**72**). The compound (**72**) later upon reacted with thiourea yielded 4'-phenyl-{[4'-(4'-benzylidene-5'-oxo-2-(pyridin-3-yl)-4,5-dihydro-1H-imidazol-1-yl)](*p*-hydroxybenzoyl)amino}methyl carbamimidothioate (**73**). The compound (**73**) in turn reacted with diethyl malonate yielded N-{1-[4',6'-dioxo-tetrahydropyrimidin-2-yl]sulfanyl}benzyl}-N-[4'-*p*-hydroxybenzylidene-5'-oxo-2-(pyridin-3-yl)-4,5-dihydro-1H-imidazol-1-yl]-benzamide (**74**).



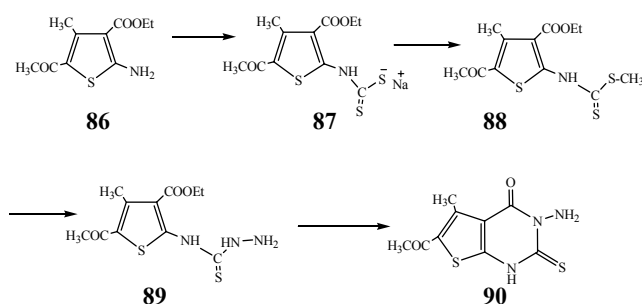
Drea and co-workers⁵⁴ reported the reaction of 5-amino-3-mercaptopyrazole (**75**) with 4-dimethylaminobenzaldehyde (**76**) which gave 5-(4'-dimethylamino)benzylidene)amino-3-mercaptopyrazole (**77**). The compound (**77**) on reaction with benzoyl chloride provided 5-(4'-dimethylamino)-chlorobenzylidene)-N-(benzoyl)amino-3-mercaptopyrazole (**78**). The compound (**78**) reacted with guanidine hydrochloride and yielded 5-{(4'-dimethylamino)benzylidene)-N-(benzoyl)-N-(guanidino)}-amino-3-mercaptopyrazole (**79**) which later on reaction with diethyl malonate gave 5-{(4'-dimethylamino)benzylidene)-N-(benzoyl)(4,6-dioxotetrahydropyrimidin-2-ylamino)methyl}-amino-3-mercaptopyrazole (**80**).



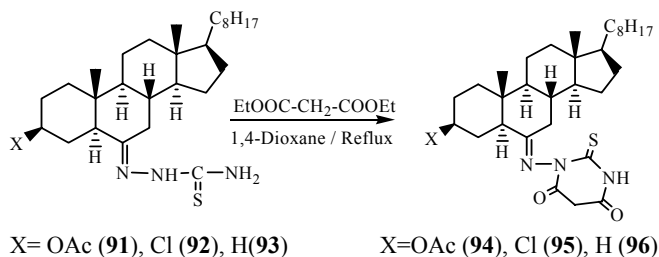
Hasanen⁵⁵ reported the reaction of 3-acetylcoumarin (**81**) with thiosemicarbazide that provided 3-acetylcoumarin thiosemicarbazone (**82**) which reacted with diethyl malonate, chloroethyl acetate and ethyl acetoacetate to yield corresponding 4,6-dihydroxy-1-(coumarin-3-ylethylidene)-aminopyrimidin-2-thione (**83**), 3-(coumarin-3-ylethylidene)amino-2-thioxoimidazolidin-4-one (**84**) and 6-methyl-1-(coumarin-3-ylethylidene)amino-2-thioxopyrimidin-4-one (**85**) in better yields.



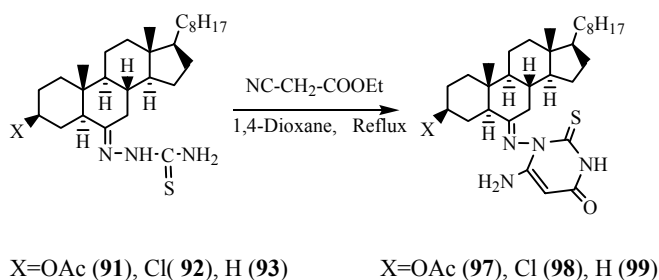
Hafez and co-workers⁵⁶ reported the reaction of 5-acetyl-3-ethyl-2-amino-4-methylthiophene carboxylate (**86**) with CS₂ which gave methyl N-(4-methyl-5-acetyl-3-carboxyethylthiophene)dithiocarbamate (**88**). The compound (**88**) reacted with hydrazine and yielded methyl N-(4-methyl-5-acetyl-3-carboxyethylthiophene)thiosemicarbazide (**89**). The compound (**89**) in warmed ethanolic sodium hydroxide solution cyclized and gave 3-amino-6-acetyl-5-methyl-2-thioxothieno[2,3-*d*]pyrimidin-4-one (**90**).



Shamsuzzaman and co-workers⁵⁷ reported the reaction of steroidal thiosemicarbazones (**91-93**) with diethyl malonate that provided steroidal pyrimidinones (**94-96**) in better yields.



Shamsuzzaman and co-workers⁵⁸ also reported another set of reaction in which steroidal thiosemicarbazones (**91-93**) reacted with ethyl cyanoacetate and yielded differently substituted steroidal pyrimidines (**97-99**) in sufficient amounts.



Synthesis of pyran derivatives

Pyran is a six membered non-aromatic ring consisting of five carbon atoms, one oxygen atom and two double bonds. The term pyran is also often applied to the saturated ring analog, which is more properly referred to as tetrahydropyran (oxane). There are two isomers of pyran that differ by the location of the double bonds. In 2H-pyran (**100**), the saturated carbon is at position 2 while as in 4H-pyran (**101**), the saturated carbon is at position 4.



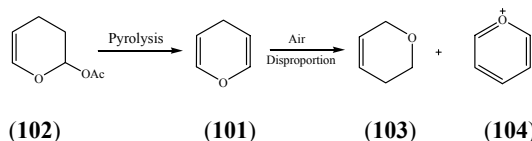
(**100**)



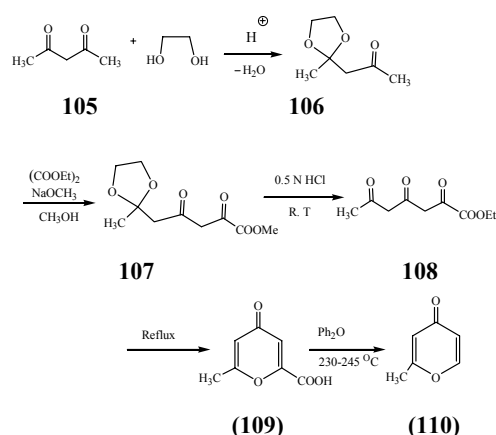
(**101**)

They are not only used in cosmetics, pigments and biodegradable agrochemicals^{59,60} but also constitute a structural unit of many natural products.⁶¹ These compounds have been reported to possess various pharmacological activities such as antiallergic, antitumor and antibacterial.^{62,63}

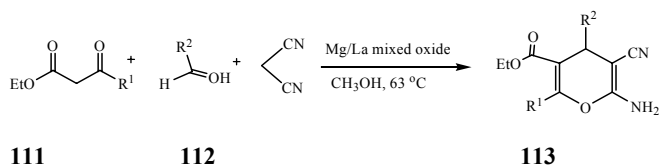
Masamune and Castellucci⁶⁴ in 1962 first isolated and characterized 4H-pyran by the pyrolysis of 2-acetoxy-3,4-dihydro-2H-pyran (**102**). It was found unstable in the presence of air so disproportionated to the dihydropyran (**103**) and the pyrylium ion (**104**).



Dorman⁶⁵ in 1967 reported the reaction of acetyl acetone (**105**) with ethylene glycol which gave 2-methyl-2-aceton-1,3-dioxolan (**106**). The compound (**106**) was acylated with diethyl oxalate in presence of sodium methoxide formed methyl 5-(2-methyl-[1,3]dioxolan-2-yl)-2,4-dioxopentanoic acid methyl ester (**107**). The compound (**107**) was treated with 0.5 N HCl to give intermediate triketone (**108**). The compound (**108**) was refluxed to complete ring closure forming 6-methyl-4H-pyran-4-one-2-carboxylic acid (**109**) which on subsequent decarboxylation yielded 2-methyl-4H-pyran-4-one (**110**).

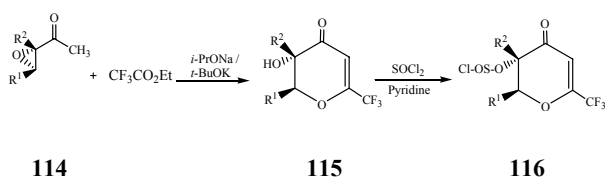


Lingaiah and co-workers⁶⁶ reported an efficient synthesis of polyfunctionalized 4H-pyran (**113a-h**) by one pot condensation of active methylenic diketo compounds (**111a-h**), aldehydes (**112a-h**) and malononitrile using basic Mg/La mixed oxide as catalyst.

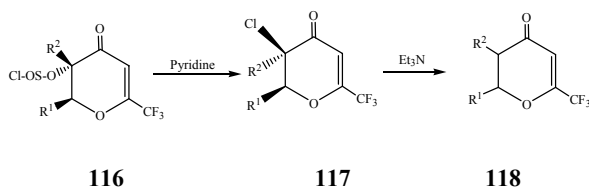


R¹: (a) C₂H₄Br, (b) C₂H₅, (c) C₃H₇, (d) CH₂Cl, (e) CH₂Br, (f) C₆H₄Cl, (g) C₆H₄Br, (h) CH₂I, **R²**: (a) C₆H₅, (b) 4-NO₂-C₆H₄, (c) 3-C₆H₄NO₂, (d) 4-Cl-C₆H₄, (e) 4-CNC₆H₄, (f) 4C₆H₄OH, (g) 4-MeC₆H₄, (h) 4-MeOC₆H₄

Tyvorskii and co-workers⁶⁷ reported the reaction of oxiranes (**114a-e**) with ethyl perfluoroalkanoate in presence of sodium *iso*-propoxide or potassium *tert*-butoxide that gave hydroxypyranones (**115a-e**). The hydroxypyranones upon reaction with thionyl chloride in dry pyridine yielded chlorosulphites (**116a-e**). These sulphites upon refluxing in presence of pyridine provided chlorosubstituted pyranones (**117a-e**) which on reaction with triethylamine yielded 2-perfluoroalkyl-4H-pyran-4-ones (**118a-e**).

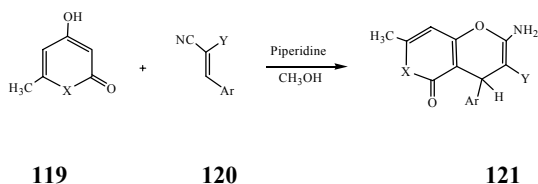


R¹: (a) H, (b) H, (c) CH₃, (d) CH₂Cl, (e) CH₂I, **R²**: (a) CH₃, (b) Ph, (c) CH₃, (d) CH₃, (e) Ph



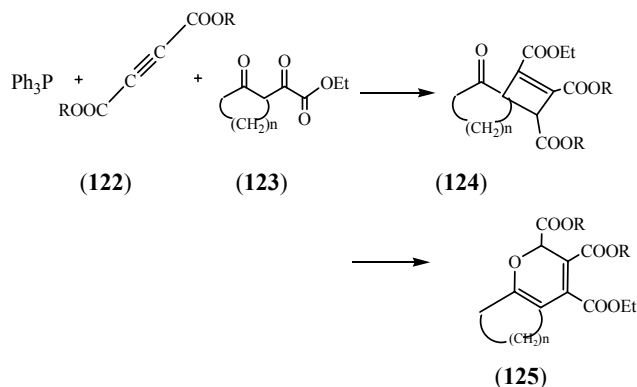
R¹: (a) H, (b) H, (c) CH₃, (d) CH₂Cl, (e) CH₂I, **R²**: (a) CH₃, (b) Ph, (c) CH₃, (d) CH₃, (e) Ph

Stoyanov and co-workers⁶⁸ reported the reaction of 4-hydroxy-6-methyl-pyranone and pyridinone derivatives (**119a-c**) with Knoevenagel products (**120a-c**) in presence of piperidine in methanol to yield substituted 2-amino-4H, 5H-pyrano[4,3-*b*]pyran-5-ones (**121a-c**).



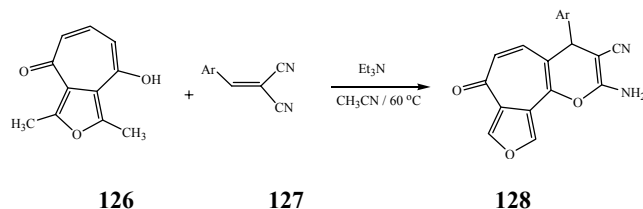
X: (a) O, (b) NH, (c) NCH₂Ph, **Ar**: (a) Ph, (b) Ph, (c) NO₂Ph, **Y**: (a) COOCH₃, (b) CN, (c) COOC₂H₅

Yavari and Bayat⁶⁹ reported that dialkylacetylene dicarboxylates (**122a-d**) reacted smoothly with triphenyl phosphine and ethyl oxo(2-oxocycloalkyl)ethanoates (**123a-d**) via intramolecular Wittig reaction to produce *spiro*cyclobutene derivatives (**124a-d**). These *spiro* systems underwent electrocyclic ring-opening reaction to produce electron-deficient 1, 3-dienes which spontaneously cyclized to 2H-pyran derivatives (**125a-d**).



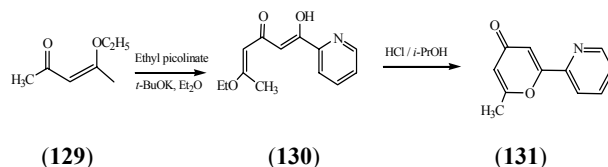
R: (a) Me, (b) Et, (c) *i*Pr, (d) *i*Bu, **n**: (a) 3, (b) 4, (c) 5, (d) 9

Arseneva and Arsenev⁷⁰ reported that 8-hydroxy-1,3-dimethyl-4H-cyclohepta[*c*]furan-4-one (**126**) on reaction with arylidenemalononitriles (**127a-h**) gave the corresponding condensed 2-amino-4H-pyrans (**128a-h**) in good yields.

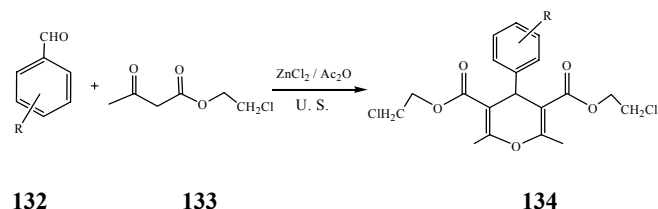


Ar (a) Cl₂C₆H₃, (b) FC₆H₄, (c) ClC₆H₄, (d) BrC₆H₄, (e) EtO-C₆H₄, (f) MeO-C₆H₄, (g) MeS-C₆H₄, (h) thienyl

Bobrov and Tyvorskii⁷¹ reported the synthesis of 6-methyl-2-(2-pyridyl)-4H-pyran-4-one (**131**). The pyranone precursor (5-ethoxy-1-hydroxy-1-pyridin-2-yl-hexa-1,4-dien-3-one) (**130**) was prepared by Claisen condensation of acetyl acetone enol ether (**129**) with ethyl picolinate.

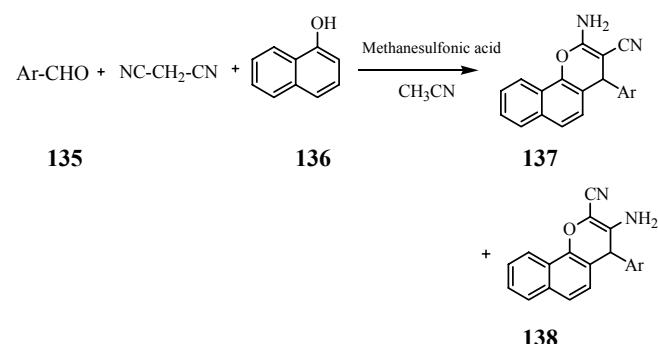


Ni and co-workers⁷² reported the reaction of aromatic aldehydes (**132a-j**) with 3-oxo-butyric acid-2-chloroethyl ester (**133**) in acetic anhydride in presence of zinc chloride, which was irradiated by an ultrasonic processor at 50 °C and 100 W to yield substituted 4-aryl-4H-pyran-3,5-dicarboxylates (**134a-j**).



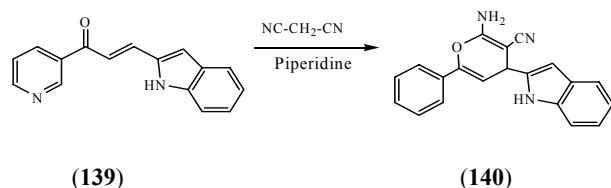
R: (a) 2-F, (b) 2,4-(CH_3)₂, (c) 4-Br, (d) 4- OC_2H_5 , (e) 2,4-Cl, Br, (f) 2,4-Cl, I, (g) 4-F, (h) 2,4- NO_2 , CH_3 , (i) 2,4-(OH)₂, (j) 3-Br

Heravi and co-workers⁷³ reported one-pot, three component reaction of aromatic aldehydes (**135a-e**), malononitrile and α -naphthol (**136**) in presence of methanesulfonic acid to yield two isomers of 2-amino-4H-chromenes **137a-e** and **138a-e** in very good yields.

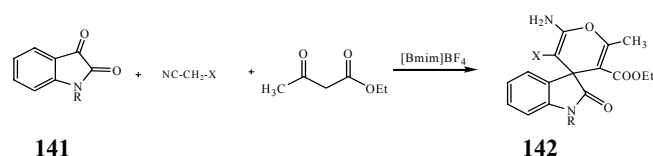


Ar: (a) $\text{Cl}_2\text{C}_6\text{H}_3$, (b) $(\text{NO}_2)_2\text{C}_6\text{H}_3$, (c) $(\text{MeO})_2\text{C}_6\text{H}_3$, (d) FClC_6H_3 , (e) $\text{ClNO}_2\text{C}_6\text{H}_3$,

El-Latif and co-workers⁷⁴ reported the reaction of 3- β -indolylacryloylpyridine (**139**) with malononitrile in presence of piperidine to yield 2-amino-4-(3-indolyl)-6-(3-pyridyl)-pyran-3-carbonitrile (**140**).

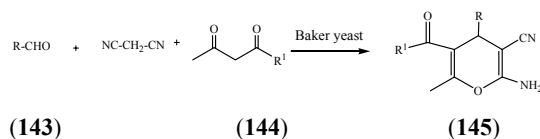


Moghadam and Miri⁷⁵ reported the reaction of isatins (**141a-b**), malononitrile or ethyl cyanoacetate and 1, 3-dicarbonyl compound in the ionic liquid to yield *spiro*[4H-pyranoxindole] derivatives (**142 a-d**) in better amounts.



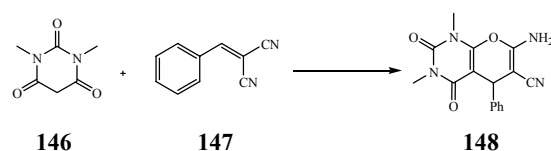
R: (a) H, (b) H (c) Bu, (d) Bu, **X:** (a) CN, (b) COOEt , (c) CN, (d) COOEt

Pratap and co-workers⁷⁶ reported the Baker's yeast catalyzed one-pot three-component cyclocondensation of aryl aldehydes (**143a-g**), malononitrile and β -dicarbonyls (**144a-c**) in dimethylacetamide solvent to obtain polyfunctionalized 4H-pyrans (**145a-g**).

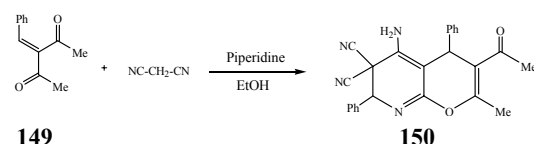


R: (a) $(\text{MeO})_2\text{C}_6\text{H}_3$, (b) $\text{Cl}_2\text{C}_6\text{H}_3$, (c) 3- ClC_6H_4 , (d) 4- HOC_6H_4 , (e) 4- FC_6H_4 , (f) 3-pyridyl, (g) 4- $\text{CH}_3\text{C}_6\text{H}_4$, **R**¹: (a) OEt , (b) Me, (c) OMe , (d) OEt , (e) Me, (f) OMe , (g) OEt

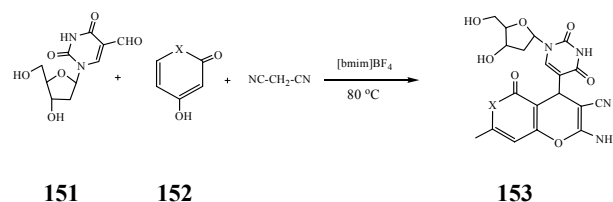
Seeliger and co-workers⁷⁷ have reported the formation of dihydropyrano[2,3-*c*]pyrimidinedione (**148**) in 80 % yields by the reaction of 1,3-dimethylbarbituric acid (**146**) with arylidenemalononitrile (**147**) upon protonation.



Martin and co-workers⁷⁸ reported the synthesis of pyrano[2,3-*b*]pyridine derivative (**150**) from malononitrile and 2-benzylidene-1,3-diketone (**149**). The compound **149** is easily accessible via Knoevenagel condensation of benzaldehyde and pentan-2,4-dione.



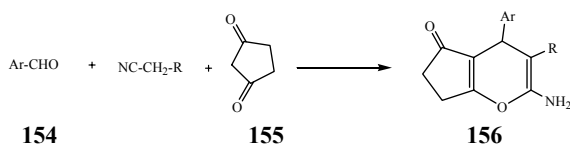
Feng and co-workers⁷⁹ reported the multi-component reactions of nucleoside (**151**), 4-hydroxy-2-pyranone (**152a**) or 4-hydroxy-pyridin-2(1H)-one (**152b**) and malononitrile in presence of ionic liquid to provide the efficient synthesis of pyrano[4,3-*b*]pyran nucleoside derivative (**153a**) and pyrano[3,2-*c*]pyridine nucleoside derivative (**153b**) which were also found as potential antiviral and anti-leishmanial agents.



X: (a) O, (b) NH

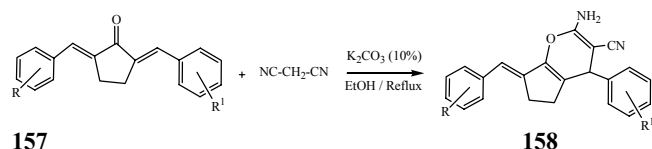
Yao and co-workers⁸⁰ reported a rapid and facile synthesis of cyclopenta [*b*] pyran derivatives namely, 2-amino-4-aryl-5-oxo-tetrahydrocyclopenta [*b*] pyran-3-carbonitriles (**156a,c**) and ethyl-2-amino-4-aryl-5-oxo-tetrahydrocyclopenta [*b*]pyran-3-carboxylates (**156b,d**) under solvent free conditions by triturating a mixture of the three components;

aromatic aldehydes (**154a,b**), malononitrile/ethyl cyanoacetate and cyclopentadione (**155**) at 80 °C.



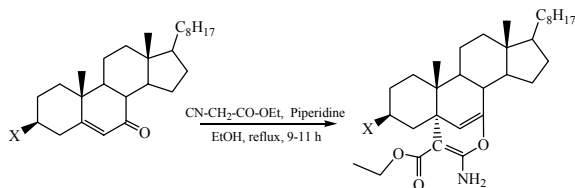
Ar: (a) C₆H₅, (b) C₆H₅, (c) ClC₆H₄, (d) ClC₆H₄, **R:** (a) CN, (b) COOEt, (c) CN, (d) COOEt

Karimi-Jaberi and Pooladian⁸¹ synthesized a series of substituted 2-amino-4H-pyran-3-carbonitriles (**158a-s**) through a one-pot condensation of malononitrile and α,α' -bis(arylidene)cyclopentanones (**157a-s**) in ethanol by using K₂CO₃ as a catalyst. Short experimental reaction times, excellent yields, no need to use cumbersome apparatus for purification of the products, inexpensiveness and commercial availability of the catalyst were the advantages of this method.



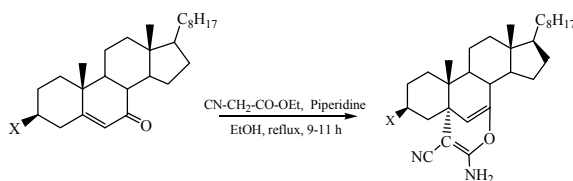
R: (a) CH₂, (b) CH₂, (c) CH₂, (d) C₂H₄, (e) C₂H₄, (f) C₂H₄, (g) C₂H₄, (h) C₂H₄, (i) C₂H₄, (j) C₂H₄, (k) C₂H₄, (l) C₃H₆, (m) C₃H₆, (n) C₃H₆, (o) C₃H₆, (p) C₃H₆, (q) C₃H₆, (r) C₃H₆, (s) C₃H₆, **R':** (a) 2-Cl, (b) H, (c) 2-Cl, 4-Cl, (d) 2-Cl, (e) H, (f) 2-Cl, 4-Cl, (g) 4-F, (h) 4-Br, (i) 4-OMe, (j) 4-Me, (k) 2-Cl, 6-F, (l) H, (m) 2-Cl, (n) 2-Cl, 4-Cl, (o) 4-F, (p) 4-Br, (q) 4-OMe, (r) 4-OMe, (s) 2-Cl, 6-F

Shamsuzzaman and co-workers⁸² reported the reaction of steroidal ketones (**159-161**) with ethyl cyanoacetate that provided substituted steroidal 4H-pyrans (**162-164**) in better yields.



X: OAc(**159**), Cl(**160**), H(**161**) **X:** OAc(**162**), Cl(**163**), H(**164**)

Shamsuzzaman and co-workers⁸³ also reported the reaction of steroidal ketones (**159-161**) with malononitrile that gave cyano appended steroidal 4H-pyrans (**165-167**) in good yields.



X: OAc(**159**), Cl(**160**), H(**161**) **X:** OAc(**165**), Cl(**166**), H(**167**)

Conclusion

In this article we have mentioned the different routes for the synthesis of pyrimidine and pyran derivatives. The steps included condensation followed by cyclization or multi component reaction (MCR), either in a step-wise manner or in one pot has been achieved successfully to obtain the aforementioned two classes of heterocycles under different conditions. Most of the preparative methods included diethyl oxalate, diethyl malonate, malononitrile and ethyl cyanoacetate as the common reagents for the synthesis of pyrimidines and pyrans appended on different heterocyclic skeletons. Also many series of substituted pyrimidine and pyran-fused six membered heterocycles possessing *N*-, *S*- and *O*- have been constructed in potential yields and with conventional methods. Hence these protocols provide convenient strategies to annelate different heterocyclic nuclei with widespread bioactive pyrimidines and pyrans thereby extending the categories of heterocyclic systems. These strategies may also provide valuable information for the further design and development of more active biological agents through various modifications and derivatizations.

Acknowledgement

Author (AMD) thanks Dr. Shamsuzzaman Professor of Chemistry, AMU Aligarh, for useful discussions during the literature survey and University Grants Commission for providing research fellowship for successful completion of this work.

References

- Domling, A., Ugi, I., *Angew. Chem. Int., Ed. Engl.*, **2000**, 39, 3168
- Domling, A., *Chem. Rev.*, **2006**, 106, 17.
- Joule, J. A., Mills, K., *Heterocyclic Chemistry* (John Wiley & Sons) Oxford 5th Edn. **2010**, p. 250
- Lagoja, M., Irene, *Chemistry and Biodiversity*, **2005**, 2, 1
- Rewcastle, G. W., Bridges, A. J., Fry, D. W., Rubin, J. R., Denny, W. A., *J. Med. Chem.*, **1997**, 40, 1820
- Fry, D. W., Becker, M. A., Switzer, R. L., *Mol. Pharm.*, **1995**, 47, 810.
- Gready, J. E., McKinlay, C., Gebauer, M. G., *Eur. J. Med. Chem.*, **2003**, 38, 719.
- Sanghvi, Y. S., Larson, S. B., Matsumoto, S. S., Nord, L. D., Smee, D. F., Willis, R. C., Avery, T. H., Robins, R. K., Revankar, G. R., *J. Med. Chem.*, **1989**, 32, 3629.
- Tenser, R. B., Gaydos, A., Hay, K. A., *Antimicrob. Agents Chemother.*, **2001**, 45, 3657.
- Nizamuddin, M. M., Srivastava, M. K., Khan, M. H., *Indian J. Chem.*, **2001**, 40, 49.
- Ram, V. J., Goel, A., Sarkhel, S., Maulik, P. R., *Bioorg. Med. Chem.*, **2002**, 10, 1275.
- Elnagdi, M. H., Al-awadi, N., Erian, A. N., In: *Compensative Heterocyclic Chemistry II*, 1st ed.; Katritzky, A. R., Rees, C. W., Scriven, E. F. V. Eds.; Pergamon Press: Oxford, **1996**, 7, p. 431.
- Elnagdi, M. H., Elmoghayar, M. R. H., Elgemeie, G. F., *Adv. Heterocycl. Chem.*, **1984**, 41, 319.

- ¹⁴Ahluwalia, V. K., Dahiya, A., Garg, V. J., *Indian J. Chem.*, **1997**, *36B*, 88.
- ¹⁵Undheim, K., Benneche, T., *Pyrimidines and their benzo derivatives. In: Comprehensive heterocyclic chemistry II*, Oxford: Pergamon; **1996**, 6. p. 93
- ¹⁶Jain, K. S., Chitra, T. S., Miniyaar, P. B., Kathiravan, M. K., Bendre, V. S., Veer, V. S., *Curr. Sci.*, **2006**, *90*, 793.
- ¹⁷Botta, M., Corelli, F., Maga, G., Manetti, F., Renzulli, M., Spadari, S., *Tetrahedron*, **2001**, *57*, 8357.
- ¹⁸Botta, M., Occhionero, F., Nicoletti, R., Mastromarino, P., Conti, C., Magrini, M., *Bioorg. Med. Chem.*, **1999**, *7*, 1925.
- ¹⁹Hammam, A. H., Zahran, M., El-Hag, F. A., Helmy, K. M. H., *Egypt. J. Pharm. Sci.*, **1996**, *37*, 565
- ²⁰Hammam, A. H., Zaki, M. E. A., El-Assasy, M. E., *Egypt. J. Pharm. Sci.*, **1997**, *38*, 291
- ²¹Rovnyak, G., Shu, V., Schwartz, J., *J. Heterocycl. Chem.*, **1981**, *18*, 327.
- ²²Heidelberg, C., Arafeld, F. J., *Cancer Res.*, **1963**, *23*, 1226.
- ²³Clercq, E. D., *J. Med. Chem.*, **1988**, *29*, 1561.
- ²⁴Baba, M., Pauvels, R., Herdweg, P., Clercq, E. D., Desmyster, J., Vadepulfe, M., *Biochem. Biophys. Res. Commun.*, **1987**, *142*, 128.
- ²⁵Clercq, E. D., *Anticancer Res.*, **1986**, *6*, 549.
- ²⁶Hirota, K., Kubo, K., Sajiki, H., Kitade, Y., Sako, M., Maki, Y. J., *Org. Chem.*, **1997**, *62*, 2999.
- ²⁷Grimaux, M. E., *Proceedings weekly sessions of the Academy of Sciences*, **1879**, *88*, 85
- ²⁸Pinner, A., *Chem. Ber.*, **1884**, *17*, 2519
- ²⁹Pinner, A., *Chem. Ber.*, **1885**, *18*, 759
- ³⁰Gabriel, S., Colman, J., *Chem. Ber.*, **1900**, *33*, 3666
- ³¹Behrend, R., *Ann. Chem.*, **1885**, *229*, 18
- ³²Hussain, S. M., El-Barbary, A. A., Mansour, S. A., *J. Heterocycl. Chem.*, **1985**, *22*, 169
- ³³Pere, M. A., Soto, J. L., Guzman, F. J., *J. Chem. Soc.*, **1985**, *1*, 87
- ³⁴Taylor, E. C., Morrison, R. W., *J. Org. Chem.*, **1967**, *32*, 2379
- ³⁵Botta, M., Dceci, M. C., Angelis, F. D., Finizia, G., Nicoletti, R., *Tetrahedron*, **1984**, *40*, 3313.
- ³⁶Andereichikov, S., Yu. G. D., Plakhina, Zh. *Org. Khim.*, **1987**, *23*, 872
- ³⁷El-Subbagh, H. I., *Sulfur Lett.*, **1990**, *11*, 249
- ³⁸Bowman, A., *J. Chem. Soc.*, **1937**, 494
- ³⁹Yossef, K. M., Omar, R. H., El-Meleigy, M., *Zagazig J. Pharm. Sci.*, **1994**, *3*, 182
- ⁴⁰Mohamed, E. A., *Chem. Pap.*, **1994**, *48*, 261
- ⁴¹Attaby, F. A., Eldin, S. M., *Arch. Pharm. Res.*, **1997**, *20*, 330
- ⁴²Stadlbauer, W., Badawey, E., Hojas, G., Roschger, P., Kappe, T., *Molecules*, **2001**, *6*, 338
- ⁴³Rivera, D. G., Peseke, K., Jomarrón, I., Montero, A., Molina, R., Coll, F., *Molecules*, **2003**, *8*, 444
- ⁴⁴Semenov, B. B., Novikov, K. A., Krasnov, K. A., Kachala, V. V., *Chem. Heterocycl. Comp.*, **2005**, *41*, 5
- ⁴⁵Abdel-Rahman, R. M., Makki, M. S. I. T., Bawazir, W. A. B., *E - J. Chem.*, **2010**, *7*, 93
- ⁴⁶Parashar, B., Bhardwaj, S., Sharma, S., Gupta, G. D., Sharma V. K., Punjabi, P. B., *J. Chem. Pharm. Res.*, **2010**, *2*, 33
- ⁴⁷Hassan, D. F., Al-Nahrain J., *Univer. Sci. J.*, **2010**, *13*, 32
- ⁴⁸Ammar, Y. A., Mohamed, Y. A., El-Sharief, A. M., El-Gaby, M. S. A., Abbas, S. Y., *Chem. Sci. J.*, **2011**, CSJ-15
- ⁴⁹Naganagowda, G., Thamyongkit, P., Klai-U-dom, R., Ariyakraingkrai, W., Luechai, A., Petsom, A., *J. Sulfur Chem.*, **2011**, *32*, 235
- ⁵⁰El-Zahari, M. I., Abdel-Karim, S. S., Haiba, M. E., Khedr, M. A., *Acta Poloniae Pharm. Drug Res.*, **2011**, *68*, 357.
- ⁵¹Dabholkar, V. V., Gavande, R. P., *Acta Poloniae Pharm. Drug Res.*, **2012**, *69*, 247
- ⁵²Abdel-Wahab, B. F., Mohamed, H. A., *Turk. J. Chem.*, **2012**, *36*, 805
- ⁵³Al. Abodi, A. J. K., Majed, N., Sahar, A. K., Al-Bayati, R. I. H., *American J. Org. Chem.*, **2012**, *2*, 143
- ⁵⁴Essa, F. O., Kadhum, K. J., Drea, A. A., *J. App. Chem.*, **2012**, *1*, 344
- ⁵⁵Hasanen, J. A., *Der. Pharma. Chem.*, **2012**, *4*, 1923
- ⁵⁶Hafez, H. N., El-Gazzar, A. R. B. A., Nawwar, G. A.M., *Eur. J. Med. Chem.*, **2010**, *45*, 1485
- ⁵⁷Shamsuzzaman, Dar, A. M., Yaseen, Z., Alam, K., Hussain, A., Gatoo, M. A., *J. Mol. Struct.*, **2013**, *1045*, 62.
- ⁵⁸Shamsuzzaman, Dar, A. M., Tabassum, S., Zaki, M., Khan, Y., Sohail, A., Gatoo, M. A., *Comp. Rend. Chim.*, **2014**, *17*, 359
- ⁵⁹Hackett, J. C., Kim, Y. W., Su, B., Brueggemeier, R. W., *Bioorg. Med. Chem.*, **2005**, *13*, 4063.
- ⁶⁰Borhade, A. V., Uphade, B. K., Tope, D. R., *J. Chem. Sci.*, **2013**, *125*, 583.
- ⁶¹Xiao, Y., Zhang, J., *Chem. Commun.*, **2009**, 3594.
- ⁶²Wang, J. L., Liu, D., Zhang, Z. J., Shan, S., Han, X., Srinivasula, S. M., Croce, C. M., Alnemri, E. S., Huang, Z., *Proc. Natl. Acad. Sci. USA.*, **2000**, *97*, 7124.
- ⁶³Fairlamb, I. J. S., Marrison, L. R., Dickinson, J. M., Lu, F. J., Schmidt, J. P., *Bioorg. Med. Chem.*, **2004**, *12*, 4285.
- ⁶⁴Masamune, S., Castellucci, N. T., *J. Am. Chem. Soc.*, **1962**, *84*, 2452
- ⁶⁵Dorman, L. C., *J. Org. Chem.*, **1967**, *32*, 4105.
- ⁶⁶Babu, N. S., Pasha, N., Rao, K. T. V., Prasad, P. S. S., Lingaiah, N., *Tetrahedron Lett.*, **2008**, *49*, 2730
- ⁶⁷Tyvorskii, V. I., Bobrov, D. N., Kulinkovich, O. G., *Tetrahedron*, **1998**, *54*, 2819
- ⁶⁸Stoyanov, E. V., Ivanov, I. C., Heber, D., *Molecules*, **2000**, *5*, 19
- ⁶⁹Yavari, I., Bayat, M., *Tetrahedron*, **2003**, *59*, 2001
- ⁷⁰Yu, M., Arsen'eva, Arsen'ev, V. G., *Chem. Heterocycl. Comp.*, **2008**, *44*, 136
- ⁷¹Bobrov, D. N., Tyvorskii, V. I., *Tetrahedron*, **2010**, *66*, 5432
- ⁷²Ni, C., Song, X., Yan, H., Song, X., Zhong, R., *Ultrason. Sonochem.*, **2010**, *17*, 367
- ⁷³Heravi, M. M., Baghernejad, B., Oskooie, H. A., *J. Chinese Chem. Soc.*, **2008**, *55*, 659
- ⁷⁴El-Latif, N. A. A., Amr, A. E. E., Ibrahiem, A. A., *Monatsh. Chem.*, **2007**, *138*, 559
- ⁷⁵Moghadam, K. R., Miri, L. Y., *Tetrahedron*, **2011**, *67*, 5693
- ⁷⁶Pratap, U. R., Jawale, D. V., Netankar, P. D., Mane, R. A., *Tetrahedron Lett.*, **2011**, *52*, 581
- ⁷⁷Seeliger, F., Berger, S. T. A., Remennikov, G. Y., Polborn, K., Mayr, H., *J. Org. Chem.*, **2007**, *72*, 9170
- ⁷⁸Martin, N., Seoane, C., Soto, J. L., *Tetrahedron*, **1988**, *44*, 5861.
- ⁷⁹Feng, X. F. D., Qua, Y., Zhang, X., Wang, J., Loiseau, P. M., Andrei, G., Snoeck, R., Clercq, E. D., *Bioorg. Med. Chem. Lett.*, **2010**, *20*, 809
- ⁸⁰Yao, C., Jiang, B., Li, T., Qin, B., Feng, X., Zhang, H., Wang, C., Tu, S., *Bioorg. Med. Chem. Lett.*, **2011**, *21*, 599

⁸¹Jaberi, Z. K., Pooladian, B., *The Scientific World Journal*, Article ID 208796, **2012**, doi:10.1100/2012/208796

⁸³Shamsuzzaman, Dar, A. M., Khan, Y., Sohail, A., *J. Photochem. Photobiol., B*, **2013**, 129, 36

⁸²Shamsuzzaman, Dar, A. M., Sohail, A., Bhat, S., Mustafa, M. F., Khan, Y., *Spectrochim. Acta Part A*, **2014**, 117, 493

Received: 21.02.2015.

Accepted: 17.06.2015.



SEMICONDUCTING MATERIALS TOWARDS PHOTOCATALYTIC AIR TREATMENT. MATERIALS, TESTS AND PRACTICAL APPLICATION

Szymon Wojtyła^[a,b] and Tomasz Baran^{[a,c]*}

Keywords: photocatalysis, semiconductor, air pollutants.

Despite the development of advanced technology (or because of its development) environmental pollution, including particularly dangerous air pollutions, are really serious today. Photocatalytic air treatment has the potential for degradation of both, organic and inorganic contaminants including particularly dangerous nitrogen oxides and volatile organic compounds from indoor as well as outdoor air. Photocatalytic methods have a great advantage - do not lead to adsorption of pollutants but lead to degradation and mineralization of organic and inorganic compounds. The attractiveness of photocatalysis results also from features such as ability of using cheap and abundant sunlight as an energy source or mild conditions of process. This article briefly summarizes the broad range of studies: from modeling and photoreactor design, through laboratory experiment to large scale application within recent 5 years. Our goal was not only to summarize a recent works but to demonstrate that the photocatalytic air cleaning is not a technology of a distant future, but is already technology available today.

* Corresponding Author

[a] SajTom Light Future Ltd., Cytrynowa 3, 43-354 Czaniec, Poland, tommaso.baran@gmail.com

[b] Faculty of Chemistry, Jagiellonian University, Ingardena 3, 30-060 Kraków, szwojtyla@gmail.com

[c] Department of Chemistry, University of Milano, Via Golgi 19 - 20133 Milano, Italy

Introduction

Heterogeneous photocatalysis is a versatile and environmentally benign treatment technology based on solar energy (light) utilization. Degradation of biological, organic and inorganic pollutants in water and air, conversion of carbon dioxide to useful compounds or water splitting with hydrogen formation can be cited as examples of photocatalytic processes.¹ Absorption of light of energy equal or greater than energy of band gap results in charge separation – electrons are promoted to conduction band leaving holes in valence band (Fig. 1). Photogenerated charges might recombine (undesirable effect) or migrate toward surface of material. At the surface charges can react with adsorbed species – electron donor D or electron acceptor A resulting in reduction or oxidation of these species and leading to a final products A_{red} and D_{ox} .

In case of photocatalytic degradation of pollutants, oxygen adsorbed at the surface plays a role of electron acceptor. One electron reduction of molecular oxygen leads to superoxide anion radical, or upon former oxidation to singlet oxygen.²⁻⁴ Subsequent reaction leads to the formation of other reactive oxygen species like H_2O_2 and $\cdot OH$. In the meantime, water (or surface $-OH$ group) can be oxidized by photogenerated hole from the valence band with formation of $\cdot OH$ radical. The presence of the several kinds of reactive oxygen species makes the photocatalysis a great method of pollutants degradation. Reaction of reactive oxygen species with organic and inorganic compounds leads to complete

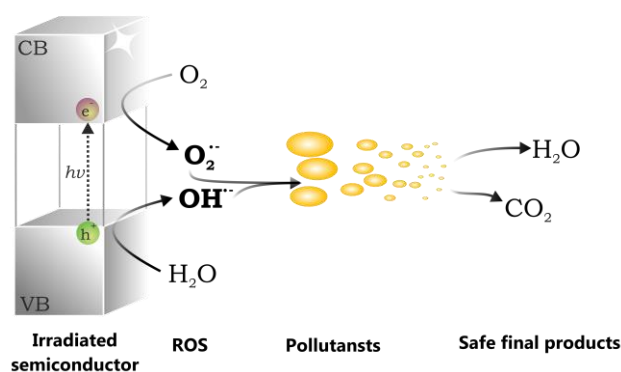


Figure 1. General mechanism of photocatalytic degradation of pollutants.

mineralization and the possible products are: CO_2 , H_2O , Cl^- , NO_3^- , SO_4^{2-} and other small and safe molecules or ions. The degradation of the pollutants follows the pseudo first-order kinetics, that indicates that the reaction is controlled by the surface chemical reaction and the reaction rate is controlled by concentration of pollutants.^{5,6} The reaction yield depends also on other factors such as oxygen or water amount. Increasing humidity enhances the formation of $\cdot OH$ radicals which overcomes the negative competitive adsorption of H_2O molecules.⁷ Slightly different conclusion was reported by Cazoir et al.⁸ In view of the results, authors suggest that mechanism of reaction strongly depends on the humidity of environment. Light (wavelength and intensity) is a crucial factor for reaction efficiency, and it will be discussed below.

Organic and inorganic air pollutions are a major issue leading to many serious illnesses. Irritation of respiratory tract and eyes, headaches, dizziness, visual disorders, and memory impairment are the symptoms that people have experienced soon after exposure to some organics. Many volatile organic compounds are known to cause cancer in humans and animals. Air pollutants are particularly dangerous because of its high mobility. Volatile organic

compounds (VOCs) are widespread components of air pollutions. Photocatalytic oxidation is considered as a very promising method of VOCs removal from indoor air. Literature mentions long list of tested model pollutants that can be photocatalytically removed from air: aliphatic and aromatic hydrocarbons (particularly dangerous polycyclic aromatic hydrocarbons), halogenated compounds, alcohols, ethers, aldehydes, sulphur- and nitrogen-containing compounds, esters, pesticides, herbicides and others.^{9–15} Among the above air pollutants are mono-nitrogen oxides NO and NO₂, a group of highly reactive gases. NO_x comes primarily from vehicles exhausts and cannot be completely eliminated by catalytic converters. NO_x has severe environmental and health effects. Nitrogen dioxide is unhealthy to breathe, especially by children, asthmatics and people with chronic obstructive pulmonary disease. NO_x may react with VOCs in the presence of sunlight to form ozone that damage lung tissue and reduction in lungs function. NO_x together with sulfur oxide are also a precursors for acid rain, and NO_x contributes to global warming.

The review is divided into three main sections that are related to materials engineering, types of photoreactors and commercial application of photocatalytic materials towards air cleaning. We would like to discuss photocatalytic degradation of air pollutants from modeling, photoreactor design, and materials study through laboratory experiment to large scale application.

Material engineering

The first issue concerning the successful photocatalytic air cleaner is related to materials. An ideal photocatalyst should have following features: i) appropriate potentials of conduction and valence band edges that allow the reactive oxygen species formation from O₂ and H₂O, ii) appropriate band gap energy, iii) long lifetime of the separated electrons and holes, iv) activity upon irradiation with light of possibly low energies, preferably with visible light, v) high stability and photo stability, vi) possible low environmental impact, vii) low cost, viii) favorable morphological properties such as high specific surface area. Band structures of several common semiconductors are shown in Fig. 2.

Properties of photocatalysts greatly depend on synthesis process. Majority of photocatalyst was prepared by one of the following general methods: sol-gel method,^{6,16} hydrothermal technique,^{6,7} ultrasonic-assisted method,¹⁷ electrochemical method,¹⁸ ultrasonic spray pyrolysis,¹⁹ microwave assisted synthesis.²⁰ Many properties of semiconductor can influence a photocatalytic reaction. Therefore, photocatalysts are modified and developed in order to increase the yield of light conversion, change the direction or selectivity of reaction, enhance the resistance to photo corrosion and poisoning, etc. The main methods of improving photocatalysts are listed below and discussed in detailed in the next subsections:

- lowering of the particles size (preparation of nanocrystalline photocatalysts),
- sensitization towards visible light (surface modification, doping, composites of semiconductors),

- modification of the photocatalyst with co-catalyst (e.g. deposition of metal nanoparticles or transition metal complexes),
- use of the supports (e.g. zeolites, carbon nanotubes, aerogels, aluminum oxide, silica, glass beads, fibers or pellets, organo-clays, paper),
- structural and morphological modifications (increase of specific surface area, presence of surface hydroxyl groups).^{1,21}

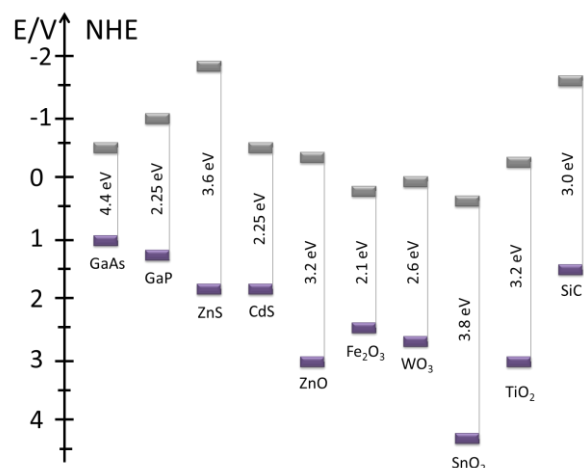


Figure 2. Band gap energies and potentials of band edges of selected semiconductors at pH = 7.

Titanium dioxide based materials are commonly used for photo-catalytic degradation of both, organic and inorganic pollutants. Success of TiO₂ results from several advantages of these wide-bandgap semiconductors such as stability in the dark and under irradiation, insolubility in water, lack of toxicity and safety for the environment. The lifetime of photogenerated charges are relatively long - this facilitates the interfacial charges transfer. Wide band gap is disadvantage of titanium dioxide that limits the use of solar light – energy of band gap is 3.2 eV for anatase, 3.0 eV rutile and 3.23 eV for brookite (see Fig. 2).^{1,22}

Many papers concerned with the use of TiO₂ as a photocatalyst have been published within last years. It should be noticed that number of scientific reports on titanium dioxide is incomparably greater than that for other materials; thus several following paragraphs will be dedicated to the use of pure and modified TiO₂. Majority of reports describes the possibility of use titanium dioxide excited by UV light and discuss various aspect of reaction e.g. properties of material, photoreactor type, the influence of model pollutants (in particular the probe of degradation especially danger compound like NO_x), the influence of oxygen and water concentration.^{10,11,23} Commercial titanium dioxide (e.g. P25-Evonic, Hombicat UV100) shows some photocatalytic activity, however nanocrystalline materials seems to be more promising. Combining advancements in nanotechnology, a nanostructure titanium dioxide with controlled particles size, surface area, and morphology has been designed, synthesized and tested as photocatalyst for pollutants degradation. Recent reports are summarized in Table 1.

Table 1. Summarizon of nanocatalytic TiO₂ based photocatalyst

TiO ₂ based photocatalyst	Pollutant and the efficiency of its degradation
TiO ₂ nanotubes ²⁴	Toluene, 30-100 % degradation in 30 min
Microporous anatase TiO ₂ nanoparticles ²⁵	Toluene, removed 77 %
TiO ₂ anatase nanoplates ²⁶	Acetaldehyde, NO, NO ₂
Zeolite based nano TiO ₂ ²⁷	Acetaldehyde
Nanofibers TiO ₂ ²⁸	Elementary mercury, 6-68 % conversion
Nano-TiO ₂ -based architectural mortar ²⁹	NO, bacteria (<i>E. coli</i>)
TiO ₂ nanoparticles layer ³⁰	Toluene, higher than 95 % and elimination rates up to 75 mg m ⁻² h ⁻¹
TiO ₂ nanotubes ³¹	Toluene, acetaldehyde, 0.09 min ⁻¹
TiO ₂ nanorods ³²	NO, 9-50 % conversion

TiO₂ nanotubes were tested as a photocatalyst for NO and NO₂ degradation under UV-A irradiation (λ in range 315–400 nm).³³ Results suggested that reaction rate of NO degradation was much faster than that of NO₂. Transformation of NO₂ to nitrate seems to be the rate-limiting step. However during 4h experiment up to 80 % of initial amount of NO_x was removed. Titanium dioxide exhibit also the activity towards degradation of SO₂.¹⁴ Photocatalytic oxidation removes up to around 40 % of the initial amount of SO₂ (14ppm).

Photo-catalyst's properties can be influenced by metal(0) particles deposition on its surface. The deposited metal can be regarded as an electron sink or a co-catalyst. The ability of charge trapping is related to the work function of the metals, which are usually higher than those of many common semiconductors. Moreover, metal as a co-catalyst offers the reaction sites and catalyzes the reactions and promotes the charge separation (increase in the lifetime of electron-hole pairs).³⁴ Pt on TiO₂ with various amounts of platinum was prepared by photocatalytic deposition and tested in photocatalytic degradation of indoor air contaminations.³⁵ Einaga et al. discussed the presence of platinum at TiO₂ on the reaction selectivity.³⁶ Coverage of TiO₂ surface with Pt has a noticeable effect on toluene oxidation activity at room temperature and the bigger amount of intermediate compounds was observed in comparison to neat TiO₂, however at higher temperature Pt on TiO₂ showed enhanced activity. It has been proved that also other metals like silver may enhance the photocatalytic activity, as has been reported for Ag on TiO₂ and Ag on ZnAl₂O₄ (*vide infra*).³⁷ Ag on TiO₂ thin films exhibited the rewarding performance for benzene, toluene, ethylbenzene and xylene degradation under visible light.¹⁶ The maximum degradation efficiency is for xylene (89 %), followed by ethylbenzene (86 %), toluene (83 %) and benzene (79 %). Similar, TiO₂ (P25) modified with Ag, Au, Pt and Pd clusters exhibits high efficiency in toluene removal.³⁸

Photosensitization of semiconductors by surface modification can be achieved by using organic or inorganic chromophores. Three various mechanisms are commonly known: i) direct photosensitization (optical charge transfer), ii) photosensitization involving an electron injection from

the excited photosensitizer to the conduction band of semiconductor, iii) photosensitization involving a hole injection from the excited photosensitizer to the valence band of semiconductor.³⁹ A series of materials based on titanium dioxide modified with platinum or chromium compounds (Cr₂O₇²⁻ on TiO₂, [PtCl₆]²⁻ on TiO₂, [CrO₃F]⁻ on TiO₂, CrF₃ on TiO₂) were studied in photocatalytic oxidation of volatile air pollutants.⁴⁰ All materials were more active than neat commercially available TiO₂ under visible light.

Doping is one of the common methods of semiconductors modification leading to band gap energy diminution. Some metals or nonmetals can provide additional energy levels within the band gap of the semiconductor. Electron excitation from the valence band to the acceptor level or from the donor level to conduction band, requires a lower photon energy compared with the direct semiconductor excitation.³⁴ C/TiO₂ can be given as an example.⁴¹ Degradation of NO_x under visible light irradiation vary from 7 % to 18 %. Ag/TiO₂ has been tested as a catalyst of transformation of phenol and oxalic acid.⁴² Shie et al. studied photodegradation kinetics of toluene using nitrogen doped titanium dioxide modified by radio frequency plasma.⁴³ Reaction efficiencies of toluene degradation for modified material were higher than those of commercial TiO₂ (P25). Visible light activity of titanium dioxide was achieved by doping with iron or cobalt ions.^{5,44} Fe-doped TiO₂ can remove indoor contaminations such as formaldehyde, benzene, ammonia under solar light. The removal percentage of above compound after 9 h of irradiation achieved 55 % (HCOH), 53.1 % (NH₃), and 37.5 % (C₆H₆), when they existed in the air individually however in case of the mixture of all gases the removal percentage decreased to 33.3 %, 28.3 %, and 28 %, respectively.⁵ Efficiency of benzene degradation varied from 2.1 % to 51.5 % in the presence of Co-doped TiO₂.⁴⁵ Other example based on lanthanum doped TiO₂ (titania nanotubes).⁶ The properties of this material were determined by the photocatalytic degradation of gaseous ethylbenzene.

Composites of two semiconductors are other group of photocatalysts. Formation of composites has various goals. The most important aim is to obtain photosensitization effect and better charge separation. A photosensitization through formation of composites of two semiconductors involves excitation of the narrow bandgap semiconductor, followed by electron transfer from its conduction band to the valence band of the wide bandgap semiconductor. Moreover, ingredient of composite can also play a role of support. Open-cell self-bonded SiC foams were used as a support for TiO₂ in the gas phase photocatalytic degradation of methylethylketone.⁴⁶ Titania-graphite composite is the other example, that has been tested for degradation of acetaldehyde upon visible light irradiation.¹² Andryushina and Stroyuk studied the influence of graphene oxide on photocatalytic activity of titanium dioxide in gas-phase alcohols and hydrocarbons oxidation.⁹ These authors found, that the presence of graphene oxide accelerated the photocatalytic oxidation of ethanol and benzene because of interaction of graphene oxide with the TiO₂ surface via anchoring functional groups and high efficiency of accepting of the photogenerated electrons. Similarly, Nikkanen et al. observed enhanced photocatalytic properties of TiO₂ coated steel by the application of silicon oxide intermediate layer.⁴⁷ Bi₂O₃/TiO₂ is an interesting example of

obtaining the photosensitization effect by formation of composite and the mechanism is presented in Fig. 3.⁴⁸ Studied material showed higher photocatalytic activity for the degradation of isopropanol in gas phase than Bi_2O_3 and TiO_2 . Two hours of irradiation resulted in degradation of 75 % of isopropanol. Authors suggested that TiO_2 acts as a principal photocatalyst while Bi_2O_3 plays a role of light harvester. Similar mechanism was observed also in other cases. $\text{LaVO}_4/\text{TiO}_2$ heterojunction nanotubes were prepared by sol-gel method in order to obtain visible light active material and the photocatalytic activity was demonstrated by catalytic degradation of gaseous toluene.¹³ Composites presented high photodegradation efficiency. The conversion of toluene ($c_0=120$ ppm) over 1 % $\text{LaVO}_4/\text{TiO}_2$ reached 75 % after 6h of irradiation (in case of P25 it was about 10 %). The enhanced performance of heterojunction nanotubes was attributed to the matching band potentials, the interconnected heterojunction of LaVO_4 versus titanium dioxide as well as small particles size and big surface area.

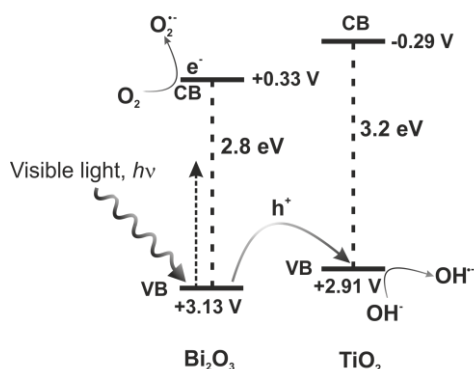


Figure 3. Mechanism for the photocatalytic activity of $\text{Bi}_2\text{O}_3/\text{TiO}_2$ heterojunction photocatalyst.⁴⁸

Over the last few years ZnO, in particular nanocrystalline ZnO, has become the object of scientific interest. However, majority of the reports about photocatalytic application of ZnO have been focused on the photodegradation of pollutants in water. The comparison of photo-activities of ZnO and TiO_2 seems to glorify the titanium oxide: the rate constant of TiO_2 for HCHO degradation was 0.05 min^{-1} which was two orders of magnitude larger than that of zinc oxide.⁴⁹ However, high photocatalytic activity towards degradation of formaldehyde in gas phase has been demonstrated for nano-ZnO on bone char.⁵⁰ Published results show, that maximum decomposition efficiency of formaldehyde was 73 % using continuous flow reactor (inlet formaldehyde concentration 2.5 mg/m^3). ZnO also exhibited good efficiency of degradation of NO_x .⁵¹ Photocatalytic activity for the decomposition of NO_x under visible light as well as UV irradiation was superior to that of commercial TiO_2 powders. ZnO/carbon quantum dots composite is an interesting example of photosensitization toward visible light.⁵² Such material was used as superior photocatalyst for the degradation of benzene and methanol, and the results showed that composites exhibit higher activity (degradation efficiency over 80 %, 24 h) compared to pure TiO_2 or ZnO. Synergistic effect for the activity and photocatalytic property has been demonstrated also for other composites e.g. $\text{g-C}_3\text{N}_4/\text{ZnO}$.⁵³

Zinc and cadmium sulfide based materials are the next big group of active photomaterials. Metal sulfides, in particular ZnS, are very promising, buoyant photocatalysts for CO_2 conversion, water splitting as well as for organic compounds degradation.⁵⁴ Some metal sulfides (CdS , CdSe , PbS , and PbSe) as well as other chalcogenides also offer a significant advantage because of their tunable response to visible light. CdS is the most commonly studied and its photocatalytic activity for degradation of vapors of ethanol and isopropanol is noticeable.^{55,56} The morphology of cadmium sulfide can be easily controlled during preparation, and various particle shapes may be obtained e.g. nanowires, nanoribbons, hollow particles. Nonetheless, the activity of CdS as a photocatalyst for total degradation of organic compounds is not promising. Partial oxidation of ethanol and isopropanol to acetaldehyde and acetone was observed.⁵⁶ Total mineralization should be the goal of photocatalytic degradation, otherwise some more dangerous coproducts can be formed.

WO_3 is an attractive photocatalyst because small band gap energy as well as their stability and photostability. Materials based on WO_3 have been tested as a photocatalysts which are able to remove very toxic pollutants such as H_2S ; authors have reported complete degradation.⁵⁷ The $\text{WO}_3/\text{Cu}_2\text{O}$ composite, synthesized by hydrothermal method, was studied as a photocatalyst for air treatment.⁵⁸ Taking phenol as degradation target, the effects of the amount and kind of catalyst and other factors e.g. light source, air flow rate and initial concentration was investigated. The degradation rate of phenol was above 98 % in case of optimal conditions and irradiation time 180 min. In turn, Ag on WO_3 showed activity for acetone degradation three and six times higher than that of pure mesoporous WO_3 and nitrogen-doped TiO_2 , respectively (under visible-light irradiation).⁵⁹ Enhanced photocatalytic properties are attributed to the largely improved electron-hole separation in the Ag on WO_3 heterojunction.

Photocatalyst based on iron oxides and oxide-hydroxide has attracted some attention in recent years because its activity under visible light is, probably, due to the possible formation of singlet oxygen.⁴ $\alpha\text{-Fe}_2\text{O}_3$ is the most stable iron oxide, an example of *n*-type semiconductor with band gap energy of 1.9–2.2 eV. $\alpha\text{-Fe}_2\text{O}_3$ prepared from hollow $\alpha\text{-FeOOH}$ urchin-like spheres was tested as a catalyst of photodegradation of organic pollutants under visible light irradiation.⁶⁰ Decomposition of the model organic contaminants is associated with ROS formation, which has been proved.⁶⁰

Besides all commonly used materials, literature gives more unique examples of photocatalysts. Cobalt oxide is one of them.⁶¹ Authors suggested the potential use of hierarchical structures of cobalt oxide as an alternative to titanium dioxide for photodegradation of organic contaminants. 3 hours of irradiation resulted in 80 % degradation of acetaldehyde. Moreover, the big advantage of Co_3O_4 is its activity under visible light. Chromium oxide is the next oxide material suggested as a photocatalyst for degradation of volatile organic compounds.⁶² Authors reported a turnover number 17 in case of the most active catalyst 0.5 mol% Cr-SiO_2 , however, the use of chromium compounds for environmental protection seems to be dangerous and should be considered very carefully. Also cerium oxide has been studied as a photocatalyst. With regard to the sample of CeO_2 -nanoparticles, the conversion

ratio of benzene at the initial stage was 2.2 %; after reaction (22 h) it decreased to 1.4 %.⁶³ Porous graphitic carbon nitride was synthesized and coupled with the MoS₂ nanosheets to form MoS₂/C₃N₄ hetero-structures in which MoS₂ served as electron-trapper to extend the lifetime of separated electron-hole pairs.⁶⁴ Bi₂WO₆ is an active photomaterial in visible light. Photocatalytic properties of Bi₂WO₆ modified with polyaniline (PANI) has been investigated using gaseous acetaldehyde as a model air contaminant.⁶⁵ CH₃CHO was degraded by the Bi₂WO₆ and PANI/Bi₂WO₆ with production of water and CO₂ under visible light irradiation. Going to another example, it has been reported, that 1 % Ag on ZnAl₂O₄ nano-particles were more active than neat materials as well as commercial P25 in photo-catalytic oxidation of gaseous toluene.³⁷ Authors suggested, that hydroxyl groups on the surface of nanomaterial are able to react with the product of oxidation, which is retained on the surface leading to the progressive deactivation of the catalyst in the gas-solid system. The BiOI/BiOCl composites showed enhanced visible light activity for removal of NO because of the large specific surface areas and pore volume, hierarchical nanostructure and modified band potentials, exceeding that of commercially available TiO₂, BiOI, and Bi₂WO₆.⁶⁶

The photocatalytic inactivation of microorganisms in air is an important aspect of photocatalytic air cleaning. Photocatalysis has ability to kill broad range of microorganisms including Gram-positive and Gram-negative bacteria, endospores, fungi, algae, protozoa and viruses, as well as prions.⁶⁷ Photocatalysis can also destroy endospores and microbial toxins. Tests in real conditions, as well as feasibility of elimination of bacteria in laboratory scale, have been studied.⁶⁸ Elimination ratio vary from few percent up to 80 % depending on the conditions and applied materials. Inactivation of *Escherichia coli*, *P. aeruginosa*, *Anabaena*, *Legionella pneumophila* are the most commonly tested processes involving neat and modified TiO₂, CuO or WO₃.^{69–72} The typical mechanism of inactivation of microorganism is shown in Fig. 4. However, not all microorganisms can be photo-inactivated. The published results showed that species like *Staphylococcus pasteurii*, *Staphylococcus saprophyticus*, *Stenotrophomonas maltophilia*, *Macroccoccus equiperficus*, *Naxibacter haematophilus*, and *Bacillus endophyticus* were resistant to photocatalytic treatment.⁶⁸

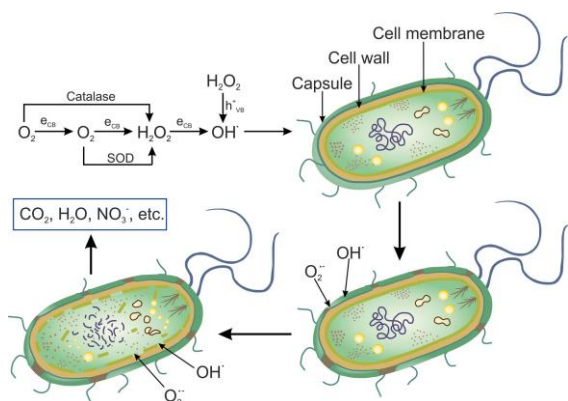


Figure 4. Mechanism of photocatalytic inactivation of bacteria.

Photoreactor design

The photo-catalytic performance for air cleaning strongly depends on the design of an efficient photocatalytic reactor. The main performance parameters of a photocatalytic reactor are the factor of mass transfer rate and the factor of light delivery, thus typical photo-reactor is constructed of two important parts: support for photocatalytic filter and a light source. The features of an ideal photoreactor are:

- high specific surface area for a large reaction area;
- energy-saving appropriate light source with appropriate wavelength,
- high mass transfer,
- high residential time.

Several types of reactors have been developed *e.g.* a flow-through photo-reactor,¹¹ bed packed photoreactor,¹⁰ honeycomb monolith reactor,⁷³ continuous flow reactor.⁵⁰ Schematic diagrams of various photoreactors for air purification are shown in Fig. 5.^{74–77} Detailed descriptions of all types of photoreactors are given elsewhere and there is no point to repeat these.^{78–80} An interesting example is the use of 3D printed gas-phase photocatalysis reactor because the 3D printer availability will allow the design and produce photo-reactor in very easy way.⁸¹

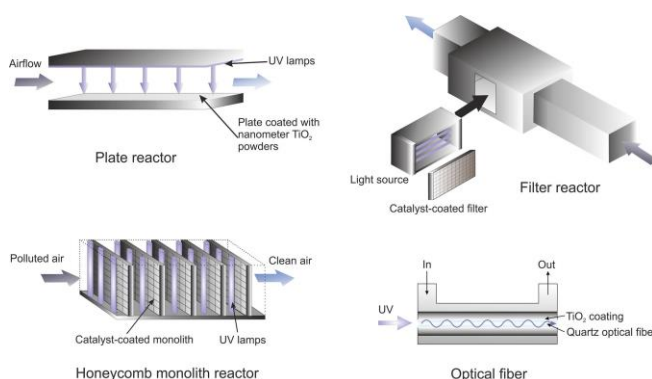


Figure 5. Schematic diagrams of various photoreactors for air purification.^{74–77}

The most common light sources for photocatalysis are the black-light-type UV lamp that emits light in the UVA band (λ_{max} 355 nm), high pressure mercury vapors lamp (λ 184, 253, 365, 404, 435, 546, 578 nm) and xenon lamp (visible light). Lately, light emitting diodes (LEDs) that can emit ultraviolet light (360 and 400 nm) or visible light are being considered as a better light source because of their many advantages. The LED save significant amount of energy in comparison to the UV lamps or HBO and XBO. LEDs are durable, robust, efficient, and can be easily installed in any configuration.⁸² Many examples of the use of LED driven photosystem for air cleaning can be given.^{40,82} Much work has been done in order to check the influence of light source and light intensity for the reaction efficiency.

The effect of light intensity (35, 225 and 435 $\mu\text{W cm}^{-2}$) on photocatalytic degradation using TiO_2 was studied and the obtained results prove that the removal efficiency increased with increasing of light intensity. It vary from 0.035 to 0.130 $\text{mg L}^{-1} \text{min}^{-1}$ for the lowest and highest light intensity respectively.⁸³

Commercial applications of photocatalysts

Within last 10 years photocatalysis has become more and more attractive for the industry with regard to the development of technologies for water and air purification. The market of photocatalytic products is increasing and photocatalysis is considered as a future technology. According to a market research report, the global market value for photocatalysts was estimated at the level of 847.5 million dollars in 2009 and was expected to reach 1.7 billion dollars in 2014. Products for the construction sector and consumer products account for the largest share of the market. The use of titanium dioxide as coating in buildings has received highest interests due to its excellent ability to purify the environment by capturing the pollutants both in the indoor and outdoor air. TiO_2 can be incorporated into coatings and paints, plastics and fabrics, concrete and plaster, glass, including pavement blocks, wood-based panels, plaster (gypsum) boards, ceiling tiles, ceramic tiles and wall papers.⁸⁴

Photocatalytically active paints can be used in outdoor applications on so called self-cleaning facades and for degradation of nitrogen oxides in street as well as in indoor application due to antimicrobial, antifungal properties of the paint or because of its ability to decompose organic and inorganic pollutants. For internal applications it is specially dedicated by producer for places, which require the elimination of noxious and toxic air substances in hospitals, schools, public buildings, shops, magazines of food, convention centers, food-processing plants, factories, poultry and livestock sheds. Many buildings in developed countries are constructed with photo catalytic materials or paints. Ecogreen PlusTM, KNOxOUT or Sto AG can be given as examples of photocatalytic paint brands. Auvinen and Wirtanen noticed, that the organic components of paints may be decomposed by photocatalytic reaction.^{85,86} Self-degrading effect leads to an increase in the concentration of organic compounds, like aldehydes and ketones, that are quite stable indoor as air pollutants and decrease the quality of the air. It should be highlighted, that to prohibit this kind of back-effect, all components of paints should be stable enough to endure highly active radicals.

An interesting application of photo-catalysis is covering the glass (windows) with photocatalyst. Such windows have two attractive features: self-cleaning (mainly from outside) and photocatalytic degradation of air pollutants (mainly the inner side). Photo-catalytic surfaces show super-hydrophilic effect, allowing dirt to be washed off - self-cleaning windows and self-cleaning glass covers for highway tunnel lamps (e.g. San Gobain BiocleanTM, Pilkington ActiveTM and SuncleanTM).⁶⁷

The use of photo-catalysis for air cleaning has caught the interest of industry. Photocatalytic reactors can be integrated with conditioning and ventilation systems. Several

companies (e.g. AirOasis, Indoor Purification Systems Inc., Daiken Chemical Co. Ltd., Life Air IAQ Ltd., Laiyang ZiXiLai Environmental Protection Technology Co. Ltd.) produce the photocatalytic air purifiers equipped with TiO_2 coated filters and UV lamps.

Slimen and coauthors studied very interesting practical aspect of photocatalysis – degradation of cigarette smoke.⁸⁷ The TiO_2 -impregnated titanium mesh filter revealed high activity for the removal of nicotine, ammonium, 3-ethenylpyridine, and tar, which constitute some of the compounds of cigarette smoke. The prototype air purifier was composed of six photocatalyst units, some additional filters and a fan. Experiments carried out in the 1 m^3 box and operated in an air flow of $>10 \text{ m}^3 \text{min}^{-1}$ showed a significant decrease in the acetaldehyde concentration ($\sim 80 \%$). Other very interesting application of photocatalysis is the use of nano-photo-filters in air quality control system of airliner cabin.⁸⁸ Long-term usable air-cleaner based on the synergy of photo-catalysis and plasma treatments has been also tested for degradation of cigarette smoke.⁸⁹ In one case of the treatment of smoke from tobacco worth 12,000 cigarettes, the air-cleaner maintained high-level air-purification activity (close to 100 % of the total suspended particulate and 88 % of total volatile organic compound) at single-pass conditions.

Conclusion

Some people consider photocatalysis as a *science fiction*. Looking at this article, it is difficult to agree with such people. This review highlights several current aspects for the preparation and improvement of photocatalysts such as surface modification, doping, formation of composites, quantum-size effects and surface coverage with metal nanoparticles. There is no one simple recipe to prepare efficient material. Various applications (bacteria inactivation, degradation of organic or inorganic pollutants) require different properties of photocatalyst. Scientists are looking for the correct direction. Often they go astray but science, as a whole, is going forward. Photo-catalysis appears (perhaps still timidly) to be working in our houses, offices, schools, hospitals and cars.

References

- ¹Carp, O., Huisman, C. L., Reller, A., *Prog. Solid State Chem.*, **2004**, 32(1–2), 33.
- ²Nosaka, Y., Daimon, T., Nosaka, A. Y., Murakami, Y., *Phys. Chem. Chem. Phys.*, **2004**, 6(11), 2917.
- ³Wojtyła, S., Pilarczyk, K., Regiel-Futyr, A., Macyk, W., XXVth IUPAC Symp. Photochem., Bordeaux, France, **2014**.
- ⁴Wojtyła, S., Baran, T., Regiel-Futyr, A., Buchalska, M., Macyk, W., *Polish Conf. Students PhD Students*, Lublin, Poland, **2014**.
- ⁵Wang, S., Yu, H., Cheng, X., *J. Chem.*, **2014**, e829892.
- ⁶Cheng, Z.-W., Feng, L., Chen, J.-M., Yu, J.-M., Jiang, Y.-F. J., *Hazard. Mater.*, **2013**, 254-255, 354.
- ⁷Zhao, W., Dai, J., Liu, F., Bao, J., Wang, Y., Yang, Y., Yang, Y., Zhao, D., *Sci. Total Environ.*, **2012**, 438, 201.

- ⁸Cazoir, D., Vildoza, D., Sleiman, M., Ferronato, C., Fine, L., Chovelon, J.-M., *Int. J. Environ. Anal. Chem.*, **2012**, 92(8), 923.
- ⁹Andryushina, N. S., Stroyuk, O. L., *Appl. Catal. B Environ.*, **2014**, 148–149, 543.
- ¹⁰Monteiro, R. A. R., Miranda, S. M., Rodrigues-Silva, C., Faria, J. L., Silva, A. M. T., Boaventura, R. A. R., Vilar, V. J. P., *Appl. Catal. B Environ.*, **2015**, 165, 306.
- ¹¹Moulis, F., Krýsa, J., *Res. Chem. Intermed.*, **2015**, 1.
- ¹²Wang, J., Ou, E., Li, J., Yang, X., Wang, W., Yan, Z., Li, C., *Mater. Sci. Semicond. Process.*, **2015**, 31, 397.
- ¹³Zou, X., Li, X., Zhao, Q., Liu, S., *J. Colloid Interface Sci.*, **2012**, 383(1), 13.
- ¹⁴Krishnan, P., Zhang, M.-H., Cheng, Y., Rieng, D. T., Yu, L. E., *Constr. Build. Mater.*, **2013**, 43, 197.
- ¹⁵Prakash, A. M., Swamy, A. V. V. S., Krishna, R. H., *Eur. Chem. Bull.*, **2012**, 2(1), 28.
- ¹⁶Peerakiatkhajorn, P., Chawengkijwanich, C., Onreabroy, W., Chiarakorn, S., *Mater. Sci. Forum*, **2012**, 712, 133.
- ¹⁷Neppolian, B., Wang, Q., Jung, H., Choi, H., *Ultrason. Sonochem.*, **2008**, 15(4), 649.
- ¹⁸Sulka, G. D., Kapusta-Kołodziej, J., Brzózka, A., Jaskuła, M., *Electrochimica Acta*, **2010**, 55(14), 4359.
- ¹⁹Huang, J., Ho, W., Lee, F. S. C., *Sci. Adv. Mater.*, **2012**, 4 (8), 863.
- ²⁰Jia, X., He, W., Zhang, X., Zhao, H., Li, Z., Feng, Y., *Nanotechnology*, **2007**, 18(7), 075602.
- ²¹Colmenares, J. C., Luque, R., *Chem. Soc. Rev.*, **2014**, 43(3), 765.
- ²²Di Paola, A., Cufalo, G., Addamo, M., Bellardita, M., Camprostrini, R., Ischia, M., Ceccato, R., Palmisano, L., *Colloids Surf. Physicochem. Eng. Asp.*, **2008**, 317(1–3), 366.
- ²³Gandolfo, A., Bartolomei, V., Gomez Alvarez, E., Tlili, S., Gligorovski, S., Kleffmann, J., Wortham, H., *Appl. Catal. B Environ.*, **2015**, 166–167, 84.
- ²⁴Nischk, M., Mazierski, P., Gazda, M., Zaleska, A., *Appl. Catal. B Environ.*, **2014**, 144, 674.
- ²⁵Lyu, J., Zhu, L., Burda, C., *ChemCatChem*, **2013**, 5(10), 3114.
- ²⁶Sofianou, M.-V., Psycharis, V., Boukos, N., Vaimakis, T., Yu, J., Dillert, R., Bahnemann, D., Trapalis, C., *Appl. Catal. B Environ.*, **2013**, 142–143, 761.
- ²⁷Izadyar, S., Fatemi, S., *Ind. Eng. Chem. Res.*, **2013**, 52(32), 10961.
- ²⁸Yuan, Y., Zhao, Y., Li, H., Li, Y., Gao, X., Zheng, C., Zhang, J., *J. Hazard. Mater.*, **2012**, 227–228, 427.
- ²⁹Guo, M.-Z., Ling, T.-C., Poon, C.-S., *Cem. Concr. Compos.*, **2013**, 36, 101.
- ³⁰Maury-Ramirez, A., Demeestere, K., De Belie, N., *J. Hazard. Mater.*, **2012**, 211–212, 218.
- ³¹Pichat, P., *Mol. Basel Switz.*, **2014**, 19(9), 15075.
- ³²Zhang, D., Wen, M., Zhang, S., Liu, P., Zhu, W., Li, G., Li, H., *Appl. Catal. B Environ.*, **2014**, 147, 610.
- ³³Nguyen, N. H., Bai, H., *J. Environ. Sci.*, **2014**, 26(5), 1180.
- ³⁴Linsebigler, A. L., Lu, G., Yates, J. T., *Chem. Rev.*, **1995**, 95(3), 735.
- ³⁵Hong, G. B., Ma, C. M., *J. Nanomater.*, **2012**, 2012, e405361.
- ³⁶Einaga, H., Mochiduki, K., Teraoka, Y., *Catalysts*, **2013**, 3(1), 219.
- ³⁷Zhu, Z., Zhao, Q., Li, X., Li, Y., Sun, C., Zhang, G., Cao, Y., *Chem. Eng. J.*, **2012**, 203, 43.
- ³⁸Klein, M., Grabowska, E., Zaleska, A., *Physicochem. Probl. Miner. Process.*, **2015**, 51(1), 49.
- ³⁹Buchalska, M., Kunciewicz, J., Świętek, E., Labuz, P., Baran, T., Stochel, G., Macyk, W., *Coord. Chem. Rev.*, **2013**, 257(3–4), 767.
- ⁴⁰Baran, T., Macyk, W., *J. Photochem. Photobiol. Chem.*, **2012**, 241, 8.
- ⁴¹Lorencik, S., Yu, Q. L., Brouwers, H. J. H., *Appl. Catal. B Environ.*, **2015**, 168–169, 77.
- ⁴²Chen, Y., Xie, Y., Yang, J., Cao, H., Zhang, Y., *J. Environ. Sci.*, **2014**, 26(3), 662.
- ⁴³Shie, J.-L., Lee, C.-H., Chiou, C.-S., Chen, Y.-H., Chang, C.-Y., *Environ. Technol.*, **2014**, 35(5–8), 653.
- ⁴⁴Zhou, G., Wang, W., Zheng, B., Li, Y., *Eur. Chem. Bull.* **2013**, 2(12), 1045.
- ⁴⁵Huang, H., Ye, X., Huang, H., Hu, P., Zhang, L., Leung, D. Y. C., *Int. J. Photoenergy*, **2013**, 2013, e890240.
- ⁴⁶Masson, R., Keller, V., Keller, N., *Appl. Catal. B Environ.*, **2015**, 170–171, 301.
- ⁴⁷Nikkanen, J.-P., Huttunen-Saarivirta, E., Salminen, T., Hyvärinen, L., Honkanen, M., Isotahdon, E., Heinonen, S., Levänen, E., *Appl. Catal. B Environ.*, **2015**, 174–175, 533.
- ⁴⁸Chakraborty, A. K., Hossain, M. E., Rhaman, M. M., Sobahan, K., *J. Environ. Sci.*, **2014**, 26 (2), 458.
- ⁴⁹Liao, Y., Xie, C., Liu, Y., Chen, H., Li, H., Wu, J., *Ceram. Int.*, **2012**, 38(6), 4437.
- ⁵⁰Rezaee, A., Rangkooy, H., Khavanin, A., Jafari, A., *J. Environ. Chem. Lett.*, **2014**, 12(2), 353.
- ⁵¹Wei, Y., Huang, Y., Wu, J., Wang, M., Guo, C., Qiang, D., Yin, S., Sato, T., *J. Hazard. Mater.*, **2013**, 248–249, 202.
- ⁵²Yu, H., Zhang, H., Huang, H., Liu, Y., Li, H., Ming, H., Kang, Z., *New J. Chem.*, **2012**, 36(4), 1031.
- ⁵³Li, X., Li, M., Yang, J., Li, X., Hu, T., Wang, J., Sui, Y., Wu, X., Kong, L., *J. Phys. Chem. Solids*, **2014**, 75(3), 441.
- ⁵⁴Dibenedetto, A., Stufano, P., Macyk, W., Baran, T., Fragale, C., Costa, M., Aresta, M., *ChemSusChem*, **2012**, 5(2), 373.
- ⁵⁵Rempel, A. A., Kozlova, E. A., Gorbunova, T. I., Cherepanova, S. V., Gerasimov, E. Y., Kozhevnikova, N. S., Valeeva, A. A., Korovin, E. Y., Kaichev, V. V., Shchipunov, Y. A., *Catal. Commun.*, **2015**, 68, 61.
- ⁵⁶Nasalevich, M. A., Kozlova, E. A., Lyubina, T. P., Vorontsov, A. V., *J. Catal.*, **2012**, 287, 138.
- ⁵⁷Alonso-Tellez, A., Robert, D., Keller, V., Keller, N., *Environ. Sci. Pollut. Res.*, **2013**, 21 (5), 3503.
- ⁵⁸Niu, F., Fu, F., Gao, X., Zhang, X., *Spec. Petrochem.*, **2014**, 31(2), 6.
- ⁵⁹Sun, S., Wang, W., Zeng, S., Shang, M., Zhang, L., *J. Hazard. Mater.*, **2010**, 178 (1–3), 427.
- ⁶⁰Hojamberdiev, M., Zhu, G., Eminov, A., Okada, K. J., *Clust. Sci.*, **2012**, 24(1), 97.
- ⁶¹Cheng, J. P., Shereef, A., Gray, K. A., Wu, J., *J. Nanoparticle Res.*, **2015**, 17(3), 1.
- ⁶²Peiris Weerasinghe, M. N., Klabunde, K. J., *J. Photochem. Photobiol. Chem.*, **2013**, 254, 62.
- ⁶³Tang, Z.-R., Zhang, Y., Xu, Y.-J., *RSC Adv.*, **2011**, 1(9), 1772.
- ⁶⁴Li, Q., Zhang, N., Yang, Y., Wang, G., Ng, D. H. L., *Langmuir*, **2014**, 30(29), 8965.
- ⁶⁵Wang, W., Xu, J., Zhang, L., Sun, S., *Catal. Today*, **2014**, 224, 147.
- ⁶⁶Dong, F., Sun, Y., Fu, M., Wu, Z., Lee, S. C., *J. Hazard. Mater.*, **2012**, 219–220, 26.

- ⁶⁷Foster, H. A., Ditta, I. B., Varghese, S., Steele, A., *Appl. Microbiol. Biotechnol.*, **2011**, 90(6), 1847.
- ⁶⁸Sánchez, B., Sánchez-Muñoz, M., Muñoz-Vicente, M., Cobas, G., Portela, R., Suárez, S., González, A. E., Rodríguez, N., Amils, R., *Chemosphere*, **2012**, 87(6), 625.
- ⁶⁹Ishiguro, H., Yao, Y., Nakano, R., Hara, M., Sunada, K., Hashimoto, K., Kajioka, J., Fujishima, A., Kubota, Y., *Appl. Catal. B Environ.*, **2013**, 129, 56.
- ⁷⁰Castillo-Ledezma, J. H., López-Malo, A., Pelaez, M., Dionysiou, D. D., Bandala, E. R., *J. Surf. Interfaces Mater.*, **2014**, 2(4), 334.
- ⁷¹Hou, Y., Li, X., Zhao, Q., Chen, G., Raston, C. L., *Environ. Sci. Technol.*, **2012**, 46(7), 4042.
- ⁷²Priester, J. H., Mielke, R., Werlin, R., Orias, E., Holden, P., Gelb, J., *Microsc. Microanal.*, **2012**, 18(Supplement S2), 556.
- ⁷³Yu, K.-P., Lee, G. W.-M., Hung, A.-J., *J. Environ. Sci. Health Part A Tox. Hazard. Subst. Environ. Eng.*, **2014**, 49(10), 1110.
- ⁷⁴Obee, T. N., *Environ. Sci. Technol.*, **1996**, 30(12), 3578.
- ⁷⁵Hossain, M. M., Raupp, G. B., Hay, S. O., Obee, T. N., *AIChE J.*, **1999**, 45(6), 1309.
- ⁷⁶Choi, W., Ko, J. Y., Park, H., Chung, J. S., *Appl. Catal. B Environ.*, **2001**, 31(3), 209.
- ⁷⁷Vohra, A., Goswami, D. Y., Deshpande, D. A., Block, S. S., *Appl. Catal. B Environ.*, **2006**, 64(1–2), 57.
- ⁷⁸Andre, J. C., Viriot, M. L., Saïd, A., *J. Photochem. Photobiol. Chem.*, **1988**, 42(2–3), 383.
- ⁷⁹Jafarikojoor, M., Sohrabi, M., Royaei, S. J., Hassanvand, A., *CLEAN – Soil Air Water*, **2015**, 43(5), 662.
- ⁸⁰Leung, M. K. H., Yiu, C. W., In *Proc. ISES World Congr. 2007 (Vol. I – Vol. V)*, Goswami, D. Y., Zhao, Y., Eds., Springer Berlin Heidelberg, 2008, pp 441–445.
- ⁸¹Stefanov, B. I., Lebrun, D., Mattsson, A., Granqvist, C. G., Österlund, L., *J. Chem. Educ.*, **2015**, 92(4), 678.
- ⁸²Sharmin, R., Ray, M. B., *J. Air Waste Manag. Assoc.*, **2012**, 62(9), 1032.
- ⁸³Pansamut, G., Charinpanitkul, T., Biswas, P., Suriyawong, A., *Eng. J.*, **2013**, 17(3), 25.
- ⁸⁴Yu, C. W. F., Kim, J., *Indoor Built Environ.*, **2012**, 1420326X12470282.
- ⁸⁵Auvinen, J., Wirtanen, L., *Atmos. Environ.*, **2008**, 42(18), 4101.
- ⁸⁶Zhang, J., Wilson, W. E., Liou, P. J., *Environ. Sci. Technol.*, **1994**, 28(11), 1975.
- ⁸⁷Slimen, H., Ochiai, T., Nakata, K., Murakami, T., Houas, A., Morito, Y., Fujishima, A., *Ind. Eng. Chem. Res.*, **2012**, 51(1), 587.
- ⁸⁸Tao, H., Meng, L., Liping, P., Jun, W., *Procedia Eng.*, **2011**, 17, 343.
- ⁸⁹Ochiai, T., Ichihashi, E., Nishida, N., Machida, T., Uchida, Y., Hayashi, Y., Morito, Y., Fujishima, A., *Molecules*, **2014**, 19(11), 17424.

Received: 06.06.2015.

Accepted: 02.07.2015.



SILICA GEL SUPPORTED γ -FERRITE AS A HETEROGENOUS CATALYST FOR HIGH YIELD SYNTHESIS OF β -LACTAMS (2-AZETIDINONES) UNDER ECO-FRIENDLY CONDITIONS VIA 1,2,4-TRIAZOLES

Kalpana Avasthi^{[a]*}, Ritu Yadav^[a] and Ashish Bohre^[b]

Keywords: : Schiff bases, β -lactams, $\text{SiO}_2/\gamma\text{-Fe}_2\text{O}_3$, heterogenous catalyst, 1,2,4-triazoles.

A mild and efficient method has been reported for the preparation of Schiff base through the condensation reaction of various aromatic aldehydes with substituted aromatic amines in the presence of silica supported γ -Ferrite (ferric oxide) as a heterogeneous catalyst under solvent-free conditions. and this Schiff base used for Environmentally benign synthesis followed by the reaction with chloroacetylchloride in green conditions to yield the β -lactams (a-l) with excellent yields. The advantages of this eco-friendly, mild economic method are such as simplicity of the reaction procedure, moderate to high product yields, and simple working steps, very short reaction times.

* Corresponding Authors

Fax: 07582-264163

E-Mail: kalpana.avasthi@gmail.com

[a] Green Synthetic Organic Laboratory, Department of Chemistry, Dr. Hari Singh Gour central University, SAGAR (M.P.) 470003, INDIA.

[b] Catalysis laboratory, Department of chemistry, Delhi University, DELHI.

issues as climate change, energy production, availability of a safe and adequate water supply, food production, and the presence of toxic substances in the environment.²¹ A number of classic organic reactions, traditionally run in organic solvents, can be carried out in water with the proper design of catalysts and reaction conditions.²²

Introduction

A large number of 3-chloro monocyclic β -lactam possess powerful antibacterial, antimicrobial, anti-inflammatory, anticonvulsant, anti-tubercular and enzyme inhibition activity.¹⁻⁴ Synthesis of Schiff bases have been described in variant conditions using sulphuric acid⁵ and glacial acetic acid.⁶ 2-Azetidinone(β -lactam) ring system is the common structural feature of a number of broad spectrum β -lactam antibiotics, including penicillin, cephalosporin, carbapenems, nocardicins, monobactams, clavulanic acid, sub-lactams and azobactams, which have been widely used as chemotherapeutic agents to treat bacterial infections and microbial diseases.⁷ The need for effective β -lactam has motivated synthetic organic and medicinal chemists to design new functionalized 2-azetidinones. The 1 H-1,2,4-triazole compounds possess important pharmacological activities such antifungal and antiviral activities. 1,2,4-triazole residues are bearing in such type of drugs for e.g fluconazole⁸, the powerful azole antifungal agent as well as the potent antiviral N-nucleoside ribavirin.⁹ Furthermore, various 1,2,4-triazole derivatives have been reported as fungicidal¹⁰, insecticidal¹¹, anti-microbial¹², and some showed antitumor activity¹³, as well as anticonvulsants¹⁴, antidepressants¹⁵ and plant growth regulator anticoagulants¹⁶. Other laboratories reported the same biological activity of the triazole family¹⁷⁻¹⁹. In connection with our work on 1,2,4-triazole having hydrazide and β -lactam moieties, we demonstrate here some potency of the reported hydrazide and β -lactams derivatives of 1,2,4 triazole. Green chemistry is the design of chemical products and processes that reduce or eliminate the way of use and generation of hazardous substances.²⁰ Advances in green chemistry address both obvious hazards and those associated with such global

Microwave assisted heterocyclic synthesis is an efficient and Eco-friendly synthetic strategy for heterocyclic compounds and has now become a modern and powerful tool for green chemistry.²³⁻²⁵ Microwave technology has recent application for the cyclization reactions of heterocyclic compounds. Nowadays such type of important reactions like nucleophilic substitution, ring formation reaction are done by these green technology, Microwave irradiation has been applied to organic reactions in the absence of solvent and/or in the presence of a solid support, such as clays, alumina and silica, resulting in shorter reaction times and better product yields than those obtained by using conventional heating.²⁶⁻²⁷ A solvent-free or solid state reaction may be carried out using the reactants alone or incorporating them in clays, zeolites, silica, alumina or other matrices²⁸. In recent years, β -zeolite²⁹, montmorillonite clays³⁰, SiO_2 supported $\gamma\text{-Fe}_2\text{O}_3$ were employed as catalysts for this purpose to obtain relatively better results.

SiO_2 is a particularly interesting oxide as it is widely used industrially as filler, adsorbent, drying agent, catalyst support and reagent. $\gamma\text{-Fe}_2\text{O}_3$ is the inorganic oxide most commonly utilized to carry out surface organic chemistry.³¹ Although some of these methods represent a convenient procedure with good to high product yields, representation of a new, efficient and facile procedure for synthesis of these compounds can be very significant. In continuation of our research, because of these economical and environmental reasons, here we hope to report a procedure. Using $\text{SiO}_2/\gamma\text{-Fe}_2\text{O}_3$ as a catalyst for the synthesis of schiff bases from carbonyl compounds and different amines in the absence of a solvent under mild reaction conditions. The structures of all the newly synthesized compounds were confirmed by elemental analysis, IR, ^1H NMR, ^{13}C NMR, and HR-MS.

Experimental

All melting points were determined in open capillaries. The IR spectra were recorded on Shimadzu FT-IR 8300 Spectrophotometer. Samples were prepared by finely dispersing powder material on a KBr carrier. ^1H NMR and ^{13}C NMR spectra were measured on a Bruker DRX-300 spectrometer in CDCl_3 at 300 MHz using TMS as an internal standard. Chemical shifts reported on δ scales. The purity of the compounds was checked by thin layer chromatography (TLC) on silica gel (G-60 mesh) using chloroform: methanol as an eluent. Synthesized sample were purified by column chromatography using silica Gel (230-400 mesh). All other chemicals were purchased from Sigma-Aldrich and the reagent grade chemicals were purchased from commercial sources and further purified before use.

Reagents

All starting materials of commercial grade were purchased from Sigma-Aldrich and used without further purification. SiO_2 and Fe_2O_3 were purchased from Merck. The purity of all compounds was checked by TLC on glass plates coated with silica gel (E-Merck G254).

Preparation and determination of silica-supported γ -ferrite catalyst

The heterogeneous silica supported catalyst was prepared in our laboratory by simple combination method. The mixture of silica and γ -ferrite in appropriate ratio was mixed together and this reagent was heated in an oven at 100°C for 1 h and then the obtained homogeneous mixture, free flowing, white-red powder substance is sensitive towards moisture and thus should be stored in a sealed flask in a desiccator for later use. The exact loading of the γ -ferrite at the surface of silica was identified by IR spectra and prepared catalyst was then used for further catalytic study.

General procedure for the synthesis of Schiff base and β -lactams (2-Azetidinones) by using catalyst.

[a] Microwave method for the synthesis of (chloroacetyl)-3-mercapto-4-methyl-1,2,4-triazole (1)

An equimolar mixture of microwave method a solid supported mixture of compounds 3-mercapto-4-methyl-1,2,4-Triazole (0.01) and chloroacetylchloride (0.01) in ethanol was mixed thoroughly in open glass vessel and subjected to the microwave irradiation at low power setting (25 %, 200 W) for 2.40–4.15 min, then allowed to cool. The reaction progress was monitored by TLC using Chloroform: methanol solvents, when reaction was completed the reaction mixture was cooled and poured into crushed ice. The product obtained was filtered, dried, wash with water and recrystallized from ethanol to get compound **1**. The compound **1** was identified by spectrophotometric analysis. Molecular formula; $\text{C}_5\text{H}_6\text{ClN}_3\text{OS}$, Yield 80 %, m.p. 108 – 109°C , brown crystals. The structure was established on the basis of spectral analysis, IR (KBr), ν_{max} 1688, 1553, 1468, 1338 (1,2,4-triazole nucleus), 2592 (Ar-SH), 2825, 1476,

1210 (N-CH₃), 718 (S-CO-S) 1615 (S-CO) cm^{-1} ; ^1H NMR (CDCl_3) δ ppm : 8.42 (s, H, Ar-H of 1,2,4 triazole), 4.48 (s, 2H, CH₂), 3.60 (s, 3H, N-CH₃). ^{13}C NMR (CDCl_3 , 100 MHz). Four characteristic signals appeared for (N-CH₃), (aliphatic CH₂), (C of 1,2,4-triazole), (CO aliphatic) in the δ (ppm) ranges 27.1, 46.1–47.1, 160.4–162.5, 187.2–188.6 ppm, respectively. All these facts collectively suggest the successful synthesis of compound **1**.

[b] Microwave method for the synthesis of (hydrazinoacetyl)-3-mercapto-4-methyl-1,2,4-triazole (2)

A mixture of compound **1** (0.01 mol) and hydrazine hydrate (0.01 mole) in ethanol was performed in open glass vessel and subjected to the microwave irradiation at low power setting (25 %, 200 W) for 2–3 min. After cooling the product was filtered and purified over a column chromatography using chloroform: methanol (7:3 v/v). The purified product was recrystallized from ethanol at room temperature to yield compound **2**. The compound **2** was identified by spectrophotometric analysis. Molecular formula; $\text{C}_5\text{H}_9\text{N}_5\text{OS}$, Yield 81 %, m.p. 136 – 139°C , pale brown crystals. The structure was established on the basis of spectral analysis, IR (KBr) ν_{max} 1688, 1553, 1468, 1338 (1,2,4-triazole nucleus), 2825, 1476, 1210 (N-CH₃), 1668 (CO-NH), 3351 (NH₂) cm^{-1} ; ^1H NMR (CDCl_3) δ (ppm) : 8.42 (s, H, Ar-H of 1,2,4-triazole), 3.73 (s, 2H, CH₂), 3.62 (s, 3H, N-CH₃), 2.1 (s, 2H, NH₂), 2.0 (s, 1H, NH). ^{13}C NMR (CDCl_3 , 100 MHz) four characteristic signals appeared for (N-CH₃), (aliphatic CH₂), (C of 1,2,4 triazole), (CO aliphatic) in the δ (ppm) ranges 27.1, 66.1, 161.4–162.3, 193.2–196.6 ppm, respectively. All these facts collectively suggest the successful synthesis of compound **2**.

[c] Microwave method for the synthesis of [(2-(aryl)hydrazine-acetyl)-3-mercapto-4-methyl-1,2,4-triazoles (3)

A mixture of the compound **2** (0.01 mol) and arylaldehyde (0.01 mol) and $\text{SiO}_2/\gamma\text{-Fe}_2\text{O}_3$ in ethanol was performed in open glass vessel for 1 minute on microwave irradiation. The progress of reaction was monitored by TLC using hexane and ethyl acetate (9:1 v/v) as eluent. $\text{SiO}_2/\gamma\text{-Fe}_2\text{O}_3$ removed by filtration and the eluate was concentrated to give a product which was recrystallized from chloroform, to give compound **3a–3l** in excellent yield. The compounds **3a–3l** was identified by spectrophotometric analysis.

[(2-(4-Chlorobenzylidene) hydrazino acetyl) -3-mercapto-4-methyl-1,2,4-triazole (3a)

Molecular formula; $\text{C}_{12}\text{H}_{12}\text{ClN}_5\text{OS}$, Yield 94 %, m.p. 152 – 55°C , light yellow crystals. The structure was established on the basis of spectral analysis, IR (KBr) ν_{max} 1678, 1555, 1468, 1332 (1,2,4-triazole nucleus), 2822, 1470, 1215 (N-CH₃), ^1H NMR (CDCl_3) δ (ppm) : 8.44 (s, H, Ar-H of 1,2,4 triazole), 3.74 (s, 2H, CH₂), 3.59 (s, 3H, N-CH₃), 8.52 (s, 1H of azomethine), 2.0 (s, 1H, NH). ^{13}C NMR (CDCl_3 , 100 MHz)/four characteristic signals appeared for (N-CH₃), (aliphatic CH₂), (C of 1,2,4-triazole), (CO aliphatic), (C of aromatic aldehyde) in the δ (ppm) ranges 27.1, 63.1, 143.4–162.3, 196.6, and 128.9–131.6 ppm respectively. All these facts collectively suggest the successful synthesis of compound **3a**.

[(2-(2,4-Dichlorobenzylidene)hydrazinoacetyl]-3-mercapto-4-methyl-1,2,4-triazole (3b)

$C_{12}H_{11}Cl_2N_5OS$ Yield 91 %, m.p. 135-140 °C, light yellow crystals, IR(KBr) ν_{max} 1678, 1468, For 1,2,4-triazole nucleus, 1214 (N-CH₃), 755 (C-Cl), 1608 (N=CH); ¹H NMR (CDCl₃) δ (ppm): 8.44 (s, H, Ar-H of 1,2,4 triazole), 3.60 (s, 3H, N-CH₃), 3.76 (s, 2H, CH₂) 8.54 (s, 1H of azomethine), 2.0 (s, 1H, NH), 7.40, 7.70, 7.98 for benzylidimine; ¹³C NMR (CDCl₃) 27.1 (N-CH₃), 63.1 (aliphatic CH₂), 143.1-161.8 (C of 1,2,4-triazole), 196.5 (CO aliphatic) 128.3-132.6 (C of aromatic aldehyde); Mass (HRMS): m/z : 344, M⁺.

[(2-(2-Bromobenzylidene)hydrazinoacetyl]-3-mercapto-4-methyl-1,2,4-triazole (3c)

$C_{12}H_{12}BrN_5OS$; Yield: 88 %, m.p. 145-147 °C, light red powder, IR(KBr) ν_{max} 1677, 1452 for 1,2,4-triazole nucleus, 635 (C-Br), 1602 (N=CH), 1212 (N-CH₃); ¹H NMR (CDCl₃) δ (ppm): 8.42 (s, H, Ar-H of 1,2,4 triazole), 3.61 (s, 3H, N-CH₃), 3.76 (s, 2H, CH₂) 8.54 (s, 1H of azomethine) 2.0 (s, 1H, NH) 7.41-7.72, 7.58 for benzylidimine; ¹³C NMR (CDCl₃): 27.1 (N-CH₃), 63.7 (aliphatic CH₂), 143.1-162.8 (C of 1,2,4-triazole), 196.5 (CO aliphatic) 121.1-132.8 (C of aromatic aldehyde), 143.3 (C of azomethine); Mass (HRMS): m/z : 354, M⁺.

[(2-(3-Bromobenzylidene)hydrazinoacetyl]-3-mercapto-4-methyl-1,2,4-triazole (3d)

$C_{12}H_{12}BrN_5OS$, Yield 90 %, m.p. 142-144 °C, red powder, IR(KBr) ν_{max} 1674, 1468, (1,2,4-triazole nucleus), 1215 (N-CH₃), 635 (C-Br), 1602 (N=CH); ¹H NMR (CDCl₃) δ (ppm) 8.44 (s, H, Ar-H of 1,2,4-triazole), 3.60 (s, 3H, N-CH₃), 3.76 (s, 2H, CH₂) 8.54 (s, 1H of azomethine), 2.0 (s, 1H, NH) 7.41, 7.82, 7.58 for benzylidimine; ¹³C NMR (CDCl₃) 27.1 (N-CH₃), 63.7 (aliphatic CH₂), 143.1-162.5 (C of 1,2,4-triazole), 196.5 (CO aliphatic) 123.1-133.8 (C of aromatic aldehyde) 143.3 (C of azomethine); Mass (HRMS): m/z: 354, M⁺.

[(2-(4-Bromobenzylidene)hydrazinoacetyl]-3-mercapto-4-methyl-1,2,4-triazole (3e)

$C_{12}H_{12}BrN_5OS$. Yield 82 %, m.p. 145-146 °C, yellow powder, IR(KBr), ν_{max} 1674, 1468, (1,2,4-triazole nucleus), 1215 (N-CH₃) 638 (C-Br), 1609 (N=CH); ¹H NMR (CDCl₃) δ (ppm) 8.44 (s, H, Ar-H of 1,2,4-triazole), 3.60 (s, 3H, N-CH₃) 3.76 (s, 2H, CH₂) 8.54 (s, 1H of azomethine), 2.0 (s, 1H, NH) 7.70-7.58 for benzylidimine; ¹³C NMR (CDCl₃) 27.1 (N-CH₃), 63.7 (aliphatic CH₂), 143.1-162.5 (C of 1,2,4-triazole), 196.5 (CO aliphatic) 125.1-132.7 (C of aromatic aldehyde), 143.3 (C, of azomethine); Mass (HRMS): m/z: 354, M⁺.

[(2-(2-Methoxybenzylidene)hydrazinoacetyl]-3-mercapto-4-methyl-1,2,4-triazole (3f)

$C_{13}H_{15}N_5O_2S$. Yield 84 %, m.p. 150-152 °C, amorphous yellow powder, IR(KBr), ν_{max} 1672, 1462, (1,2,4-triazole nucleus), 1215 (N-CH₃), 2865 and 1170 (OCH₃) 1590

(N=CH). ¹H NMR (CDCl₃) δ (ppm) 8.42 (s, H, Ar-H of 1,2,4-triazole), 3.60 (s, 3H, N-CH₃), 3.76 (s, 2H, CH₂) 8.54 (s, 1H of azomethine), 2.0 (s, 1H, NH), 7.72, 7.26 for benzylidimine, 3.82 for 3H of OCH₃. ¹³C NMR (CDCl₃) 27.1 (N-CH₃), 63.8 (aliphatic CH₂), 143.1-162.6 (C of 1,2,4-triazole), 196.5 (CO aliphatic), 111.2-157.7 (C of aromatic aldehyde), 143.3 (C, of azomethine), 55.6 (C of OCH₃). Mass (HRMS): m/z: 305, M⁺.

[(2-(3-Methoxybenzylidene)hydrazinoacetyl]-3-mercapto-4-methyl-1,2,4-triazole (3g)

$C_{13}H_{15}N_5O_2S$ Yield 94 %, m.p. 151-152 °C, yellow powder, IR(KBr), ν_{max} 1672, 1462, (1,2,4-triazole nucleus), 1215 (N-CH₃), 2860, 1165 (OCH₃), 1598 (N=CH). ¹H NMR (CDCl₃) δ (ppm) 8.44 (s, H, Ar-H of 1,2,4-triazole), 3.60 (s, 3H, N-CH₃), 3.76 (s, 2H, CH₂) 8.54 (s, 1H of azomethine), 2.0 (s, 1H, NH), 7.52, 7.06 for benzylidimine, 3.83 for 3H of OCH₃. ¹³C NMR (CDCl₃): 27.1 (N-CH₃), 63.8 (aliphatic CH₂), 143.1-162.6 (C of 1,2,4-triazole), 196.5 (CO aliphatic), 111.2-160.7 (C of aromatic aldehyde), 143.3 (C, of azomethine), 55.8 (C of OCH₃). Mass (HRMS): m/z: 305, M⁺.

[(2-(4-Methoxybenzylidene)hydrazinoacetyl]-3-mercapto-4-methyl-1,2,4-triazole (3h)

$C_{13}H_{15}N_5O_2S$. Yield 96 %, m.p. 154-156 °C, dark yellow powder, IR(KBr), ν_{max} 1672, 1462, (1,2,4-triazole nucleus), 1215 (N-CH₃), 2866, 1162 (OCH₃) 1598 (N=CH). ¹H NMR (CDCl₃) δ (ppm): 8.44 (s, H, Ar-H of 1,2,4-triazole), 3.60 (s, 3H, N-CH₃), 3.76 (s, 2H, CH₂) 8.54 (s, 1H of azomethine), 2.0 (s, 1H, NH), 7.82, 7.06 for benzylidimine, 3.83 for 3H of OCH₃. ¹³C NMR (CDCl₃): 27.1 (N-CH₃), 63.8 (aliphatic CH₂), 143.1-162.6 (C of 1,2,4-triazole) 196.5 (CO aliphatic) 114.2-162.7 (C of aromatic aldehyde), 143.3 (C of azomethine), 55.8 (C of OCH₃). Mass (HRMS): m/z: 305, M⁺.

[(2-(3,4,5-Trimethoxybenzylidene)hydrazinoacetyl]-3-mercapto-4-methyl-1,2,4-triazole (3i)

$C_{15}H_{19}N_5O_4S$. Yield 88 %, m.p. 156-158 °C, yellow powder, IR(KBr), ν_{max} : 1672, 1460 (1,2,4-triazole nucleus), 1215 (N-CH₃), 2865 and 1170 (OCH₃), 1598 (N=CH). ¹H NMR (CDCl₃) δ (ppm): 8.44 (s, H, Ar-H of 1,2,4-triazole), 3.60 (s, 3H, N-CH₃), 3.76 (s, 2H, CH₂) 8.54 (s, 1H of azomethine), 2.0 (s, 1H, NH), 7.14 for benzylidimine, 3.83 for 6H of OCH₃. ¹³C NMR (CDCl₃) 27.1 (N-CH₃), 63.8 (aliphatic CH₂), 143.1-162.6 (C of 1,2,4-triazole), 196.5 (CO aliphatic), 104.2-152.7 (C of aromatic aldehyde), 143.3 (C of azomethine), 56.1, 60.4 (C of OCH₃). Mass (HRMS): m/z: 365, M⁺.

[(2-(2-Methylbenzylidene)hydrazinoacetyl]-3-mercapto-4-methyl-1,2,4-triazole (3j)

$C_{13}H_{15}N_5OS$. Yield 93 %, m.p. 158-160 °C, red powder, IR(KBr), ν_{max} : 1672, 1460, (1,2,4-triazole nucleus), 1215 (N-CH₃), 2927 (CH₃), 1549 (N=CH). ¹H NMR (CDCl₃) δ (ppm): 8.44 (s, H, Ar-H of 1,2,4-triazole), 3.60 (s, 3H, N-CH₃), 3.76 (s, 2H, CH₂), 8.52 (s, 1H of azomethine), 2.0 (s,

1H, NH), 7.24, 7.70 for benzylideneimine, 2.48 for 3H of CH₃. ¹³C NMR (CDCl₃): 27.1 (N-CH₃), 63.8 (aliphatic CH₂), 143.1-162.6 (C of 1,2,4-triazole), 196.5 (CO aliphatic), 124.2-135.3 (C of aromatic aldehyde), 143.3 (C of azomethine), 16.8 (C of CH₃). Mass (HRMS), m/z: 289, M⁺.

[(2-(3-Methylbenzylidene)hydrazinoacetyl)-3-mercapto-4-methyl-1,2,4-triazole (3k)]

C₁₃H₁₅N₅OS. Yield 88 %, m.p. 159-161 °C, light red powder, IR(KBr): ν_{\max} 1672, 1460, (1,2,4-triazole nucleus), 1215 (N-CH₃), 2927 (CH₃), 1549 (N=CH); ¹H NMR (CDCl₃) δ (ppm): 8.44 (s, H, Ar-H of 1,2,4-triazole), 3.60 (s, 3H, N-CH₃), 3.76 (s, 2H, CH₂), 8.52 (s, 1H of azomethine), 2.0 (s, 1H, NH), 7.24, 7.70 for benzylideneimine, 2.48 for 3H of CH₃. ¹³C NMR (CDCl₃): 27.1 (N-CH₃), 63.8 (aliphatic CH₂), 143.1-162.6 (C of 1,2,4-triazole), 196.5 (CO aliphatic), 124.2-135.3 (C of aromatic aldehyde), 143.3 (C of azomethine), 16.8 (C of CH₃). HRMS: m/z: 289, M⁺.

[(2-(4-Methylbenzylidene)hydrazinoacetyl)-3-mercapto-4-methyl-1,2,4-triazole (3l)]

C₁₃H₁₅N₅OS. Yield 89 %, m.p. 160-161 °C, light yellow powder, IR(KBr): ν_{\max} 1672, 1460, (1,2,4-triazole nucleus), 1215 (N-CH₃), 2928 (CH₃), 1547 (N=CH). ¹H NMR (CDCl₃) δ (ppm): 8.44 (s, H, Ar-H of 1,2,4-triazole), 3.60 (s, 3H, N-CH₃), 3.76 (s, 2H, CH₂), 8.52 (s, 1H of azomethine), 2.0 (s, 1H, NH), 7.27, 7.70 for benzylideneimine, 2.38 for 3H of CH₃. ¹³C NMR (CDCl₃): 27.1 (N-CH₃), 63.8 (aliphatic CH₂), 143.1-162.6 (C of 1,2,4-triazole), 196.5 (CO aliphatic), 126.2-140.3 (C of aromatic aldehyde), 143.3 (C of azomethine), 21.8 (C of CH₃). HRMS: m/z: 289, M⁺.

General microwave method for the synthesis of [4-[4-chlorophenyl]-3-chloro-2-oxoazetidineimino]-acetyl-3-mercapto-4-methyl-1,2,4-triazole (4a)

An equimolar mixture of compound **3a** (0.01) and triethylamine (0.01) in ethanol then added chloroacetyl chloride dropwise in ice bath then reaction mixture was performed in open glass vessel for about 2 min, the progress of reaction was monitored by TLC using hexane and ethyl acetate (9:1 v/v) as eluent, and the reaction mixture was concentrated to give a product which was recrystallized from chloroform, to give compounds **4a-4l** were synthesized in the similar manner using compound **3a-3l**. The synthesized compounds were identified by spectrophotometric analysis.

Synthesis of N-[[4-(4-chlorophenyl)-3-chloro-2-oxo-azetidine-imino]acetyl-3-mercapto-4-methyl-1,2,4-triazole, (4a)]

Yield 87 %, m.p. 210-215 °C, light red crystals. The structure was established on the basis of spectral analysis, IR(KBr): ν_{\max} 1668, 1545, 1332 (1,2,4-triazole nucleus), 2826, 1469, 1213 (N-CH₃). ¹H NMR (CDCl₃): δ (ppm): 8.44 (s, H, Ar-H of 1,2,4-triazole), 3.74 (s, 2H, CH₂), 3.58 (s, 3H, N-CH₃), 5.49 (s, 1H of CH-Cl), 2.0 (s, 1H, NH). ¹³C NMR (CDCl₃) four characteristic signals appeared for (N-CH₃), (aliphatic CH₂), (C of 1,2,4-triazole), (CO aliphatic), (C of aromatic aldehyde), (CO of β -lactam ring), (C of β -lactam

ring) in the δ (ppm) ranges 26.1, 62.1, 163.4-142.3, 196.6, 128.9-132.6, 197.2, 76.2 ppm. Mass (HRMS): m/z: 385, M⁺. Anal.: Calcd for molecular formula C₁₄H₁₃Cl₂N₅O₂S: C 43.53; H 3.49; Cl 18.36; N 18.13; found C 43.50, H 3.45, Cl 18.30; N 18.10.

Synthesis of N-[[4-(2,4-dichlorophenyl)-3-chloro-2-oxo-azetidineimino]-acetyl-3-mercapto-4-methyl-1,2,4-triazole (4b)]

Yield 85 %, m.p. 215-220 °C, light yellow crystals, IR(KBr): ν_{\max} 1664, 1545, 1332 (1,2,4-triazole nucleus), 2826, 1466, 1214 (N-CH₃). ¹H NMR (CDCl₃) δ (ppm): 8.44 (s, H, Ar-H of 1,2,4-triazole), 3.72 (s, 2H, CH₂), 3.60 (s, 3H, N-CH₃), 5.42 (s, 1H of CH-Cl), 2.0 (s, 1H, NH), 5.08 (d, 1H, N-CH-Ar), 7.32-7.64 (m, 6H, Ar). ¹³C NMR (CDCl₃) 27.1 (N-CH₃), 62.1 (aliphatic CH₂), 143.1-161.6 (C of 1,2,4-triazole), 196.5 (CO aliphatic), 125.3-142.0 (C of aromatic aldehyde), 163.2 (CO of β -lactam ring), 64.3 (C of β -lactam ring). Mass (HRMS): m/z: 420, M⁺. Anal.: Calcd for C₁₄H₁₂Cl₃N₅O₂S: C 39.97; H 2.88; Cl 25.28; N 16.65; O 7.62; S 7.61; Found C 39.96; H 2.83; Cl 25.23; N 16.62; O 7.52; S 7.61.

Synthesis of N-[[4-(2-bromophenyl)-3-chloro-2-oxo-azetidine-imino]-acetyl-3-mercapto-4-methyl-1,2,4-triazole (4c)]

Yield 88 %, m.p. 235-238 °C, pale yellow crystals, IR(KBr): ν_{\max} 1664, 1542 (1,2,4-triazole nucleus), 635 (C-Br), 2826, 1214 (N-CH₃), 1762 (C=O), 755 (C-Cl). ¹H NMR (CDCl₃) δ (ppm): 8.44 (s, H, Ar-H of 1,2,4-triazole), 3.75 (s, 2H, CH₂), 3.60 (s, 3H, N-CH₃), 5.47 (s, 1H of CH-Cl), 2.0 (s, 1H, NH), 5.04 (d, 1H, N-CH-Ar), 7.16-7.54 (m, 8H, Ar). ¹³C NMR (CDCl₃) 27.1 (N-CH₃), 62.0 (aliphatic CH₂), 143.1-163.6 (C of 1,2,4-triazole), 196.4 (CO aliphatic), 121.3-142.0 (C of aromatic aldehyde), 163.4 (CO of β -lactam ring), 63.6 (C of β -lactam ring). Mass (HRMS): m/z: 430, M⁺. Anal.: Calcd for C₁₄H₁₃BrClN₅O₂S: C 39.07; H 3.08; Br 18.58; Cl 8.28; N 16.25; O 7.42; S 7.44. Found: C 39.06; H 3.07; Br 18.20; Cl 8.23; N 16.22; O 7.41; S 7.41.

Synthesis of N-[[4-(3-bromophenyl)-3-chloro-2-oxo-azetidine-imino]-acetyl-3-mercapto-4-methyl-1,2,4-triazole (4d)]

Yield 87 %, m.p. 232-238 °C, dark yellow crystals. IR(KBr) ν_{\max} 1662, 1542, (1,2,4-triazole nucleus), 637 (C-Br) 2823, 1214 (N-CH₃), 1760 (C=O), 763 (C-Cl). ¹H NMR (CDCl₃) δ (ppm): 8.44 (s, H, Ar-H of 1,2,4-triazole), 3.75 (s, 2H, CH₂), 3.60 (s, 3H, N-CH₃), 5.44 (s, 1H of CH-Cl), 2.0 (s, 1H, NH), 5.08 (d, 1H, N-CH-Ar), 7.26-7.44 (m, 8H, Ar). ¹³C NMR (CDCl₃): 27.1 (N-CH₃), 62.0 (aliphatic CH₂), 143.1-162.6 (C of 1,2,4-triazole), 196.4 (CO aliphatic), 122.5-145.0 (C of aromatic aldehyde), 163.4 (CO of β -lactam ring), 64.6 (C of β -lactam ring). Mass (HRMS): m/z: 430, M⁺. Anal.: Calcd for C₁₄H₁₃BrClN₅O₂S: C 39.04; H 3.04; Br 18.55; Cl 8.23; N 16.26; O 7.43; S 7.42. Found C 39.01; H 3.02; Br 18.50; Cl 8.25; N 16.24; O 7.40; S 7.40.

Synthesis of N-[[4-(4-bromophenyl)-3-chloro-2-oxo-azetidine-imino]acetyl-3-mercapto-4-methyl-1,2,4-triazole (4e)]

Yield 77 %, m.p. 234-239 °C, dark yellow crystals. IR(KBr): ν_{\max} 1662, 1546 (1,2,4-triazole nucleus), 638 (C-Br), 2825, 1214 (N-CH₃), 1768 (C=O), 769 (C-Cl). ¹H NMR

(CDCl₃): δ (ppm): 8.44 (s, H, Ar-H of 1,2,4-triazole), 3.72 (s, 2H, CH₂), 3.62 (s, 3H, N-CH₃), 5.40 (s, 1H of CH-Cl), 2.2 (s, 1H, NH), 5.02 (d, 1H, N-CH-Ar), 7.16-7.94 (m, 8H, Ar). ¹³C NMR (CDCl₃): 27.0 (N-CH₃), 61.0 (aliphatic CH₂), 143.8-160.6 (C of 1,2,4-triazole), 196.4 (CO aliphatic), 122.4-145.9 (C of aromatic aldehyde), 163.2 (CO of β -lactam ring), 64.8 (C of β -lactam ring). Mass (HRMS): m/z: 430, M⁺. Anal.: Calcd for C₁₄H₁₃BrClN₅O₂S: C 39.04; H 3.04; Br 18.55; Cl 8.23; N 16.26; O 7.43; S 7.42. Found: C 39.00; H 3.01; Br 18.59; Cl 8.20; N 16.27; O 7.41; S 7.45.

Synthesis of N-[[4-(2-methoxyphenyl)-3-chloro-2-oxo-azetidineimino]acetyl-3-mercapto-4-methyl-1,2,4-triazole (4f)]

Yield 82 %, m.p. 224-229 °C, yellow crystals. IR(KBr): ν_{\max} 1672, 1460 (1,2,4-triazole nucleus), 1215 (N-CH₃), 2868 and 1173 (OCH₃), 1763 (C=O), 766 (C-Cl). ¹H NMR (CDCl₃): δ (ppm): 8.44 (s, H, Ar-H of 1,2,4-triazole), 3.75 (s, 2H, CH₂), 3.62 (s, 3H, N-CH₃), 5.45 (s, 1H of CH-Cl), 2.4 (s, 1H, NH), 5.05 (d, 1H, N-CH-Ar), 6.86-7.14 (m, 8H, Ar), 3.84 (s, 3H, OCH₃). ¹³C NMR (CDCl₃): 27.2 (N-CH₃), 63.0 (aliphatic CH₂), 142.8-161.6 (C of 1,2,4-triazole), 196.4 (CO aliphatic), 112.4-155.9 (C of aromatic ring), 163.5 (CO of β -lactam ring), 64.2 (C of β -lactam ring). Mass (HRMS): m/z: 381, M⁺. Anal.: Calcd for C₁₅H₁₆ClN₅O₃S: C 47.18; H 4.22; Cl 9.27; N 18.36; O 12.53; S 8.42. Found: C 49.10; H 4.21; Cl 9.20; N 18.37; O 11.41; S 8.48.

Synthesis of N-[[4-(3-methoxyphenyl)-3-chloro-2-oxoazetidine-imino]acetyl-3-mercapto-4-methyl-1,2,4-triazole (4g)]

Yield 85 %, m.p. 234-237°C, deep yellow powder. IR (KBr): ν_{\max} 1672, 1458 (1,2,4-triazole nucleus), 1215 (N-CH₃), 2868 and 1175 (OCH₃), 1768 (C=O), 762 (C-Cl). ¹H NMR (CDCl₃): δ (ppm): 8.42 (s, H, Ar-H of 1,2,4-triazole), 3.73 (s, 2H, CH₂), 3.61 (s, 3H, N-CH₃), 5.42 (s, 1H of CH-Cl), 2.6 (s, 1H, NH), 5.07 (d, 1H, N-CH-Ar), 6.83-7.24 (m, 8H, Ar), 3.82 (s, 3H, OCH₃). ¹³C NMR (CDCl₃): 27.4 (N-CH₃), 62.2 (aliphatic CH₂), 162.8-141.4 (C of 1,2,4-triazole), 196.2 (CO aliphatic), 112.5-165.9 (C of aromatic ring), 162.5 (CO of β -lactam ring), 64.2 (C of β -lactam ring), 53.8 (C of OCH₃). Mass (HRMS): m/z: 381, M⁺. Anal.: Calcd for C₁₅H₁₆ClN₅O₃S: C 47.18; H 4.22; Cl 9.27; N 18.36; O 12.56; S 8.40. Found: C 48.10; H 4.23; Cl 9.28; N 18.38; O 12.41; S 8.42.

Synthesis of N-[[4-(4-methoxyphenyl)-3-chloro-2-oxo-azetidineimino]acetyl-3-mercapto-4-methyl-1,2,4-triazole (4h)]

Yield 87%, m.p. 237-239 °C, deep brown crystals. IR(KBr): ν_{\max} 1672, 1468, (1,2,4-triazole nucleus), 1218 (N-CH₃), 2867 and 1165 (OCH₃), 1769 (C=O), 762 (C-Cl). ¹H NMR (CDCl₃): δ (ppm): 8.42 (s, H, Ar-H of 1,2,4-triazole), 3.72 (s, 2H, CH₂), 3.63 (s, 3H, N-CH₃), 5.43 (s, 1H of CH-Cl), 2.2 (s, 1H, NH), 5.10 (d, 1H, N-CH-Ar), 6.93-7.14 (m, 8H, Ar), 3.84 (s, 3H, OCH₃). ¹³C NMR (CDCl₃): 27.2 (N-CH₃), 62.1 (aliphatic CH₂), 162.2-142.4 (C of 1,2,4-triazole), 196.1 (CO aliphatic), 114.5-155.9 (C of aromatic ring), 164.5 (CO of β -lactam ring), 64.1 (C of β -lactam ring), 54.8 (C of OCH₃). Mass (HRMS): m/z: 381, M⁺. Anal.: Calcd for C₁₅H₁₆ClN₅O₃S: C 47.18; H 4.22; Cl 9.28; N 18.34; O 12.58; S 8.41. Found: C 47.12; H 4.21; Cl 9.26; N 18.32; O 12.51; S 8.40.

Synthesis of N-[[4-(3,4,5-trimethoxyphenyl)-3-chloro-2-oxo-azetidineimino]acetyl-3-mercapto-4-methyl-1,2,4-triazole (4i)]

Yield 75 %, m.p. 278-279 °C, shiny yellow powder. IR (KBr): ν_{\max} 1672, 1461 (1,2,4-triazole nucleus), 1216 (N-CH₃), 2862 and 1175 (OCH₃), 1479 (C=C aromatic), 1765 (C=O), 764 (C-Cl). ¹H NMR (CDCl₃): δ (ppm): 8.43 (s, H, Ar-H), 2.0(s, 1H, NH), 5.07 (d, 1H, N-CH-Ar), 6.53-7.8 (m, 4H, Ar), 3.82 (s, 9H, OCH₃). ¹³C NMR (CDCl₃): 27.0 (N-CH₃), 62.5 (aliphatic CH₂), 162.5-142.0 (C of 1,2,4 triazole), 196.7 (CO aliphatic), 104.5-152.9 (C of aromatic ring), 163.5 (CO of β -lactam ring), 64.2 (C of β lactam ring), 57.1 (C of OCH₃). Mass (HRMS): m/z: 441, M⁺. Anal.: Calcd for C₁₇H₂₀ClN₅O₅S: C 46.21; H 4.54; Cl 8.08; N 15.84; O 18.10; S 7.25. Found: C 46.18; H 4.51; Cl 8.06; N 15.82; O 18.11; S 7.24.

Synthesis of N-[[4-(2-methyl-phenyl)-3-chloro-2-oxo-azetidineimino]acetyl-3-mercapto-4-methyl-1,2,4 triazole (4j)]

Yield 92 %, m.p. 232-234 °C, yellow powder. IR(KBr): ν_{\max} 1676, 1460 (1,2,4-triazole nucleus), 1214 (N-CH₃), 1472 (C=C aromatic), 1742 (C=O), 762 (C-Cl). ¹H NMR (CDCl₃) δ (ppm): 8.39 (s, H, Ar-H of 1,2,4-triazole), 3.68 (s, 2H, CH₂), 3.61 (s, 3H, N-CH₃), 5.45 (s, 1H of CH-Cl), 2.1 (s, 1H, NH), 5.12 (d, 1H, N-CH-Ar), 6.93-7.51 (m, 8H, Ar), 2.62 (s, 3H, OCH₃). ¹³C NMR (CDCl₃): 26.8 (N-CH₃), 62.3 (aliphatic CH₂), 162.7-141.1 (C of 1,2,4 triazole), 195.7 (CO aliphatic), 124.5-142.9 (C of aromatic ring), 162.5 (CO of β -lactam ring), 64.8 (C of β -lactam ring), 17.1 (C of CH₃). Mass (HRMS): m/z: 365, M⁺. Anal.: Calcd for C₁₅H₁₆ClN₅O₂S: C 49.24; H 4.44; Cl 9.68; N 19.24; O 8.70; S 8.75. Found: C 47.18; H 4.41; Cl 9.66; N 18.92; O 8.01; S 7.94.

Synthesis of N-[[4-(3-methylphenyl)-3-chloro-2-oxo-azetidineimino]acetyl-3-mercapto-4-methyl-1,2,4 triazole (4k)]

Yield 92 %, m.p. 230-232 °C, light yellow powder. IR(KBr): ν_{\max} 1672, 1460 (1,2,4-triazole nucleus), 1215 (N-CH₃), 2929 (CH₃), 1472 (C=C aromatic), 1740 (C=O), 760 (C-Cl). ¹H NMR (CDCl₃) δ (ppm): 8.49 (s, H, Ar-H of 1,2,4-triazole), 3.78 (s, 2H, CH₂), 3.62 (s, 3H, N-CH₃), 5.43 (s, 1H of CH-Cl), 2.3 (s, 1H, NH), 5.02 (d, 1H, N-CH-Ar), 7.13-7.52 (m, 8H, Ar), 2.31 (s, 3H, CH₃). ¹³C NMR (CDCl₃): 27.8 (N-CH₃), 62.1 (aliphatic CH₂), 161.7-142.1 (C of 1,2,4-triazole), 197.7 (CO aliphatic), 122.5-144.9 (C of aromatic ring), 161.5 (CO of β -lactam ring), 64.7 (C of β -lactam ring), 20.1 (C of CH₃). Mass (HRMS): m/z: 365, M⁺. Anal.: Calcd for C₁₅H₁₆ClN₅O₂S: C 49.25; H 4.41; Cl 9.69; N 19.14; O 8.74; S 8.76. Found: C 48.28; H 4.31; Cl 9.62; N 19.12; O 8.71; S 8.74.

Synthesis of N-[[4-(4-methyl-phenyl)-3-chloro-2-oxo-azetidineimino]acetyl-3-mercapto-4-methyl-1,2,4 triazole (4l)]

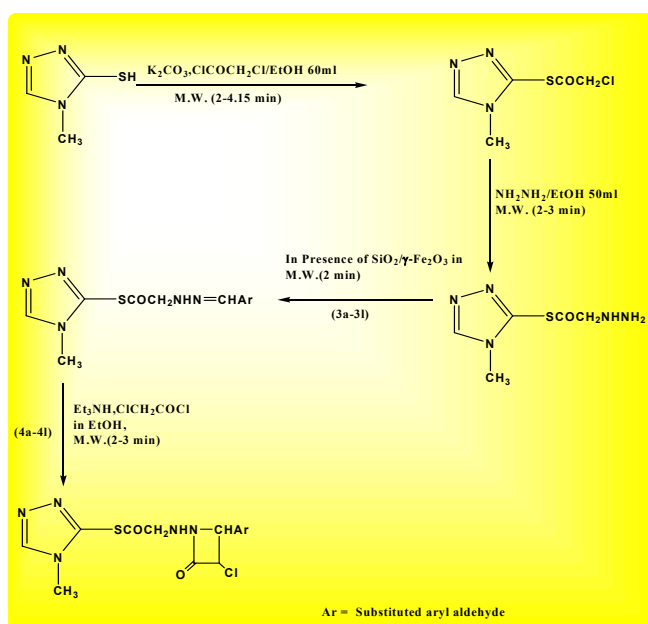
Yield 91 %, m.p. 235-235 °C, light red powder, IR (KBr): ν_{\max} 1676, 1461 (1,2,4 triazole nucleus), 1217(N-CH₃), 2928 (CH₃), 1474 (C=C aromatic), 1742 (C=O), 765 (C-Cl). ¹H NMR (CDCl₃): δ (ppm): 8.36 (s, H, Ar-H of 1,2,4-triazole), 3.68 (s, 2H, CH₂), 3.51 (s, 3H, N-CH₃), 5.40 (s, 1H of CH-Cl), 2.0(s, 1H, NH), 5.02(d, 1H, N-CH-Ar), 7.13-7.32 (m, 8H, Ar), 2.30 (s, 3H, CH₃). ¹³C NMR (CDCl₃): 27.0 (N-

CH₃), 62.3 (aliphatic CH₂), 162.7-141.1 (C of 1,2,4-triazole), 195.7 (CO aliphatic), 124.5-144.0 (C of aromatic ring), 164.5 (CO of β -lactam ring), 63.9 (C of β -lactam ring), 18.1 (C of CH₃). Mass (HRMS): m/z : 365, M⁺. Anal.: Calcd for C₁₅H₁₆ClN₅O₂S: C 49.25; H 4.41; Cl 9.69; N 19.14; O 8.74; S 8.75. Found C 47.28; H 4.39; Cl 9.52; N 19.08; O 8.69; S 8.71.

Results and Discussion

Recently, the interest in the sulfur containing moieties has been significantly surged since a wide range of biological activities associated with the scaffold have been identified. The present two pot procedure is efficient, general and versatile. Further application of the methodology to synthesize heterocyclic is in progress in our laboratory.

3-Mercapto-4-methyl-1,2,4-triazole on reaction with chloroacetylchloride yielded (chloroacetyl)-3-mercapto-4-methyl-1,2,4-triazole (**1**). The formation of compound **1** was confirmed by the appearance of a signal at 8.42 ppm (s, H, Ar-H of 1,2,4-triazole), 4.48 (s, 2H, CH₂), and 3.60 (s, 3H, N-CH₃) in ¹H NMR spectra and IR spectral band due to 718 (S-CO-S) 1615 (S-CO) cm⁻¹, respectively, also confirmed the formation of compound **1**, and on amination with hydrazine hydrate, yielded of (hydrazineacetyl)-3-mercapto-4-methyl-1,2,4 triazole compound **2**. In the ¹H NMR spectra of **2** a singlet peak at 2.1 ppm was observed due to 2H of NH₂ and a singlet peak at 2.0 ppm was due to (s, 1H) NH. Furthermore, in the IR spectra, the bands at 1668 cm⁻¹ (C=O of amide) and 3351 cm⁻¹ (NH₂) also confirmed the formation of compound **2**. The compound **2** on condensation with various aromatic aldehydes yielded α -(arylidene-hydrazino)acetyl]-3-mercapto-4-methyl-1,2,4-triazoles (**3a-l**), the formation of (**3a-l**) was supported by the appearance of singlet peaks at 8.52 ppm due to (1H) azomethine group. The ¹H NMR spectra and IR spectra (the bands at 1635, 1647 cm⁻¹ for N=CH, acyclic) also confirmed the formation of **3a-3l** compounds.



Scheme 1. Reaction routes

The compounds (**3a-l**) on reaction with triethylamine in presence of chloroacetylchloride underwent cyclization process afforded [{4-[4-aryl]-3-chloro-2-oxoazetidine-imino}acetyl-3-mercapto-4-methyl-1,2,4-triazoles (**4a-l**). In ¹H NMR spectra peaks at 4.69 (s, 1H of C-CH-Cl) 2.52 for (s, 1H, N-CH-Ar) groups have confirmed the formation of 2-azetidinones. In the IR spectra of (**4a-l**) the bands at 1710, 1721 cm⁻¹ for C=O (cyclic) of azetidinone ring also confirmed the formation of azetidinones (Scheme 1). All the Schiff base prepared in presence of heterogenous catalysts and all cyclization reactions proceeds under microwave irradiation were completed within 1-4 min. The impact of microwave irradiation in presence of catalyst for the synthesis of compounds (**3a-l**) and (**4a-l**) have been synthesized within effective high yield result shown in Table 1.

Table 1. Microwave synthesis for schiff base **3a-l** catalysed by heterogenous catalyst (SiO₂/γ-Fe₂O₃) and β -lactams **4a-l**.

Compound	Power, W	Microwave	
		Yield, %	Time, min
3a	800	94	1
3b	800	91	1.5
3c	800	88	1
3d	800	90	2
3e	800	82	2
3f	800	84	2
3g	800	94	2
3h	800	96	1
3i	800	88	3
3j	800	93	2
3k	800	88	1
3l	800	89	1
4a	800	87	2
4b	800	85	2.5
4c	800	88	2
4d	800	87	3.5
4e	800	77	3.5
4f	800	82	2
4g	800	85	1
4h	800	87	2.5
4i	800	75	2
4j	800	92	1.5
4k	800	92	2.5
4l	800	91	2

On microwave irradiation power.

Conclusions

In the chemical synthesis, MW methodology has opened up new route and opportunities for the synthetic chemists and researchers by providing novel methods not practical by conventional methods, this is a wide application in synthetic organic chemistry. MW assisted reactions are found to be rapid, efficient and safe. The approach is eco-friendly and this pollution preventive strategy is now an important part of modern combinatorial and green chemistry. Recent synthetic studies on various processes by utilizing MW irradiation have shown the high potential of MW irradiation in obtaining high yield products. The experimental procedures in microwave methods are simple

and economic. More research should have been performed to explore novel chemical compounds which can be synthesized under MW-assisted methodology.

Acknowledgement

The authors are thankful to USIC, Delhi University, Delhi (India) for providing spectral and analytical data of the compounds. We are also thankful to Head, Department of Chemistry Dr. H. S. Gour, University, Sagar (India) for giving the facilities to carryout the work. Author also thankful to UGC, New Delhi for providing financial assistantship of RGNF for Disability.

References

- ¹Abdulla, R. F., Fuhr, K. H., *J. Med. Chem.*, **1975**, 18, 625.
- ²Feigelson, G. B., Curran, W. V., Ziegler, C. B., *US* 5,189,158, **1994**,
- ³Doherty, J. B., Dorn, C. P., Durette, P. L., Finke, P. E., Maccoss, M., Mills, S. G., Shah, S. K., Sahoo, S. P., Polo, S. A., Hagmann, W. K., *Willey Online*, Book page no. 9410143
- ⁴Khalifullah, A. K., Selim, M. A., El-Hamd, R. M. A., Elmaghraby, M. A., Soleiman, H. A., Raslan, M., *Indian J. Chem.*, **1995**, 34B, 1066.
- ⁵Parikh, K. A., Oza, P. S., Parikh, A. R., *Indian J. Chem.*, **2000**, 39B, 716.
- ⁶Gheorghe, R., Mioara, A., *Bull. Chem. Technol. Maced.*, **2001**, 20.
- ⁷Santosh, K., Niranjana, M. S., Chaluvvaraju, K. C., Jamakhandi, C. M., Dayanand, K., *J. Current Pharm. Res.*, **2010**, page no. 139.
- ⁸Tsukuda, T., Shiratori, Y., Watanabe, M., Ontsuka, H., Hattori, K., Shirai, M., Shimma, M., *Bioorg. Med. Chem. Lett.*, **1998**, 8, 1819.
- ⁹Witkoaski, J. T., Robins, R. K., Sidwell, R. W., Simon L. N., *J. Med. Chem.*, **1972**, 15, 1150.
- ¹⁰Heubach, G., Sachse, B., Buerstell, H., *Ger. Offen.*, 2,826,760, **1979**.
- ¹¹Tanaka, G., *Japan Kokai*, 74-95973; *Chem. Abst.*, **1975**, 82, 156320h.
- ¹²Kumar, S. P., Mishra, D., Ghosh, G., Panda, B. B., Panda, C. S., *Int. J. Chem. Tech. Res.*, **2010**, 2(4), 1959.
- ¹³Hanna, N. B., Dimitrijevič, S. D., Larson, S. B., Robsin, R. K., Revankar, G. R., *J. Heterocycl. Chem.*, **1988**, 25, 1857.
- ¹⁴Amir, M., Khan, M. S. Y., Zaman, M. S., *Indian J. Chem.*, **2008**, B43, 2189.
- ¹⁵Chiu, S., Huskey, S.-E. W., *Drug. Metabol. Dispos.*, **1998**, 26, 838.
- ¹⁶Al-Masoudi, A., Al-Soud, A. Y., Al-Salihi, N. J., *Chem. Heterocycl. Compd.*, **2006**, 28, 1377.
- ¹⁷Raval Jignesh P., Patel Hemul V., Patel Pradip S., Desai Kishor R., *J. Saudi Chem. Soc.*, **2010**, 14, 417.
- ¹⁸Omar, A. M. E., Aboul Wafa, O. M., *J. Heterocycl. Chem.*, **1984**, 21, 1415.
- ¹⁹Francois, C., Claudine, J., *FR* 2539127; **1984**, *Chem. Abstr.* **1985**, 102, 95677n
- ²⁰Gupta, R., *Green Chem. Lett. Rev.*, **2013**, 6(2), 151.
- ²¹Metwally, N. H., *Green Chem. Lett. Rev.*, **2011**, 4(3), 225.
- ²²Thakur, A. J., *Green Chem. Lett. Rev.*, **2012**, 5(3), 457.
- ²³Caddick, S., *Tetrahedron.*, **1995**, 51, 10403.
- ²⁴Galema, S. A., *Chem. Soc. Rev.*, **1997**, 26, 233.
- ²⁵Lidstrom, P., Tierney, J., Wathey, B., Westman, J., *Tetrahedron* **2001**, 57, 9225
- ²⁶Katritzkey, A. R., Singh, S. K., *Arkivoc*, **2003**, 13, 68.
- ²⁷Nagendrappa, G., *Resonance.*, **2002**, 59.
- ²⁸Pereira, C., Gigante, B., Curto, M. J. M., Carreyre, H., Perot, G., Guisnet, M., *Synthesis.*, **1995**, 21, 1077.
- ²⁹Rode, C. V., Garade, A. C., Chikate, R. C., *Catal. Surv. Asia.*, **2009**, 13, 205.
- ³⁰Ang, B. C. Yaacob, I. I., *J. Nanomater.*, **2013**, 40, 32.
- ³¹Chin, A. B., Yaacob, I. I., *J. Mater. Process. Technol.*, **2007**, 191(1–3), 235.

Received: 18.04.2015.
Accepted: 03.07.2015.



PATHOLOGICAL PROCESSES IN LIVER AND INTUSSUSCEPTIVE GROWTH OF CAPILLARY ASSOCIATED WITH IT

G. R. Karapetyan^{[a]*} and N. S. Kukurtchyan^[a]

Keywords: TEM, intussusceptive angiogenesis, liver.

The growth of new blood vessels contributes to numerous malignant, ischemic, inflammatory, infectious and immune disorders. There are two forms of vascular remodeling associated with physiological and pathological processes; angiogenesis and arteriogenesis. It is shown in this study that, practically in all investigated models, the process of intussusceptive angiogenesis, etc. is the first step. Chemical agents lead to the development of intussusceptive angiogenesis in liver that could be the main reason for hemodynamic disturbance.

* Corresponding Authors

Fax: +374 -10-28 19 51

E-Mail: sapootraa_a@yahoo.com

[a] H. Buniatian Institute of Biochemistry, of National Academy of Sciences of Republic Armenia, Paruir Sevag str. 5/1, 0014, Yerevan, Republic of Armenia.

INTRODUCTION

Blood vessels constitute the first organ in the embryo and form the largest network in our body. When deregulated, the formation of new blood vessels contributes to numerous malignant, ischemic, inflammatory, infectious and immune disorders. Angiogenic stimulation promotes intense structural and functional changes in liver architecture and physiology.

Angiogenesis and arteriogenesis are two forms of vascular remodeling associated with physiological and pathological processes. Angiogenesis is a process of growth of new capillaries from the existing capillaries through capillary sprouting or intussusceptions.^{16,33} Non-spruting angiogenesis by means of intussusception – "growth within itself", is an important mode of capillary formation and is termed intussusceptive microvascular growth. Intussusceptive angiogenesis plays a role in tumor vascularisation.^{4,13,14,11} The presence of numerous tiny holes in vascular corrosion casts are shown, upon serial sectioning of tissue and subsequent transmission electron microscopy, to correspond to slender transcapillary tissue pillars or posts.⁹

Among features of the vasculature of the liver, not found in other tissues, are the hepatic sinusoids, characteristics of which include the presence of hepatic sinusoidal endothelial cells that possess distinctive fenestrations and pericytes or hepatic stellate cells.^{32,34} Additionally to the induction of proliferation of EC, effective angiogenesis also requires stabilization of nascent blood vessels, and formation of interendothelial cell junctions and lumens.³⁰

Pathological angiogenesis is different from that associated with physiological processes.²⁸ While physiological hepatic angiogenesis during liver regeneration leads to the formation of new functional sinusoids, pathological angiogenesis,

present in many chronic liver diseases, is characterized by the appearance of capillarized vascular structures.^{12,26} Angiogenesis is a recurring factor in the disease progression.⁸

Vascular imaging makes possible to quantify the number and spacing of blood vessels, measure blood flow and vascular permeability, as well as analyze cellular and molecular abnormalities in blood vessel walls. Microscopic methods ranging from fluorescence, confocal and multiphoton microscopy to electron microscopic imaging are particularly useful in elucidating structural and functional abnormalities of angiogenic blood vessels.²⁵

Goal

The aim of this study is to compare the mechanism of angiogenesis at different types of pathological influence on the liver.

MATERIALS AND METHODS

Reagents

Powdered paraformaldehyde; OsO₄; sodium cacodylate; 90% ethyl alcohol, acetone, epon 812, epon hardener MNA, epon hardener DDSA, epon accelerator DNP-30, uranyl acetate, sodium citrate, and lead nitrate, were of analytical grade from Sigma.

Animals

All procedures involving animals were approved by the Institutional Review Board/ Institutional Animal Care and Use Committee (H. Buniatian Institute of Biochemistry, Yerevan, NAS RA) and conformed to the European Communities Council directives (86/609/EC).

For experiments (Crush Syndrome, Intoxication by CCL₄) the liver of two-month-old male rats weighing 150-200 g and for additional study the liver of frog from Yerevan water area was used.

Treatment of material

The bioplates were put at 4°C in a mixture of paraformaldehyde in cacodilate buffer and glutaraldehyde for 12 hours, followed by post fixation in 1% OsO₄ solution for 2 hours; dehydration in ascending series of spirits; saturation in a mixture of acetone and epon resins of different proportions and pouring in gelatinous capsules into epon.

Obtaining of ultrathin slices and its treatment:

The ultrathin slices (up to 500 Å) were made using ultracut LKB (Swedish) and Reichert (Austria). Ultrathin slices were double contrasted with uranyl acetate and lead citrate.

Observation under transmission electron microscopy (TEM) and optical microscope

The ultrathin slices were observed under the transmission electron microscope (Phillips CM 10) with resolution X 10-20.000. Semithin slices 0,5-1 μm were stained for further light optical investigation.

RESULTS

The results of our study, from two types of angiogenesis intussusceptive, have shown that angiogenesis was dominant. Practically in all investigated groups the process of intussusceptive angiogenesis was observed.

However there were still some differences of the development of this process depend on the type of influence.

So, in the liver of frog lived in Yerevan water area polluted with different elements the process of angiogenesis was presented. It was shown that as a response on ecological influence etc water pollution alterations among the organelles of hepatocytes were observed this could be a physiological reaction of the tissue to the pathological influence.¹⁹

The sinusoid was divided by the way of transluminal bridge formation, and it's important to say that such new capillaries are quite different in size and asymmetric. Practically very close to the transluminal bridge Cupfer cells were observed. This could be explained as a protective response of liver on the influence of pollutant of water (Fig. 1).

Several cells appear to play a role in the process of intussusception, such as the endothelial cells, pericytes, macrophages and blood cells.⁵ The part of the cell body of the endothelial cells that formed the pillar frequently contained a high density of microfilaments, excluding all other cellular organelles.²⁷

Endothelial cells are quite large and the Disse space is observed. We opine that endothelial cells take part in the formation of transluminal bridge cover from two opposite sides. In the zone of close contact of endotheliocytes of two

opposite walls of lumenar cover of sinusoid the subplazmalemmas structure composed of thin filaments, was observed. Thin microfilaments organized in structure in the place of close contact of transluminal bridge made by endotheliocyte were observed in liver and in heart.¹⁹

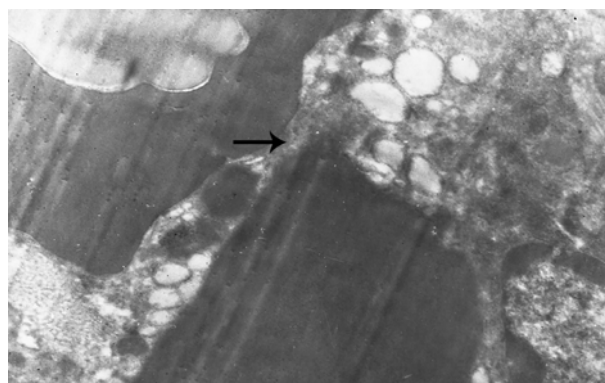


Figure 1. Formed transluminal bridge in frog liver. X 20.000

Organ's toxic injuries are widespread cause of the diseases and death in populations.^{2,15,31,29,22,3} We, therefore, studied two different types of influence on the liver particularly on the angiogenesis process that takes place in it. As a first model we studied the experimental model of Crush Syndrome etc 2h compression.

It is well known that at the compression period the catecholamine level increases which leads to cramp of arterioles and precapillaries lead to the retardation in the speed of blood flow, endovascular aggregation of erythrocytes and development of thrombus formation. Progression of microcirculation dysfunction lead to development of acute hypoxia that results in ischemia of different organs and tissues.^{21,23,17} At the experimentally induced Crush syndrome (2h of compression) the process of the transluminal bridge formation - the key of intussusceptive angiogenesis - takes place following the aggregation of erythrocytes in sinusoids, which become more critical at 4 hr. of decompression period (Fig. 2). The angiogenesis process takes place by the same mechanism mentioned above.

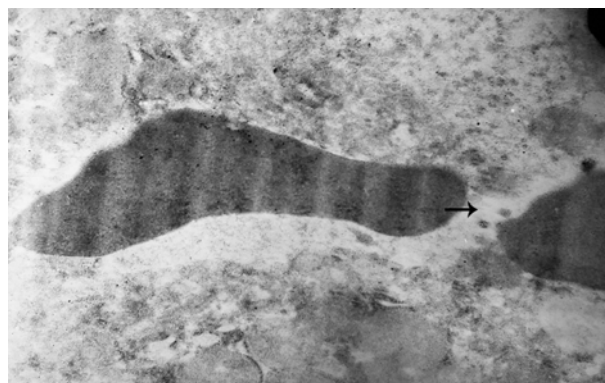


Figure 2. Formed transluminal bridge at Crush Syndrome. X 10.000

The experimentally induced intoxication by CCl_4 was chosen as the second model. It is well known that CCl_4 is an industrial toxin which leads to different pathological alteration in organism and in liver particularly.¹⁸ In this case we aimed to study if there are any changes observed in sinusoids structure. The results of our study have shown that the influence of CCl_4 is a leading factor in the development of angiogenesis process. The process of transsluminal bridge formation occurs. At the same time numerous bridges could be formed, leading to the formation of further capillaries with a different lumen diameter (Fig. 3 and 4).

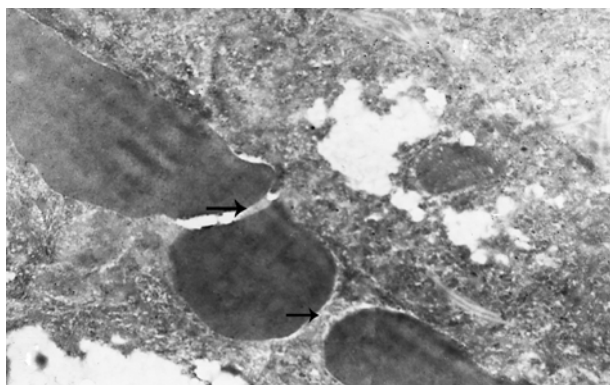


Figure 3. Formed transluminal bridge at CCl_4 toxicity. X 10.000

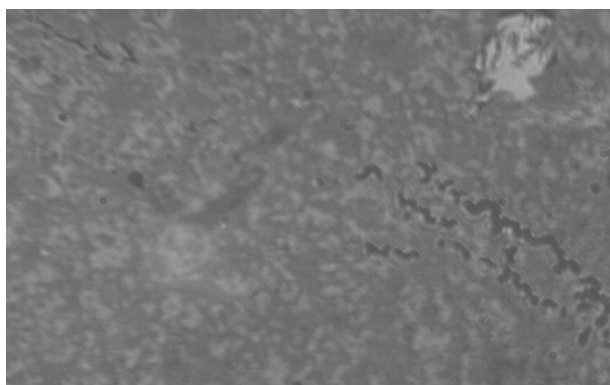


Figure 4. New vessel formation by the way of intussusception at CCl_4 toxicity. Semithin slices stained by Azur II, X 1.250

The results of current study have shown that the process of intussusceptive angiogenesis is observed in all investigated groups. This could be a response to acute influence as it does not need much energy to process it. Therefore it must be more economical and preferable for tissues.

DISCUSSION

Liver has different important functions in the organism and one of the most important is its detoxication function. Therefore it's also a target organ for many toxic agents which lead to its injury.

The influence of different pathological agents on the organism, especially those on the liver lead to microcirculation dysfunction. Such dysfunctional blood vessels are unable to provide expanding tissues and organs

with oxygen and nutrients, as well as remove the metabolic waste. This could be a reason for further progression of microcirculation dysfunction that leads to the development of acute hypoxia and as result ischemia of different organs and tissues.^{21,23,17}

Ischemic damage of different organs and tissues is still one of the most acute problems in medicine and biology. In ischemia the organism reacts by activation of angiogenesis process to provide normal metabolism processes to tissues. However, if in some case this process is normal, known as physiological angiogenesis, the influence of pathological agents is quite different. It must be mentioned that the role of angiogenesis etc., its different types are very important in the progression and development of different diseases such as diabetes, cardiovascular ischemic complications, cancer etc.^{24,5,7}

During angiogenesis, endothelial cells from intact blood vessels quickly infiltrate avascular regions via vascular sprouting. This process is fundamental to many normal and pathological processes such as wound healing and tumor growth, but its initiation and control are poorly understood. Sprouting angiogenesis is believed to be a major type of vasculature development in both liver regeneration and cancer development.¹

Another type of angiogenesis, different from sprouting, is intussusceptive angiogenesis. In contrast to sprouting angiogenesis, which is a well established mode of new blood vessel formation, intussusceptive angiogenesis is a relatively new concept in vascular biology. Intussusceptive angiogenesis is wide spread process and could be recognized as a ubiquitous phenomenon in vertebrates.⁴ This process was first observed in postnatal remodeling of capillaries in the lung.⁶ In this developmental process, a new concept of vessel formation was found where preexisting vessels split in two new vessels by the formation of transvascular tissue pillar into the lumen of the vessel. Intussusception is believed to take place after vasculogenesis or angiogenesis to expand the capillary plexus. Intussusceptive microvascular growth is a fast process that can take place within hours or even minutes with a little amount of energy, because it doesn't need proliferation of endothelial cells.

Our data indicate the fact that intussusceptive angiogenesis may play an important role in the malignant angiogenesis and chronically liver diseases.

The process of intussusceptive angiogenesis is found to occur practically in all investigated models (groups). However, some differences were observed in some studied processes. It must be noted that the transluminal bridge formation points to the presence of intussusceptive form of angiogenesis. It is well known that CCl_4 is a strong industrial toxin and has its negative toxic influence on liver as well as ischemia. Toxins released during Crush Syndrome also have a damaging influence on liver.

Transmission electron microscopy revealed four consecutive steps.⁵ Pillar formation and remodeling is not only observed in capillary plexuses but also within smaller arteries and veins.¹⁰ It was mentioned in literature that alteration in blood flow dynamics in arterial branches could

stimulate the process of angiogenesis etc that could promote pillar formation.¹ Several cells appear to play a role in the process of intussusception, such as the endothelial cells, pericytes, macrophages and blood cells.⁵

The part of the cell body of the endothelial cells that formed the pillar frequently contained a high density of microfilaments, excluding all other cellular organelles.²⁷

CONCLUSION

The influence of different pathological processes lead to intussusceptive angiogenesis development in liver, that could be the main reason for hemodynamic disturbance.

ACKNOWLEDGEMENT

Current work was performed by support of H. Buniatian Institute of Biochemistry Natl. Acad. Sci. of RA.

REFERENCES

- ¹Kurz, H., *J. Neurooncol.*, **2000**, 50, 1-19.
- ¹Andrew X., Zhu, D. G., Duda, D. V., Sahani, R., Gain, K., *Nature Rev. Clin. Oncol.*, **2011**, 8, 292-301.
- ²Bass, N. M., Ockner, B. A., *Hepatology: a textbook of liver disease*, 3rd ed., Philadelphia, **1996**, 962-1017.
- ³Bond, G. R., Hite, L. K. *Acad. Emergency Med.*, **1999**, 6(11), 1115-1120.
- ⁴Burri, P., Djonov, V., *Mol. Aspects Med.*, **2002**, 23(6S), S1-27.
- ⁵Burri, P. H., Hlushchuk, R. and Djonov, V., *Dev. Dynam.*, **2004**, 231, 474-88.
- ⁶Caduff, J. H., Fischer, L. C., and Burri, P. H., *Anatom. Record.*, **1986**, 216, 154-164.
- ⁷Carmeliet, P., *Nature*, **2005**, 438, 932-936.
- ⁸Coulon, S., Heindryckx, F., Geerts, A., Van Steenkiste, C., Colle, I., Van Vlierberghe, H., *Liver Int.*, **2011**, 31(2), 146-62.
- ⁹Djonov, V., Schmid, M., Tschanz, S. A. and Burri, P. H., *Circ. Res.*, **2000**, 86, 286-292.
- ¹⁰Djonov, V. G., Kurz, H. and Burri, P. H., *Dev. Dynam.*, **2002**, 224, 391-402.
- ¹¹Domenico, R., Djonov, V., *Cancer Lett.*, **2012**, 316, 126-131.
- ¹²García-Monzón, C. Sánchez-Madrid, F., García-Buey, L., García-Arroyo, A., García-Sánchez, A. and Moreno-Otero, R., *Gastroenterology*, **1995**, 108(1), 231-241.
- ¹³Haymo, K., P., Burri, H., Djonov, V. G., *Physiology*, **2003**, 18(2), 65-70.
- ¹⁴Hillen, F., Griffioen, A. W., *Cancer Metastasis Rev.*, **2007**, 26(3-4), 489-502.
- ¹⁵Holland, E. G., Degruy, F. V., *Am. Fam. Physician.*, **1997**, 56(7), 1781-1792.
- ¹⁶Hudlicka, O., Brown, M., Egginton, S., *Physiol. Res.*, **1992**, 72, 369-417.
- ¹⁷Ismailov, R. M., Shevchuk, N. A., Khusanov, H., *Biomed. Eng. Online*, **2005**, 4(1), 24
- ¹⁸Karapetyan, G. R., *J. Med. I Sci. Arm.*, **2008**, V. XLVIII, N 2, 60-66.
- ¹⁹Karapetyan, G. R., Kukurtchyan, N. S., *11th Conf. Arm. Electron Microsc. Soc., (AEMS)*, Yerevan, Armenia, **2003**, 95.
- ²⁰Karapetyan, G. R., Kukurtchyan, N. S., Kevorkian, G. A., *FEBS Congr.*, **2013**, p. 23.
- ²¹Lameire, N. H., De Vrise, A. S., Vanholder, R., *Curr. Opin. Crit. Care*, **2003**, 9(6), 481-490.
- ²²Lewis, J. H., *Curr. Pract. Med.*, **1999**(2): 49-58.
- ²³Malinoski, D. J., Slater, M. S., Mullins, R. J., *Crit. Care Clin.*, **2004**, 20(1), 171-192.
- ²⁴Martin, A., Komada, M. R., & Sane, D. C., *Med. Res. Rev.*, **2003**, 23, 117-145.
- ²⁵McDonald, DM., Choyke, PL., *Nat Med.*, **2003**, 9 (6): 713-25.
- ²⁶Medina, J., García-Buey, L., and Moreno-Otero, R., *Aliment. Pharmacol. Ther.*, **2003**, 17(1), 1-16.
- ²⁷Paku, S., Dezso, K., Bugyik, E., Tovari, J., Timar, J., Nagy, P., Laszlo, V., Klepetko, W., Dome, B., *J. Pathol.*, **2011**, 179(3), 1573-1585.
- ²⁸Papetti, M. and Herman, I.M., *Am. J. Physiol.*, **2002**, 282, C947-C970.
- ²⁹Plevris, J. N., Schina, M., Hayes, P. C., *Aliment. Pharmacol. Ther.*, **1998**, 12(5), 405-418.
- ³⁰Sanz-Cameno, P., Martín-Vílchez, S., Lara-Pezzi, E., Borque, M. J., Salmerón, J., Muñoz de Rueda, P., Solís, J. A., López-Cabrera, M. and Moreno-Otero, R., *Am. J. Pathol.*, **2006**, 169, 1215-1222.
- ³¹Schiodt, F. V., Rochling, F. A., Casey, D. L., Lee, W. M., *New England J. Med.*, **1997**, 337(16), 1112-1117.
- ³²Semela, D. and Dufour, J. F., *J. Hepatol.*, **2004**, 41(5): 864-880.
- ³³Simons, M., *Circulation*, **2005**, 111, 1556-66.
- ³⁴Song, J. W., Munn, L. L., *Proc. Natl. Acad. Sci. USA*, **2011**, 108(37), 15342-15347.

Received: 21.05.2015.

Accepted: 04.07.2015.